
Electronic Thesis and Dissertation Repository

8-24-2021 10:30 AM

CO₂ Derived Carbon Capture Using Microalgae in a PhotoBioCREC Unit

Maureen D. Cordoba Perez, *The University of Western Ontario*

Supervisor: de Lasa, Hugo, *The University of Western Ontario*

A thesis submitted in partial fulfillment of the requirements for the Doctor of Philosophy degree in Chemical and Biochemical Engineering

© Maureen D. Cordoba Perez 2021

Follow this and additional works at: <https://ir.lib.uwo.ca/etd>

 Part of the Biochemical and Biomolecular Engineering Commons, and the Catalysis and Reaction Engineering Commons

Recommended Citation

Cordoba Perez, Maureen D., "CO₂ Derived Carbon Capture Using Microalgae in a PhotoBioCREC Unit" (2021). *Electronic Thesis and Dissertation Repository*. 8093.
<https://ir.lib.uwo.ca/etd/8093>

This Dissertation/Thesis is brought to you for free and open access by Scholarship@Western. It has been accepted for inclusion in Electronic Thesis and Dissertation Repository by an authorized administrator of Scholarship@Western. For more information, please contact wlsadmin@uwo.ca.

Abstract

Microalgae has the potential to contribute to carbon dioxide capture, resulting in the production of alternative fuels and valuable chemical products. To accomplish this, high efficiency photobioreactors must be conceptualized, designed and established, in order to achieve high inorganic carbon conversion, superior light utilization, and unique fluid dynamics.

In this PhD Dissertation, experiments with *Chlorella vulgaris* were carried out, in a 0.175L especially designed *PhotoBioCREC* unit, under controlled radiation and high mixing conditions. This unique design involves 1 mm-2 mm alumina particles, which keep photoreactor walls always clean, without compromising photon transmittance. Sodium bicarbonate (NaHCO_3) was supplied as the inorganic carbon containing culture media. The NaHCO_3 concentrations studied were in the 18 mM to 60 mM range. The NaHCO_3 concentrations, the total organic carbon concentrations and absorbed radiation were measured every 24 hours. The pH was readjusted every day to the required 7.00 level, with the temperature being maintained at $24.3^\circ\text{C} \pm 0.5^\circ\text{C}$.

Results showed 29.6% as the best carbon conversion achieved, with a total organic carbon (TOC) selectivity up to 33% ± 2.0 , by *Chlorella vulgaris*. It was found that quantum yield efficiencies, for *Chlorella vulgaris* culture, in a NaHCO_3 solution media, were in the 1.9%-2.3% range. It was also proven that maximum reaction rates for organic carbon formation were achieved with a 28 mM NaHCO_3 concentration, displaying a $1.18 \pm 0.05 \text{ mmole L}^{-1}\text{day}^{-1}$ value. Based on the experimental data obtained, a kinetic model for inorganic carbon consumption and organic carbon formation was successfully developed and validated for concentrations of NaHCO_3 in the 18 mM to 60 mM range.

Thus, the findings of the present PhD Dissertation allowed one to establish best operational conditions, in the *PhotoBioCREC* unit, for *Chlorella vulgaris* growth, in sodium bicarbonate solutions, with high inorganic carbon and photon energy utilization.

Furthermore, the rotating flow design, in the near transmission wall region of the *PhotoBioCREC* prototype, was also demonstrated in a 10.3 L *PhotoBioCREC Swirl Reactor* prototype. It was proven in this PhD Dissertation, that this scaled-up unit could also benefit from the flow rotational principles of the *PhotoBioCREC*. It is anticipated that future studies, which will include the developed microalgae growth kinetics, will allow one to demonstrate via numerical simulation and experimentation, the value of scaled *PhotoBioCREC Swirl Reactor* units, for CO₂ derived carbon capture using *Chlorella vulgaris* culture.

Keywords

Microalgae, kinetics, carbon utilization, bicarbonates, quantum yield, efficiency.

Summary for Lay Audience

The combustion of fossil fuels leads to greenhouse emissions that play a significant role in climate change. Carbon dioxide (CO₂) is one of the main components of these emissions. Plants consume CO₂ in the process of photosynthesis. However, CO₂ fixation in plants is not significant enough to prevent the increase of the CO₂ concentration in the atmosphere. For this reason, action must be taken to enhance CO₂ fixation and to reduce these emissions.

Microalgae, like plants, offer a unique method for CO₂ fixation, through photosynthesis. They can be grown at controlled conditions, in photobioreactors. This approach can allow power plants to reduce carbon emissions, by capturing CO₂ in bicarbonate solutions, feeding them later, to photobioreactors, for microalgae growth. The organic matter produced can be used for energy production in the same power station, or alternatively, as a precursor of other products such as biofuels, pharmaceuticals, and food.

Photobioreactors for algae production are however, still under development. Light supply at a constant rate during microalgae growth, is a challenge since microalgae, tend to grow on the photobioreactor walls. Moreover, light absorption efficiency has not usually yet been reported in the technical literature even though light is the photosynthesis driving force.

The objective of this study was to design a new photobioreactor for microalgae cultivation powered by visible light. This objective was successfully accomplished by using sodium bicarbonate solutions in a 0.175 L vortex flow *PhotoBioCREC* unit, with a *Chlorella vulgaris* culture. Inorganic carbon depletion and organic carbon formation were monitored. The promising efficiency of the reactor was demonstrated in terms of its ability to convert inorganic carbon into organic carbon and to transform visible photon energy to produce microalgae. The study was completed, with fluid dynamic and photo absorption studies in a 10.3 L volume *PhotoBioCREC Swirl Reactor*. Experiments in this larger unit, provided valuable reactor engineering information, required to implement in the near future microalgae growth in scaled-up *PhotoBioCREC* units, with an induced vortex flow.

A mis padres (To my parents) Bernardino y Rafaela,

Mis hermanos (my siblings): Heilyn, Andrea, Roxana y Jose Pablo.

Acknowledgments

I am very grateful to God, for his blessings and grace, and for being my strength during the uncertain times during this journey.

My heartfelt appreciation and gratitude to Professor Hugo de Lasa, for giving me the opportunity to develop this project, for his guidance, dedication, and patience over the years. Thank you, Dr. de Lasa for caring about me, and for the support that you and your family gave me during these years.

I would like to acknowledge the financial support from the University of Costa Rica. As well, I am grateful to the staff of the Oficina de Asuntos Internacionales y Cooperación Externa, and the Chemical Engineering Department.

I would like to thank Dr. Pastor Solano, for helping me in the first stages of this research, for challenging me with his questions, and for our conversations about different subjects. I am also grateful to Jose Muñoz, always willing to help and being the happy spirit. Also, I would like to express my gratitude to Ms. Florencia de Lasa for her valuable contribution.

I am grateful to all the members of the CREC group: Samira, Imtiaz, Abdul, Amanda, Cesar, Sandra, Steve, Bianca, Nicolas and Salvador. Thank you all for the feedback and advise over the years, for the constructive conversations during lunch or coffee time. A special thanks to Nicolas for giving me the opportunity to know his family and become part of mine.

I am also grateful for all the amazing people I met during this journey. Special thanks to Marianna Kroll, for her kindness and joy, my first summer in Canada was amazing because of you. My friends that I made along the way: Amanda, Daisy, Erika, Housyn, Aaron, Lee, Anabel and Mingyar, thanks for all the laugh and all the lovely memories.

Thanks to my family and friends in Costa Rica, your messages and calls keep me going when I was missing home. Don Manuel, Marcela, Adolfo and Melisa: you are priceless, I am grateful for your trust and support, I am here because of you.

I am eternally grateful for my parents Bernardino Córdoba Gómez and Rafaela Pérez Díaz, I have accomplished my goals because of their support, hard work, confidence, and

motivation. Dad, I always remember your words “you can achieve anything if you put your mind to it”.

Finally, I would like to thank my love, Gureet, for being always there for me, for cheering me up in the difficult times. You make my days happier, and I couldn’t have asked for a better husband, you are one of God’s blessings in my life.

Table of Contents

Abstract	ii
Summary for Lay Audience	iv
Acknowledgments.....	vi
Table of Contents	viii
List of Tables	xii
List of Figures	xiii
Nomenclature	xvii
Chapter 1	1
1 Introduction	1
Chapter 2.....	7
2 Literature Review.....	7
2.1 Microalgae	7
2.2 Photosynthesis in Microalgae	7
2.2.1 Light and Dark reactions of Photosynthesis	7
2.2.2 Photorespiration	9
2.3 Inorganic Carbon Supply and Uptake Mechanism	10
2.3.1 Sources of Inorganic Carbon	10
2.3.2 Mechanism of CO ₂ Fixation in Photosynthesis	14
2.4 Light and Photosynthesis efficiency	16
2.4.1 Light.....	16
2.4.2 Quantum Yield.....	17
2.5 Other Factors to consider for Microalgae Growth.....	18
2.5.1 Temperature	18
2.5.2 Nutrients.....	19

2.5.3 Culture pH.....	20
2.5.4 Mixing.....	20
2.6 Microalgal Growth.....	21
2.6.1 Phases of the growth cycle.....	21
2.6.2 Growth Models	22
2.7 Microalgal Cultivation Systems.....	23
2.7.1 Open Systems.....	24
2.7.2 Closed systems.....	25
2.8 Genetic Engineering of Microalgae	28
2.9 Microalgae Biomass Separation Process	29
2.10CO ₂ Capture by Microalgae	30
2.11Conclusions.....	32
Chapter 3	33
3 Research Objectives	33
3.1 Specific Objectives	33
Chapter 4.....	34
4 Materials and Methods	34
4.1 Microalgae Strain.....	34
4.2 Growth media.....	34
4.2.1 Modified Bold Basal Medium (MBBM)	34
4.2.2 Inorganic Carbon Source	35
4.3 Experimental Setup.....	36
4.3.1 PhotoBioCREC Unit.....	36
4.3.2 Experiments in the <i>PhotoBioCREC</i> Unit.....	37
4.4 Analytical Methods	39
4.4.1 Total Organic Carbon (TOC).....	39

4.4.2 Inorganic Carbon Concentration.....	39
4.5 Irradiation Measurements	39
4.6 Algal Biomass Characterization	40
4.6.1 Elemental Analysis	40
4.6.2 Microalgae cell image analysis.....	41
Chapter 5	44
5 Carbon Uptake by <i>Chlorella vulgaris</i> in a PhotoBioCREC Unit	44
5.1 Carbon Concentration	44
5.1.1 pH Changes during Microalgae Growth.....	46
5.2 Carbon Conversion by CPCC90 <i>Chlorella vulgaris</i>	47
5.3 Conclusions.....	49
Chapter 6.....	51
6 Macroscopic Radiation Energy Balances and Quantum Yields	51
6.1 Methodology	51
6.2 Observed Photon Absorption and Quantum Yields.....	53
6.3 Conclusions.....	58
Chapter 7	59
7 Kinetics of Microalgae Culture	59
7.1 Introduction.....	59
7.2 Kinetic Model Development.....	61
7.3 Kinetic Parameters	64
7.4 Kinetic Model	68
7.5 Biomass Composition	71
7.6 Conclusions.....	72
Chapter 8.....	74
8 <i>PhotoBioCREC</i> Scaled Swirl Reactor Prototype	74

8.1 Description of the <i>PhotoBioCREC</i> Swirl Reactor	74
8.2 Image Analysis for Tangential and Axial Velocity Determination in the <i>PhotoBioCREC Swirl Reactor</i>	77
8.3 Fluid Dynamics of the <i>PhotoBioCREC Swirl Reactor</i>	78
8.4 Irradiation Measurements in the <i>PhotoBioCREC Swirl Reactor</i>	80
8.5 Conclusions.....	84
Chapter 9	85
9 Conclusions, Future Work and Research Outcomes.....	85
9.1 Conclusions.....	85
9.2 Future work.....	86
9.3 Research Outcomes.....	87
Bibliography	88
Curriculum Vitae	101

List of Tables

Table 2.1 Microalgae Culture Species for CO ₂ Capture Reported in the Technical Literature with the following reported: a) Inorganic carbon source, b) pH, c) Temperature, d) Carbon conversion, e) Macroscopic Radiation Energy Balances.....	30
Table 4.1 Modified Bold Basal Media (Stein, 1973).....	34
Table 4.2 Trace Metal solution (Stein, 1973)	35
Table 4.3 Nominal and Experimental Concentrations of NaHCO ₃ used in the Experiments.	35
Table 5.1 pH Measurements during CPCC90 <i>Chlorella vulgaris</i> Growth.....	46
Table 7.1 Microalgae Kinetic Models Reported in the Technical Literature.	60
Table 7.2 Kinetic Parameters for Inorganic Carbon Consumption.....	64
Table 7.3 Reaction Rate Constants for Total Organic Carbon Formation and Growth Phase time.	66
Table 7.4 Maximum Selectivity for the Different Inorganic Carbon Concentrations Based on Equation 7.12. Average values of 3 runs and standard deviations are reported.	68
Table 7.5 Elemental Analysis of the Cells of the CPCC90 <i>Chlorella vulgaris</i> Using Combined CHNS and EDX Elemental Analyses. Reported results are an average value for repeats with a ±0.003 being the largest standard deviation.	72

List of Figures

Figure 1.1 World Total Energy Supply by source in 2018. Note: <i>Category “Other” includes geothermal, solar, wind, tide/wave/ocean, heat and other sources</i> (IEA, 2020)	2
Figure 2.1 Schematic representation of the light and dark reactions of photosynthesis. Abbreviations: RuBP = ribulose-1,5-biphosphate; 3PG = 3-phosphoglycerate; and G3P = glyceraldehyde 3-phosphate (Rasmussen & Minteer, 2014)	8
Figure 2.2 Schematic representation of CO ₂ capturing from flue gas using carbonates (Gris et al., 2014).	12
Figure 2.3 A Schematic Model for Inorganic Carbon Transport and CO ₂ Accumulation Processes in Eukaryotic Algal Cells (Giordano et al., 2005).....	15
Figure 2.4 Typical growth characteristics of a microorganism in a batch reactor (Blanch et al., 1996).	22
Figure 2.5 Schematic diagram of a Raceway Pond with arrows showing the recirculation of the cultured algae and water (Razzak et al., 2017)	25
Figure 2.6 Schematic diagram of a closed microalgae system with continuous recirculation of suspended algae (Razzak et al., 2017).	26
Figure 2.7 Schematic diagram of an algae culture dewatering process (Razzak et al., 2017).29	
Figure 4.1 Schematic Description of the <i>PhotoBioCREC</i> Unit. Left: Longitudinal cross section showing the microalgae culture level, the baffle positions and the fiber optic conduit placed at 5cm from the bottom, for irradiation measurements with a spectrophotometer. Right: Various photobioreactor dimensions (Cordoba-Perez & de Lasa, 2020).	37
Figure 4.2 Different stages of CPCC90 <i>Chlorella vulgaris</i> growth in the <i>PhotoBioCREC</i> unit.	38

Figure 4.3 Irradiation Spectrum for Fluorescent Lamp. Zones highlighted in “green” describe the fraction of the spectrum where chlorophyll displays absorption wavelengths, which are included in quantum yield calculations.....	40
Figure 4.4 CPCC90 <i>Chlorella vulgaris</i> Cells Analysis with a) EDX and b) SEM. Samples correspond to a 12-day cultivation time and grown with nominal concentration of 60 mM of NaHCO ₃	41
Figure 4.5 Microscope Images of CPCC90 <i>Chlorella vulgaris</i> cells: a) Show inoculum cells, b) show a case where a 28 mM NaHCO ₃ solution was used and after 10 days of cultivation time, c) show a case where a 60 mMNaHCO ₃ solution was used and after 12 days of culture. Contrast and cells boundary definition have been modified to improve the resolution of the images.....	42
Figure 4.6 Cell size Distribution for Different Concentrations of Inorganic Carbon, as Sodium Bicarbonate: a) blue bars: 18 mM, b) orange bars: 28 mM, c) yellow bars: 40 mM, d) violet bars: 60 mM.....	43
Figure 5.1 Total Inorganic Carbon and Total Organic Carbon Concentration Changes with Culture Time for the Different Nominal Concentrations of NaHCO ₃ : (A) 18 mM, (B) 28 mM, (C) 40 mM and (D) 60 mM (standard deviation of 3 repeats).....	44
Figure 5.2 Conversion Efficiency of Inorganic Carbon provided as NaHCO ₃ into Organic Carbon in the <i>PhotoBioCREC</i>	48
Figure 6.1 <i>PhotoBioCREC</i> Unit Setup for Irradiation Measurements (Cordoba-Perez & de Lasa, 2020).....	52
Figure 6.2 Rate of photon Absorption (Equation 6.1) for the Experiments with Concentrations of Sodium Bicarbonate of: (A) 18 mM, (B) 28 mM, (C) 40 mM and (D) 60 mM. Vertical bars represent the standard deviation of three runs.	54
Figure 6.3 Rate of Organic Carbon Formation for the Different Concentrations of NaHCO ₃ : (A) 18 mM, (B) 28 mM, (C) 40 mM, and (D) 60 mM. Vertical bars represent the standard deviation of three runs.	55

Figure 6.4 Percentual Quantum Yield (Equation 6.3) for <i>Chlorella vulgaris</i> with: (A) 18 mM NaHCO ₃ , (B) 28 mM NaHCO ₃ , (C) 40 mM of NaHCO ₃ and (D) 60 mM of NaHCO ₃ . Vertical bars represent the standard deviations of three runs.	56
Figure 7.1 NaHCO ₃ Concentration Changes with culture time. Experimental and model predicted values (Equation 7.8) for nominal initial concentrations of (A) 18 mM, (B) 28 mM, (C) 40 mM, (D) 60 mM. Note: reported results include at least 3 repeats.	65
Figure 7.2 Concentrations of Total Organic Carbon with Culture Time. Experimental and model predicted values (Equation 7.9 for growth phase) for Nominal concentrations of NaHCO ₃ : (A) 18 mM, (B) 28 mM, (C) 40 mM and (D) 60 mM.	67
Figure 7.3 Maximum Concentrations of Total Organic Carbon as a Function of Initial NaHCO ₃ Concentration. Note $\gamma = 0.42 \pm 0.04$ and $\delta = 0.02 \pm 0.004$ of Equation 7.12.	68
Figure 7.4 Comparison between Experimental Results and Predicted Values from the Proposed Kinetic Model (Equation 7.9), for the determination of Total Organic Carbon Concentration for Different Initial Nominal Concentrations of NaHCO ₃ : (A) 18 mM, (B) 28 mM, (C) 40 mM, and (D) 60 mM.	70
Figure 7.5 Comparison of Predicted and Observed Total Organic Carbon for the sodium Bicarbonate Concentrations of the present study.....	71
Figure 8.1 General Schematic Diagram of the <i>PhotoBioCREC Swirl Reactor</i> and the Experimental System.	75
Figure 8.2 Diagram of the PhotoBioCREC Swirl Reactor a) inner reflectors and front annular section view, (b) unit side view (Valadés-Pelayo et al., 2015).....	76
Figure 8.3 Schematic Diagram Showing Lamps and their Relative Location in the Reflectors. The (a) axonometric view and (b) top view. Dimensions reported in centimeters (Valadés-Pelayo et al., 2015).....	77

Figure 8.4 Image Analysis. Particle trajectories are tracked in different frames, establishing the x and y position. Particles highlighted in black represent the particles tracked. The red lines provide a reference for x and y position changes of the selected particles.	78
Figure 8.5 Effect of Swirl Flow on Particle Tangential Velocity.....	79
Figure 8.6 Effect of Swirling Flow on Particle Axial Velocity.....	80
Figure 8.7 Comparison of the Visible Radiation spectra for water (continuous line) and water with alumina particles (dash lines). Measurements were performed at Z=0 cm and four azimuthal positions in the 400 nm-70 nm range. Standard deviations $\pm 2\%$	81
Figure 8.8 Axial Radiation distribution Profile at Various axial Positions. Measurements effected at four azimuthal positions.....	82
Figure 8.9 Dimensionless Transmitted Radiative Flux at Z=0 cm and at Different Azimuthal Positions shown in the Diagram.	83

Nomenclature

MBBM	Modified Bold Basal Medium
C_{in}	Inorganic carbon concentration ($mmole\ L^{-1}$)
C_{org}	Organic carbon concentration ($mmole\ L^{-1}$)
C_{in_0}	Initial inorganic carbon concentration ($mmole\ L^{-1}$)
C_{org}^{max}	Maximum organic carbon concentration in ($mmole\ L^{-1}$)
k_{in}	Reaction rate constant for inorganic carbon in ($mmole\ L^{-1}day^{-1}$)
k_{or}	Reaction rate constant for organic carbon ($mmole\ L^{-1}day^{-1}$)
K	Constant ($L\ mmole^{-1}$)
N_{in}	Moles of inorganic carbon
N_{org}	Moles of organic carbon
P_a	Rate of absorbed photons in culture media ($moles\ of\ photons\ s^{-1}$)
P_i	Rate of photons reaching the <i>PhotoBioCREC</i> Unit walls ($moles\ of\ photons\ s^{-1}$)
P_t	Rate of photons transported through the microalgae media $moles\ of\ photons\ s^{-1}$)
r_{in}	Molar rate of inorganic carbon consumption ($mmole\ L^{-1}day^{-1}$)
r_{org}	Molar rate of organic carbon formation ($mmole\ L^{-1}day^{-1}$)
t	Time (day)
t_{lag}	Lag phase time (day)
t_f	Time representing the end of the growth phase (day)
TOC	Total organic carbon
V_f	Liquid hold-up (mL)
α	Stoichiometric coefficient
β	Stoichiometric coefficient
γ	Model parameter
δ	Model parameter
η	Carbon conversion efficiency (%)
θ_v	Matrix sites
τ	Growth phase time (day)

Chapter 1

1 Introduction

Energy requirements for transportation, industry and housing are steadily increasing with human population growth (Taylor & Tainter, 2016). Over the years, fuel energy consumption has increased, with this being either localized (e.g., power stations) or distributed (e.g., car, buses) and leading to greater greenhouse gas emissions (Taylor & Tainter, 2016).

Prior to the industrial age, there was a balance between the carbon consumed by humans, animals, and plants as a source of energy, and the CO₂ absorbed by plants, the soil, and the ocean. However, at present, the natural carbon cycle has been disturbed by both the anthropogenic release of carbon dioxide (CO₂) via combustion into the atmosphere, and extensive land usage (Stocker et al., 2013). This is the consequence of the excessive use of fossil derived fuels, as required for human transportation, for the ever-expanding manufacturing industrial sector and for other energy usage intensive industries, such as cement production (Stocker et al., 2013). As a result, the concentration of carbon dioxide (CO₂) in the atmosphere is steadily growing (Buis, 2019), with this being a matter of great concern for the world community, for both the present and future of humankind (IPCC, 2014).

It is predicted that renewable energies such as wind, hydropower, geothermal and biomass will all contribute to significantly reducing fossil fuel energy generation dependence. Despite these efforts to increase energy supply by renewable resources, energy supplied by coal, oil and natural gas still accounts for up to 81.2% of the energy used worldwide (IEA, 2020), as reported in Figure 1.1.

To address this issue, one should mention that there is no single path or process capable of providing the energy required worldwide to reduce the dependence on fossil fuels. However, among several possible options, photosynthetic microorganisms have the

potential to contribute to the utilization of carbon dioxide efficiently, by capturing CO₂ to produce renewable biomass and biofuels, among other valuable products, through a “neutral carbon emission process” (Chisti, 2007; Gharabaghi et al., 2015).

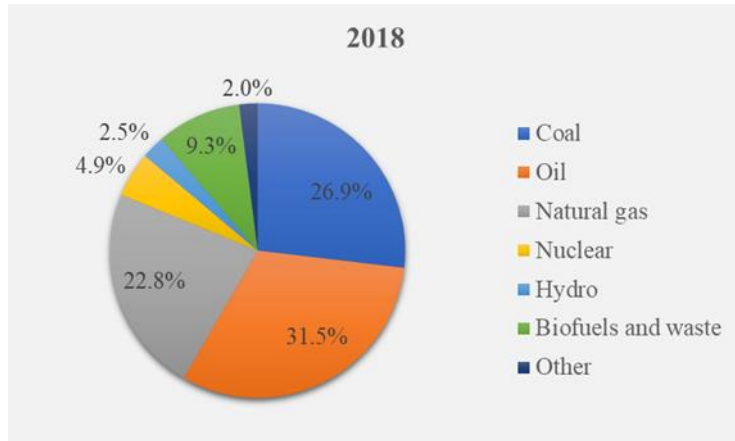


Figure 1.1 World Total Energy Supply by source in 2018. Note: *Category “Other” includes geothermal, solar, wind, tide/wave/ocean, heat and other sources* (IEA, 2020).

Microalgae species have the advantage of growing faster than plants, since most of the photonic energy is used for cell division, resulting in a rapid biomass accumulation (Li et al., 2008; Sayre, 2010). The resulting microalgae composition includes pigments, lipids, oils, fatty acids, and bioactive compounds. The produced microalgae have many applications such as animal and human food, cosmetics and biofuels, among other uses (Chisti, 2007; Metting, 1996; Spolaore et al., 2006).

Despite the claimed potential of carbon capture and microalgae biomass production through this process, the production of biofuels and bulk products such as proteins for food is not yet economically viable (Singh & Dhar, 2019). To achieve the feasibility of carbon capture by microalgae, the efficiency of the cultivation process must consider factors such as nutrients, carbon source, temperature, pH, and light supply as well as the complete utilization of the biomass components (Carvalho et al., 2014., Singh & Dhar, 2019).

When micro and macro nutrients are supplied satisfactorily, mixing, temperature and pH are controlled adequately, the main factors affecting the growth rate are the carbon source and the light supply.

Even if microalgae can grow with the CO₂ concentration in the atmosphere (0.04%¹), its growth rate is highly enhanced at higher concentrations of CO₂ (Wang et al., 2008), its growth rate is highly enhanced at higher concentrations of CO₂ (Wang et al., 2008). It is a common practice to supply a pure CO₂ stream or an enriched air-CO₂ stream to microalgae culture, resulting in high energy costs due to the low solubility and diffusion of CO₂ in water (Vadlamani et al., 2017).

A different approach involves the direct supply of CO₂ from industrial flue gas such as the one produced in a power plant. The main drawbacks of this alternative are the possible exposure of microalgae to: a) high temperature, b) high CO₂ concentrations and c) Inhibitory effects of compounds such as sulfur oxides (Pires et al., 2012; Thomas et al., 2016).

One should note however, that in order to be viable, the described microalgae culture processes have to address the issues of CO₂ capture and storage. In this respect, CO₂ storage in soluble carbonates (bicarbonate/carbonate) offer a valuable alternative to keep CO₂ in a much easier to handle liquid phase (González-López et al., 2012). This is the case given the following: a) it requires less energy and reduced transportation cost (Gris et al., 2014), b) it provides high CO₂ solubility and stable CO₂ retention (i.e., 9.6 g NaHCO₃/100 g water versus 0.1688 g CO₂/100 g water at 20 °C) (Kim et al., 2017; Perry et al., 1997). Furthermore, these bicarbonate solutions can provide the inorganic carbon requirements for microalgae growth. Since the growth rates of microalgae are influenced

¹ From: The atmosphere: Getting a Handle on Carbon dioxide. By Alan Buis, NASA's Jet Propulsion Laboratory. Carbon dioxide data is from 2009.

by the availability of dissolved inorganic carbon species in the medium (Vadlamani et al., 2017), the use of soluble carbonates species can result in a much higher carbon fixation efficiency (Adamczyk et al., 2016).

In this respect, recent research studies have reported the positive impact of bicarbonate solutions on microalgae growth, given the favourable lipid accumulation in the resulting microalgae (Chi et al., 2011, 2013; Gris et al., 2014; Kim et al., 2017; Vadlamani et al., 2017). Thus, and on this basis, an integrated process of CO₂ capture via the absorption of an enriched solution of carbonate-bicarbonates, offers the possibility of providing microalgae and benefiting from reduced liquid phase recirculating costs (Gris et al., 2014).

Concerning the light supply, one should mention that the rate of photosynthesis is a function of the irradiance to which microalgae cell compartments are exposed (Dillschneider & Posten, 2013). Thus, the light absorbed by the culture media is a critical parameter to be considered in photobioreactor design. This is also significant given that culturing microalgae in photobioreactors, may lead to unknown and variable irradiation gradients. Furthermore, when the source of irradiation is the sun, the incident light intensity is subject to the influence of daily and seasonal changes, as well as weather (Dillschneider & Posten, 2013). Hence, a significant challenge is to provide uniform irradiation intensities to all microalgae cells within the photobioreactor, with this irradiation not being affected by operational issues such as microalgae growth becoming fixed on the reactor walls (Razzak et al., 2017). Furthermore, other parameters that may influence photobioreactor performance also have to be considered, in the engineering of these units such as: a) biomass concentration, b) microalgae culture mixing, c) cell shear, d) temperature control and e) gas-liquid mass transfer (Olivieri et al., 2014).

Even though light is the driving force for photosynthesis (Dillschneider & Posten, 2013), microalgae growth and photobioreactor design have been approached without considering the efficiency of light utilization by microalgae, for inorganic carbon fixation. This key parameter is designated as Quantum Yield (de Lasa et al., 2005,

Markager, 1993). In addition, and as far we are aware of, the simultaneous investigation of microalgae carbon conversion and quantum yield efficiency during microalgae growth, is not reported in the technical literature. This lack of information limits the evaluation of microalgae growth efficiency. This becomes even more problematic in the engineering of photobioreactors, where central issues for microalgae growth optimization are the reaction rate, the visible radiation absorbed and media hydrodynamics (Razzak et al., 2017).

Given the above, the goal of present PhD research is to establish the carbon conversion and photon absorption, and as a result, the Quantum Yields, by utilizing the principles of photoreaction engineering in a novel *PhotoBioCREC* unit, using microalgae CPCC *Chlorella vulgaris* and sodium bicarbonate (NaHCO_3). It is proposed in this PhD research to study these relevant issues for microalgae growth, in the context of a microalgae growth kinetics model, applicable to a wide range of inorganic carbon concentrations.

To address these matters the following chapters are proposed for the PhD Dissertation:

Chapter 2 summarizes the state-of-the-art technologies for microalgae cultivation, the factors affecting microalgae growth, the kinetic available models, and the Quantum Yield parameter.

Chapter 3 presents the main research objectives of the PhD Dissertation.

Chapter 4, provides a detailed explanation of materials, analytical methods, and experimental setup, with details of the designed *PhotoBioCREC* unit, are provided.

Chapter 5 reports the carbon conversion, for the different bicarbonate carbon concentrations and their changes with run time. On this basis, the extent of the biochemical conversion of inorganic carbon into organic carbon by CPCC *Chlorella vulgaris*, is established.

Chapter 6 describes the implementation of Macroscopic Energy Balances and the quantification of Quantum Yields in the *PhotoBioCREC* unit. Some results reported in

Chapter 5 and Chapter 6 were published in Industrial and Engineering Chemistry Research 2020, 59 (33), 14710-14716 (Impact factor: 3.720).

Chapter 7 reports the kinetic parameters of microalgae growth under controlled mixing and radiation conditions. A kinetic model for both inorganic and organic species is proposed and validated. This chapter is based on a manuscript published in *Processes* 2021, 9, 1296 (Impact factor: 2.847).

Chapter 8 presents the scaled *PhotoBioCREC Swirl Reactor* prototype. It includes preliminary results obtained with this unit including irradiation measurements and fluid dynamics.

Chapter 9 reports the conclusions, research outcomes and future work recommendations of this PhD Dissertation.

Chapter 2

2 Literature Review

This chapter presents a review of the main concepts regarding microalgae culture, photobioreactor design and efficiency of carbon capture by microalgae processes.

2.1 Microalgae

Microalgae are algal bodies that can be observed only with a microscope due to their tiny cell size. Algae are heterogenous assemble of organisms mostly photosynthetic that produce oxygen and live in aquatic habitats. In addition, the algae lack the body and reproductive features of the land plants (Graham et al., 2009).

Microalgae can grow under different conditions since they assume many types of metabolisms, and are capable of a metabolic shift, as a response to changes in the environmental conditions (Gouveia, 2011). If microalgae grow using light as the only energy source and inorganic carbon as the carbon source, the cultivation conditions are designated as photoautotrophic (Gouveia, 2011). When grown heterotrophically, algae utilize an organic carbon source (e.g., glucose or acetate) as both a carbon source and energy source for growth (Harel & Place, 2004). In addition, microalgae can grow mixotrophically, using both light and organic carbon as the energy source, and inorganic or organic carbon as a carbon source, depending on the availability (Gouveia, 2011).

2.2 Photosynthesis in Microalgae

2.2.1 Light and Dark reactions of Photosynthesis

Plants, algae, and cyanobacteria can carry out oxygenic photosynthesis. Photosynthesis can be considered as a redox reaction driven by light energy (Mauzerall, 2013). In this reaction, carbon dioxide and water are converted to carbohydrates and oxygen (Pandey et al., 2014b). The process can be described as two sets of reactions: light reactions and dark

reactions. Figure 2.1 is a representation of the process which takes place in the chloroplast.

Under the light irradiation, light energy is converted into chemical energy that drives the conversion of CO_2 to carbohydrates. The production of both adenosine triphosphate (ATP), and the biochemical reductant nicotinamide adenine dinucleotide phosphate (NADPH_2) takes place in the photosystem II (PS II) and photosystem I (PS I) centers (Masojídek et al., 2013). The photophosphorylation reaction start with the extraction of two electrons from water once light reaches the reactions centers. These electrons are transferred through a chain of electron carriers to produce one molecule of NADPH_2 . As a product of the water splitting, O_2 is released. At the same time, protons from the stroma are transported into the lumen, which results in a pH gradient that drives the ATP synthesis, and which is catalyzed by a protein complex called ATP synthase (Masojídek et al., 2013). The reaction can be expressed as:

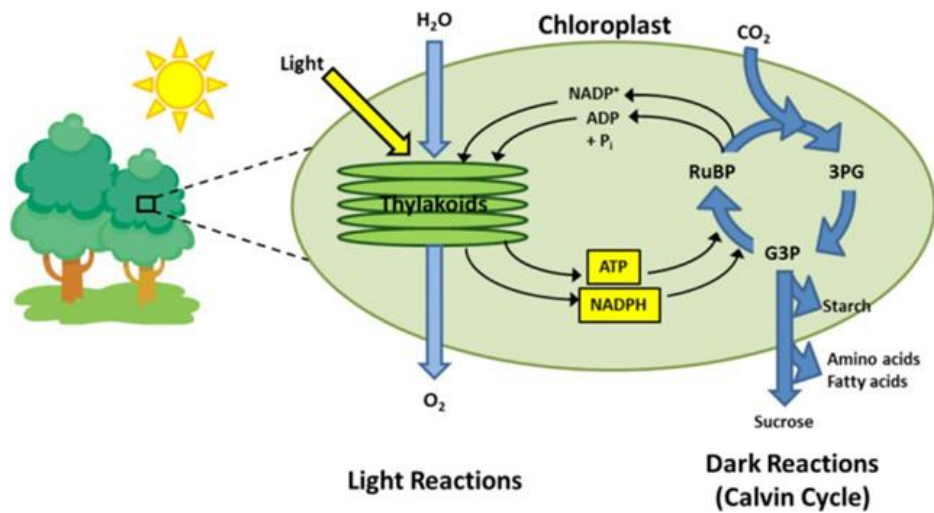
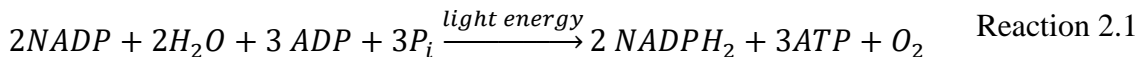
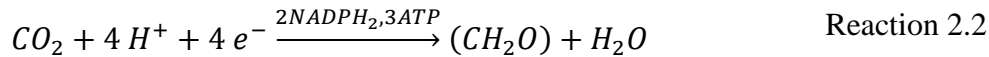


Figure 2.1 Schematic representation of the light and dark reactions of photosynthesis.

Abbreviations: RuBP = ribulose-1,5-biphosphate; 3PG = 3-phosphoglycerate; and G3P = glyceraldehyde 3-phosphate (Rasmussen & Minteer, 2014)

On the other hand, during the dark reactions, carbon dioxide fixation occurs via NADPH₂ and ATP, in the presence of enzymes. The overall reaction can be written as (Masojídek et al., 2013):



The mechanism of this reaction was developed by Calvin and Benson (1940-1950) and it is divided in four phases (Masojídek et al., 2013):

- a) Carboxylation phase: the enzyme ribulose 1,5-bisphosphate carboxylase/oxygenase (Rubisco) catalyzes the addition of CO₂ to the 5-carbon sugar named ribulose bisphosphate (Ribulose-bis-P) to form two molecules of phosphoglycerate (Glycerate-P).
- b) Reduction phase: phosphoglycerate is reduced to 3-carbon products (Triose-P) using the energy provided by ATP and NADPH₂.
- c) Regeneration phase: Ribulose phosphate (Ribulose-P) is regenerated for further CO₂ fixation. The process involved a complex series of reactions combining molecules of 3- to 7-carbon sugar phosphates.
- d) Production phase: products such as carbohydrates, fatty acids, amino acids and organic acids are synthesized.

2.2.2 Photorespiration

During photosynthesis, the conversion of organic carbon into CO₂ can proceed, catalyzed by Rubisco enzyme in a reaction designated as “photorespiration” (Long et al., 2006). This competing reaction depends on the concentration of O₂ and CO₂ (Falkowski & Raven, 2007). If the concentration of O₂ is higher than that of the CO₂ and if this is accompanied by high irradiation, the equilibrium is shifted towards photorespiration. This happens because the affinity of Rubisco enzyme to CO₂ is low (Masojídek et al., 2013).

2.3 Inorganic Carbon Supply and Uptake Mechanism

2.3.1 Sources of Inorganic Carbon

Microalgae need an enriched CO₂ source for faster growth. Considering that the concentration of CO₂ in the atmosphere is low (approximately 0.04%²), this affects its diffusion to the culture medium. Moreover, the high surface tension of water and the low mass transfer coefficient between air and the culture medium, reduces CO₂ diffusion (Thomas et al., 2016). As a result, the microalgae culture energy required, to provide sufficient carbon from atmospheric air, is high (Lam et al., 2012).

The supply of carbon to microalgae cultures can be achieved using flue gases from the combustion of fossil fuel, such as coal and oil in a power plant (Kumar et al., 2018; Vuppaldadiyam et al., 2018). This is an approach that may contribute to a near-zero carbon emission process. As well, carbon dioxide can be stored as soluble carbonates which can be supplied to microalgae culture.

2.3.1.1 Flue Gases

Flue gases are the product of combustion of fuels, which could be an inexpensive and rich source of CO₂ (Yadav et al., 2015). The produced flue gas composition is affected by the fuel source (coal, oil, natural gas) and the conditions of the combustion system (i.e., air-fuel ratio) (Thomas et al., 2016). As a result, CO₂ concentration in flue gas emissions varies from 10%-15% in coal-fired power plants, and 5%-6% in natural gas power plants (U.S. DOE 2010).

Even though flue gas can be supply directly to microalgae culture, it exposes the microalgae to extreme conditions such as high temperature, a high concentration of CO₂

² From: The atmosphere: Getting a Handle on Carbon dioxide. By Alan Buis, NASA's Jet Propulsion Laboratory. Carbon dioxide data is from 2009.

and nitrogen oxide (NOx), and the presence of inhibitory compounds such as sulfur oxide (SOx) (Pires et al., 2012). This can result in a decline in photosynthesis efficiency in microalgae, due to the low solubility of CO₂ at high temperatures (Ho et al., 2011).

Sulfur is incorporated into the plastids of the microalgae cells as sulfate. An excess of it is stored in the vacuoles, which causes a reduction in the formation of amino acids (Thomas et al., 2016). The problem associated with sulfur oxides is associated to its accumulation over time, that leads to pH reduction and a further decline of bicarbonates content of the medium (Thomas et al., 2016). Results of experiments with 50 ppm of SOx showed that there was no significant effect on the specific growth rate. However, at higher concentration of 400 ppm the pH dropped significantly (Matsumoto et al., 1997; Negoro et al., 1991).

In the case of nitrogen oxides, the main compound is nitric oxide (NO). It is considered that NO in the gaseous phase, dissolves in the culture medium and is consumed by algal cells (Matsumoto et al., 1997; Pires et al., 2012). Experiments conducted with 300 ppm of NO resulted in no growth of *Nannochloropsis sp.* and a prolonged lag phase and low growth rate for *Nannocloris sp* (Pires et al., 2012). On the other hand, experiments reported by Lizzul et al. (2014) with *Chlorella sorokiniana* showed that its growth was not affected by 50 ppm of NO in the flue gas supplied, and that the concentration of NO in the effluent gas was reduced by 95%. Thus, these results suggest that microalgae strain is a factor to consider, when using flue gas as carbon source (Lara-Gil et al. 2014; Yen et al., 2015).

2.3.1.2 Soluble Carbonates

The use of flue gas for microalgae growth presents other challenges that can be overcome with the use of soluble carbonates. When there is no land available near a power plant to use flue gases directly for microalgae growth, the gas needs to be transported, adding cost to CO₂ capture and transportation (Chi et al., 2011; Thomas et al., 2016). The compression process of CO₂ requires considerable energy. As well, temporary storage

may be needed at night (Chi et al., 2011). In this case, the capture of CO₂ in the form of soluble carbonates such as sodium bicarbonate (NaHCO₃) and sodium carbonate (NaCO₃) offers a possible solution. This could reduce the cost of transportation since the transport of aqueous bicarbonate solutions requires much less energy (Gris et al., 2014).

Figure 2.2 shows a representation of the integrated process of CO₂ capture in soluble bicarbonate/carbonate solutions. The process starts with the absorption of CO₂ from flue gases in an enriched solution of carbonate or bicarbonate. The resulting solution is provided as the carbon source to microalgae in a photobioreactor. After biomass separation, the gas-liquid phase containing the unconverted bicarbonates and CO₂ is recirculated back to the absorption unit (Gris et al., 2014).

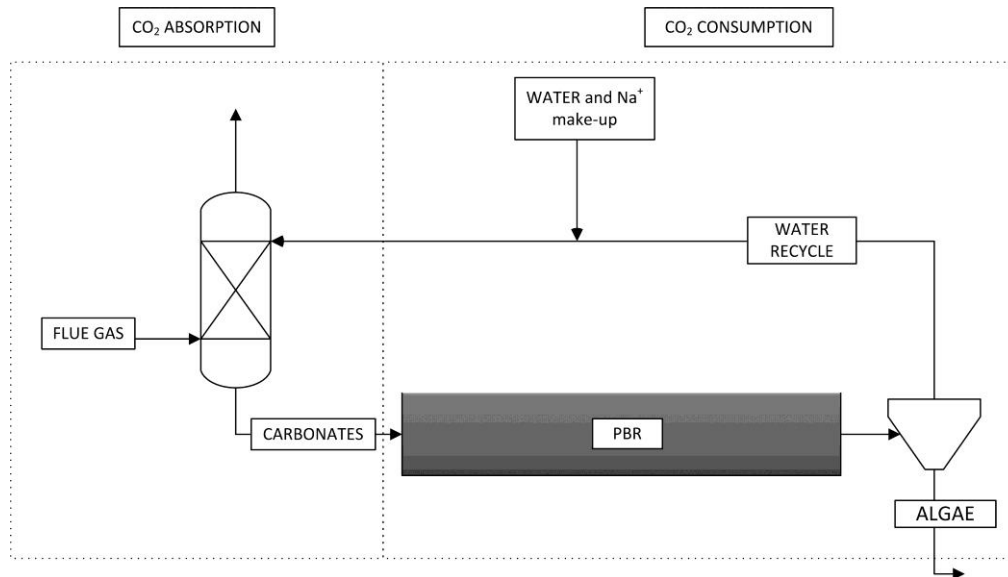


Figure 2.2 Schematic representation of CO₂ capturing from flue gas using carbonates (Gris et al., 2014).

Studies have reported that the ion bicarbonates can serve as an alternative carbon source to grow microalgae (Chi et al., 2011, 2013; Gris et al., 2014; Kim et al., 2017; Vadlamani et al., 2017). Growing microalgae with soluble carbonates has the following advantages: (1) the carbon source can be stored during winter season (considering different scenarios), (2) carbonates have higher solubility compared to CO₂, (3) the carbon source

has a longer retention time, and (4) the carbon source once dissolved as bicarbonate does not require extra energy to be spent for pumping air (Kim et al., 2017; Lam et al., 2012).

However, there is a limitation related to the tolerance of the microalgae strain to high salt concentration. The exposure of microalgae to a high level of salt can lead to the inactivation of some enzymes and eventually to growth inhibition (Kim et al., 2017; Torzillo & Vonshak, 2013).

Tu et al. (2018) studied the effect of NaHCO_3 concentration for *Chlorella* sp. LPF growth. It was reported that concentrations from 0.1 g/L to 60 g/L enhanced the growth by 42%. The growth rate was reduced by only 13%, when NaHCO_3 at 80 g/L was used. Similarly, *Chlorella vulgaris* have been cultivated with different carbon sources including CO_2 (3%), NaHCO_3 , sodium acetate and molasses which were added to the culture media with 0.5 g/day rate. It was found that the highest cell density was achieved with bicarbonates solutions as carbon source (Abedini et al., 2015).

Moreover, studies have also reported that microalgae growth under salt content can enhance lipid production. Abedini et al (2015) reported that the fatty acid content of microalgae when using bicarbonate was higher compared to when CO_2 was employed. It was also very close to the maximum achieved by sodium acetate for *Chlorella vulgaris*. Likewise, *Chlorella* sp. LPF lipid production was enhanced by the addition of NaHCO_3 (Tu et al., 2018).

The consumption of bicarbonate ion by the microalgae increases the pH of the culture, due to the release of hydroxyl ions (OH^-) (Aizawa & Miyachi, 1986). Experiments with *Dunaliella* sp. showed that when sodium bicarbonate was used as a carbon source, the pH of the medium increased up to 10 in three days of cultivation (Kim et al., 2017). One should note that pH regulation may be required, when culturing microalgae in bicarbonate solutions, and this depending on the microalgae specie's tolerance to high pH.

2.3.2 Mechanism of CO₂ Fixation in Photosynthesis

The concentration level of CO₂ in the atmosphere is near 0.04%. This low concentration is considered a limitation for the photosynthesis process. The concentration of dissolved CO₂ decreases with temperature while the solubility of CO₂ is influenced by the pH, sediment, and soil respiration, among other factors (Spalding, 2008). This results in a short- and long-term variability of available CO₂ for photosynthesis (Spalding, 2008). Therefore, photoautotrophic microorganisms evolved a mechanism to concentrate CO₂ (carbon concentrating mechanisms or CCMs). This allows them to survive at low inorganic carbon concentration in the medium (Solovchenko & Khozin-Goldberg, 2013).

Microalgae and cyanobacteria can consume both CO₂ and HCO₃⁻ through the cell membrane (Chi et al., 2011). When CO₂ dissolves in water, three inorganic carbon species are produced: CO_{2(aq)}, carbonate and bicarbonate ions. The equilibrium concentration of the various carbonate species in aqueous solution are controlled by the pH of the solutions: (a) at a pH < 4.5 free CO₂ molecules or carbonic acid H₂CO₃ (b) 4.5 < pH < 8.5: bicarbonate (HCO₃⁻) and (c) pH > 8.5: carbonate (CO₃⁻²) (Hage & Carr, 2011).

Three possibilities have been reported in the literature for carbon uptake by microalgae: (1) conversion of bicarbonates into CO₂, by using extracellular carbonic anhydrase, which can freely diffuse into the cells, (2) direct assimilation of CO₂ through the plasmatic membrane and (3) direct uptake of bicarbonates through carriers such as proteins in the membrane (Giordano et al., 2005; Huertas et al., 2000; Spalding, 2008).

Figure 2.3 reports a schematic model of an inorganic carbon transport and CO₂ accumulation process in eukaryotic algal cells. The model incorporates the possible transport of dissolved inorganic carbon in the plasmalemma and/or chloroplast envelope (Giordano et al., 2005).

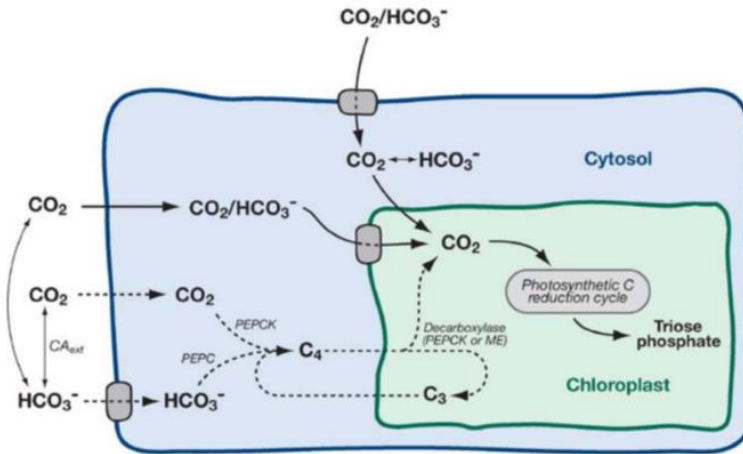


Figure 2.3 A Schematic Model for Inorganic Carbon Transport and CO₂ Accumulation Processes in Eukaryotic Algal Cells (Giordano et al., 2005).

CO₂ uptake in the eukaryotic photosynthetic microorganism is mediated by membrane transport mechanisms. For some species such as *Chlamydomonas*, the membrane is the chloroplast envelope (Kaplan & Reinhold, 1999). Two steps are considered for carbon uptake by cells: (a) the diffusion of CO₂ from the bulk solution via the unstirred layer, and (b) the subsequent mediated transfer through the chloroplast envelope (Kaplan & Reinhold, 1999). In the case of HCO₃⁻, the photosynthetic microorganism can utilize it as a source of carbon, through the enzyme that converts it to CO₂. This enzyme is called carbonic anhydrase (CA). It catalyzes the reversible interconversion of HCO₃⁻ and CO₂ (Kaplan & Reinhold, 1999).

Many photosynthetic microorganisms, both freshwater, and marine are capable of directly utilizing available bicarbonate ions (HCO₃⁻) (Colman & Rotatore, 1995; Kaplan & Reinhold, 1999). There is evidence, that when using *Scenedesmus obliquus* microalgae species, HCO₃⁻ is consumed directly by the cells. These cells can photosynthesize even when the pH is greater than 10, and bicarbonate and carbonate ions are the major inorganic carbon species (Moroney & Somanchi, 2002).

However, more research is needed to better understand the different paths for carbon uptake by microalgae, since most of the conclusions arrived at, have been made from studies with cyanobacteria.

2.4 Light and Photosynthesis efficiency

2.4.1 Light

Visible irradiation (light) is essential for microalgae growing under photoautotrophic conditions. This is the case given that microalgae obtain the needed metabolic energy, from these visible light photons. Both low and high light intensities are unfavorable for photosynthesis, leading to photo-limitation and photoinhibition, respectively (Carvalho et al., 2014). The absorption of light in photosynthetic microorganisms occurs by different pigments such as chlorophylls, phycobilins, and carotenoids with each pigment having a specific wavelength absorption band (Nwoba et al., 2019).

The rate of photosynthesis is a function of the irradiance to which microalgae cells are exposed. Irradiance is defined as the total amount of radiation reaching a point from all direction in space, at every wavelength (Dillschneider & Posten). However, the photosynthesis of microorganisms can only occur within the 400 nm - 700 nm wavelength range (visible light), designated as the photosynthetically active radiation (PAR), which corresponds to approximately 45% of sunlight wavelengths (Dillschneider & Posten, 2013; Melis, 2009). In addition, chlorophylls can capture up to 2% of the PAR. This was established in the present study, by considering the fraction of the PAR, with photons having a wavelength of 431 nm, 663.8 nm, 457.1 nm, and 643.6 nm in the absorption chlorophyll bands, as reported by Lanfer Marquez & Borrmann (2009). For this reason, the optimization of light supply is critical for microalgae growth.

Light distribution on microalgae cells depends on the type of photobioreactor and cell density. For instance, the water depth of open ponds is limited by the distance that the light can travel to reach the photosynthetic cells, which is usually between 15 cm–20 cm (Chisti, 2016).

. In high cells densities cultures however, the light path length can be limited to 2 mm given the significant absorbed or scattered light (Dillschneider & Posten, 2013).

2.4.2 Quantum Yield

Quantum yield is a measure of the efficiency of light utilization in the photosynthesis process and is expressed as units of substrate used or product formed (e.g., moles of carbon) per moles of photon (Markager, 1993).

The quantum yield of photosynthesis has to be derived from measurements of light intensity, specifically rate of absorbed energy, and rate of photosynthesis (Emerson, 1958). Among the different units used to report the rate of photosynthesis the are mol of oxygen (O_2) produced, mol of carbon used or incorporated in plant biomass per moles of photon (Markager, 1993).

Before the application of the quantum theory to photochemistry, the efficiency of photosynthesis was calculated as the number of calories stored per number of calories absorbed. Researchers who first studied the quantum yield or quantum efficiency of photosynthesis (ϕ) used the number of oxygen molecules produced per photon of light absorbed (Emerson, 1958). The expression for quantum yield reported by Emerson (1958) is presented in Equation 2.3 and in Equation 2.4:

$$\phi = \frac{\text{number of molecules converted}}{\text{number of quanta absorbed}} \quad \text{Equation 2.3}$$

$$\phi = \frac{\text{moles converted}}{\text{einsteins absorbed}} \quad \text{Equation 2.4}$$

On this basis, the maximum quantum yield (ϕ_{max}) is defined as “the largest quantity of product formed, or substrate consumed relative to the smallest number of photons absorbed” (Falkowski & Raven, 2007). Maximum quantum yields of 0.12 moles O_2 /Einsteins were reported at 680 nm for experiments with *Chlorella pyrenoidosa* at 10 °C (Govindjee et al., 1968). Emerson & Lewis (1941) reported maximum values of quantum yield for different microalgae species including *Chlorella vulgaris*. These

experiments were conducted at 10 °C with a value of 0.092 moles O₂/Einstein (Emerson & Lewis, 1941).

Razzak et al (2017) highlighted the importance of integrating radiation and kinetics in the design of photobioreactors to establish the energy efficiency. This approach has been successfully implemented in photocatalytic reactors and can be developed for microalgae culture (de Lasa et al., 2005).

2.5 Other Factors to consider for Microalgae Growth

Carbon is the main nutrient for microalgae growth. Light plays a critical role since it is the driving force for the photosynthesis process. However, there are other factors that have an influence in the growth rate of microalgae such as temperature, macronutrients for instance nitrogen and phosphorous, and micronutrients. All these factors are critical for the metabolic processes that take place during photosynthesis.

2.5.1 Temperature

Temperature impacts microalgae productivity: it influences growth and affects the solubility of CO₂ in water. Rubisco enzyme activity shows a reduction with a low temperature in microalgae growth, which affects the photosynthesis process, and carbon uptake by the cells (Zhao & Su, 2014). On the other hand, high temperatures are associated with the inhibition of the microalgal metabolic behavior, reducing the solubility of CO₂, and increasing the photorespiration intensity, which results in a reduction in the photosynthetic efficiency (Zhao & Su, 2014; Zhu et al., 2008).

Even though microalgae can grow in a wide range of temperatures, there is an optimum temperature which results in a higher growth rate. For instance, *Chlorella* can normally grow within a 5°C to 30°C range, with a 25 °C optimum (Singh & Singh, 2015). Moreover, Converti et al (2009) reported that the specific growth rate of *Chlorella vulgaris* was not affected by an increase of temperature from 25°C to 30°C. However, when the temperature increased to 38°C, the growth rate was interrupted (Converti et al.,

2009). Masahiko et al. (2000) reported the isolation of microalgae *Chlorella sorokiniana* from hot springs in Japan. These microalgae species were successfully grown in temperatures from 25 °C-40 °C.

In addition, the production of a specific microalgae component can be achieved. For example, an increase in total carotenoid and in the percentage of astaxanthin, were reported for the *Chlorococcum sp.* green algae, when temperature was increased from 20°C to 35°C under nitrogen starvation conditions (Liu & Lee, 2000).

Since photosynthesis needs light, irradiation in photobioreactor can increase the temperature of the culture. In addition, when using flue gas as a source of inorganic carbon (Chiu et al., 2011; Morita et al., 2001), the temperature must be monitored and controlled to avoid inhibition of microalgae growth.

Given the above, a system was designed to avoid temperature increasing during irradiation time in the *PhotoBioCREC* unit during experiments carried out for this research. The experimental setup is presented in Chapter 4.

2.5.2 Nutrients

Along with inorganic carbon supply, microalgae require nitrogen and phosphorous for their metabolic process. Nitrogen is an essential constituent of all structural and functional proteins in algal cells, while phosphorous mediates the energy transfer and nucleic acid synthesis (Gonçalves et al., 2017; Hu, 2004). Moreover, trace elements such as iron, cobalt, zinc, manganese among others, must be provided, due to their critical role in a variety of metabolic pathways, which involve the utilization of essential algal resources such as light, nitrogen, phosphorous and CO₂ (Andersen, 2005). It is important to highlight that the requirement of nutrients is specific for each species of microalgae.

Studies have pointed out that the use of wastewater as a source of nutrients for microalgae biomass, instead of using synthetic fertilizer, could improve the sustainability

of microalgae process as well as its economic feasibility (Abdel-Raouf et al., 2012; De Godos et al., 2009; Jutidamrongphan et al., 2015).

Nitrogen limitation has been reported to increase the lipid content, for some green microalgae. Furthermore, a low concentration of nitrogen has been shown to slow down the growth rate of microalgae. To address the role of nitrogen, researchers have been working on optimizing the cultivation time and lipid accumulation period (Abedini et al., 2015; Pandey et al., 2014b).

Regarding the nutrients, a medium recommended by the Canadian Phycological Culture Center (CPCC), University of Waterloo, was used to ensure the supply of all micro and macro nutrients required by the microalgae CPCC90 *Chlorella vulgaris*, which is the strain used in this research. Further details of the medium and its composition is presented later in Chapter 4.

2.5.3 Culture pH

The value of the pH in the culture affects the solubility of CO₂ and minerals. It also influences the metabolism of microalgae (Carvalho et al., 2014). Microalgal species have an optimal pH in the range of 7-9, but some species have an optimum pH within more acid or basic ranges (Pandey et al., 2014a). Factors such as composition and buffering capacity of the medium, temperature (affects the solubility of CO₂), amount of dissolved CO₂ and metabolic activity of the algal cells, all influences the pH of the culture (Carvalho et al., 2014).

For these reasons, the pH was monitored during microalgae growth experiments presented in this dissertation. Based on the recommended pH by the CPCC for *Chlorella vulgaris*, the pH of the culture was adjusted to 7.0. More details are given in Chapter 4.

2.5.4 Mixing

Mixing is the most important requisite for obtaining constant high yields of microalgae biomass when there are no nutrients or light limitation conditions. Mixing inside any

photobioreactor can influence the hydrodynamic stress, the photon and the gas transfer in the culture medium (Carvalho et al., 2014).

On the other hand, mixing keeps the algal cell in suspension. It eliminates thermal stratification, and allows an even nutrient distribution, while enhancing gas-liquid mass transfer to prevent oxygen accumulation (Gupta et al., 2015; Kumar et al., 2015). Moreover, mixing helps to expose the cells to light, which contributes to avoiding photo-limitation and photoinhibition, due to the enhancement of light utilization (Kumar et al., 2015).

In stirred photobioreactors, the impellers and baffles determine the effectiveness of mixing and the O₂ transfer. In air driven bioreactors, gas spargers achieve mixing and O₂ transfer (Gupta et al., 2015). In open ponds, mixing is provided by baffles and paddlewheels; circulation is another option to ensure good mixing (Gupta et al., 2015; Kumar et al., 2015).

The critical role of mixing was considered in the design of the *PhotoBioCREC* unit which results are presented in this dissertation. The use of a magnetic stirrer in addition to baffles with the designed semiconical shape of the photobioreactor provides the required mixing as later explained in Chapter 4.

2.6 Microalgal Growth

2.6.1 Phases of the growth cycle

During the growth of microalgae or any microorganism, different phases of growth can be observed as presented in Figure 2.4.

First and during the lag phase, growth rate is considered null (Monod, 1949). Different factors influence the duration of the lag phase. These factors include microalgae adaptation to the media nutrient composition and the growth phase from which the inoculum was derived (Blanch et al., 1996).

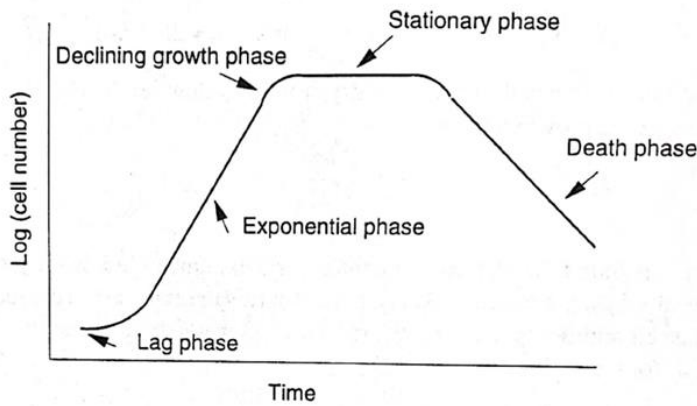


Figure 2.4 Typical growth characteristics of a microorganism in a batch reactor (Blanch et al., 1996).

Following this, there is a steady microalgae growth period, designated as the exponential phase. During this phase, cells culture progress with cell division, with cell properties considered unaltered and growth rate being constant (Monod, 1949). Once the growth phase is completed, the growth rate slows down significantly, leading to a stationary phase where growth rate is arrested. Finally, the culture phases are completed with a last one, designated as a phase where cell population number decreases (Blanch et al., 1996; Monod, 1949).

2.6.2 Growth Models

During cell division, the rate of increase of cell number can be considered proportional to the number of cells. Equation 2.5 and Equation 2.6 show the first models that were developed and used to calculate microalgae growth:

$$r_x = \mu X \quad \text{Equation 2.5}$$

$$r_x = kX(1 - \beta X) \quad \text{Equation 2.6}$$

Where r_x is the volumetric rate of increase in dry cell weight; μ (specific growth rate) and k are constants (hr^{-1}), β is a parameter with a value less than unity accounting for

growth inhibition, and X is the cell concentration expressed in terms of dry cell weight per volume.

Equation 2.5 does not include however growth limitation, leading to an inaccurate unlimited growth (Blanch et al., 1996). To overcome this, Verhulst (1844), and Pearl and Reed (1920) proposed the addition of an inhibition term, which is presented in Equation 2.6 (Blanch et al., 1996).

Monod (1949) proposed as an alternative a model that includes the effect of nutrient concentration, assuming that only one substrate (S) influences the rate of cell propagation (Equation 2.7).

$$\mu = \frac{\mu_{max}S}{K_s + S} \quad \text{Equation 2.7}$$

Where μ_{max} is the maximum specific growth rate of cells, K_s is the value of the limiting nutrient concentration, which results in a growth rate of half the maximum value.

The Monod's model as per Equation 2.7 is widely used due to its simplicity. However, a drawback of the Monod Model is that it cannot described microalgae growth inhibition, due to high substrate concentration or microalgae growth under nutrient absence (E. Lee et al., 2015).

As alternatives, other models have been proposed to account for these two conditions, such as the Andrew Model (1968) and the one by Martínez Sancho et al (1997). Regarding the latter, the addition of parameters is recommended to account for (a) the effect of nutrient absence, (b) the growth limited by low nutrient, and (c) the growth inhibit by high nutrient concentration (E. Lee et al., 2015).

2.7 Microalgal Cultivation Systems

Different photobioreactor configurations and cultivation strategies for biomass production have been reported. Microalgae can grow as suspended cultures and as

immobilized cultures. As suspended cultures, open ponds and closed reactors with their different configurations are listed. Matrix-immobilized microalgae and algal biofilms are considered (Christenson & Sims, 2011).

In general, photobioreactors can be classified as indoor or outdoor systems, as well as open or closed systems. Raceways and open ponds are the most common open systems. On the other hand, closed systems include vertical columns such as annular and airlift photobioreactors with its different configurations (internal loop, internal loop concentric and external loop). Moreover, there are tubular photobioreactors with tubes arranged in multiple possible orientations such as vertical, horizontal, inclined, spiral and helicoidal. One should also mention the existence of flat panel photobioreactors. Each configuration has advantages and disadvantages (Acién Fernández et al., 2013; Dillschneider & Posten, 2013; Kumar et al., 2015).

2.7.1 Open Systems

Raceway ponds are the most used open system for algae cultivation since the 1950s. A raceway pond is an open outdoor pond, as shown in Figure 2.5, with a shallow recirculation channel and a paddlewheel for mixing and recirculate the culture (Shi, 2014). Construction and material cost are low for raceway reactors. As well, the energy requirements for mixing are low. Furthermore, since solar energy is used for photosynthesis, there is no cost associated to providing energy (Acién Fernández et al., 2013).

However, raceway and open ponds, in general, required a relatively large area (Chisti, 2016). The efficiency of light utilization is low, and the gas-liquid mass transfer is poor (Duan & Shi, 2014). Moreover, there is no temperature control, the risk of culture contamination is high (i.e., air pollution, heavy metal accumulation, insect larvae), and the final microalgae density is low (Acién Fernández et al., 2013; Kumar et al., 2015).

Even though raceways have the problems mentioned above, they are the most popular devices used for microalgae cultures, because their potential for commercial application

is greater than in other systems. In 2015, large scale production of microalgae took place in raceway reactors, and it corresponded near to 95% of the total algal worldwide output. *Spirulina* and *Dunaliella* were some of the strains cultivated in raceways ponds (Kumar et al., 2015).

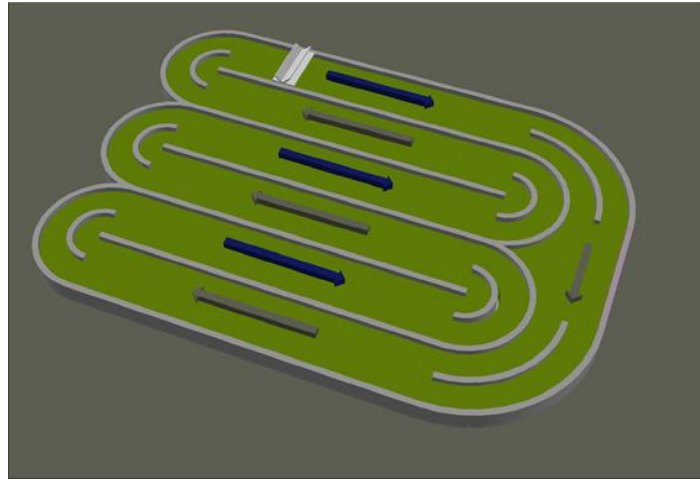


Figure 2.5 Schematic diagram of a Raceway Pond with arrows showing the recirculation of the cultured algae and water (Razzak et al., 2017)

Furthermore, the use of open systems for carbon sequestration is not recommended because of the deficient time of sparged gas into the culture, which provides very little time for the algal biomass to fix the CO₂ from the flue gas (Kumar et al., 2011). To overcome this challenge, Vadlamani et al., (2019) reported that the use of NaHCO₃ in open ponds led to higher biomass and lipid productivities, compared to the use of CO₂ in open ponds.

2.7.2 Closed systems

Closed photobioreactors were developed to overcome the problems associated with open pond systems. They can be located indoors, provided with artificial light or natural light via light collection and distribution systems as shown in Figure 2.6. Direct sunlight can be used when they are located outdoors (Shi, 2014). In order to capture solar light,

materials must be transparent with long shelf lives such as polymethyl methacrylate, borosilicate glass or simply plastic films (Dillschneider & Posten, 2013).

In these systems, the risk of contamination is low due to reduced exposure between the culture and the atmosphere. In addition, control of operating conditions is more feasible in closed systems and water loss due to prevention of evaporation (Dillschneider & Posten, 2013).

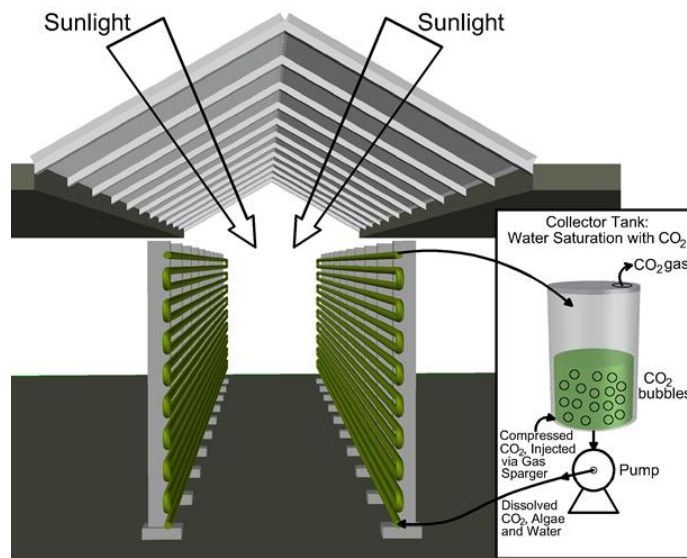


Figure 2.6 Schematic diagram of a closed microalgae system with continuous recirculation of suspended algae (Razzak et al., 2017).

Many designs and configurations of closed photobioreactors have been studied. The most common are vertical column photobioreactor, tubular photobioreactor, and flat panel photobioreactor.

2.7.2.1 Tubular Photobioreactor

A tubular photobioreactor is the most used closed system. It is constituted by solar collector tubes, arranged in multiple possible orientations such as vertical, horizontal, inclined, spiral, helicoidal and variations of these (Carvalho et al., 2014). Culture flows and recirculates by aeration or mechanical pumps (Acién Fernández et al., 2013).

Aeration and oxygen removal usually take place in specific gassing and degassing compartments, while gassing at several points along the tubular track is possible. The flow regimen within the tubes can be regarded as plug flow with a minimal backward and forward mixing. Tubular reactors can attain high biomass productivities with a small tube diameter (Dillschneider & Posten, 2013; Wang et al., 2012). The significant disadvantages of this photobioreactors are related to the accumulation of excessive dissolved oxygen and the excessive power consumption for liquid impulsion (Acién Fernández et al., 2013).

2.7.2.2 Flat panel Photobioreactor

Flat panels consist of joined transparent plates to store the culture, on which the culture is illuminated from one or both sides. The dimensions of this type of photobioreactor are diverse, with heights lower than 1.5 m and widths less than 0.10 m being preferred, and this to avoid the use of high mechanical resistance materials (Acién Fernández et al., 2013).

Flats panels are characterized by a high surface area to volume ratio and open gas disengagement systems. Agitation is provided by bubbling air or using a motor (Shi, 2014). High photosynthetic efficiencies have been reported for flat panel photobioreactors; given that they are suitable for mass cultures of algae. Compared to horizontal tubular reactors, the accumulation of dissolved oxygen concentration is relatively low in flat panel photobioreactors (Carvalho et al., 2014).

2.7.2.3 Vertical column Photobioreactor

Vertical tubular photobioreactors were among the first closed algal biomass culture systems described in the literature, but their high cost discouraged their use (Carvalho et al., 2014). The first design of this type of bioreactor, known as a bubble column, consists of a cylindrically shaped transparent vessel. The bioreactor is aerated by a gas distributor feeding gas bubbles with controlled diameter and thus providing high gas/liquid exchange area unto the system (Dillschneider & Posten, 2013). Gas sparging provides

good mixing, enhances CO₂ mass transfer and removes the O₂ produced during photosynthesis (Kumar et al., 2011).

Another type of vertical photobioreactor is designated as the airlift PBR. This unit differs from bubble columns, given it includes two separate and interconnected zones: (a) the riser (up flow section), and (b) the downcomer (downflow section). Gas is sparged in the riser section, resulting in a gas holdup. The circulation of the liquid phase occurs due to the density difference between the liquid in the riser and in the downcomer. This leads to close loop circulation which provides enhanced exposure of the cells to visible light (Gupta et al., 2015). Vertical column PBRs with mixing caused by gas bubbles are considered a valuable option given they provide high volumetric gas transfer coefficients and little culture shear stresses (Wang et al., 2012).

2.8 Genetic Engineering of Microalgae

The optimization of strains and expansion of genetic toolsets for manipulating the strains into producing high yields of target products, is a possible route towards microalgae process scale up (Sproles et al., 2021). Most of the studies in genetic engineering of microalgae have been carried out for *Chlamydomonas reinhardtii*, which is considered a model organism for the development of molecular tools for strain selection (Talebi et al., 2013).

Efforts have been localized on targeting specific parts of metabolic pathways within photosynthetic microorganisms' cells to change the flux of metabolites towards a desired product (Sproles et al., 2021). Metabolic pathways can be modified by overexpression or silencing of certain genes to achieve higher biomass yield and desired products such as fatty acids, a key feedstock for biofuel production (Fayyaz et al., 2020., Sproles et al., 2021).

Chlorella vulgaris metabolic pathway was modified by overexpressing an endogenous ω-3 fatty acid desaturase gene driven by its own promoter to synthesize α-linolenic, a polyunsaturated fatty acid (Norashikin et al., 2018). In addition, the genetic

transformation of *Chlorella vulgaris* through electroporation has been reported by Kumar et al. (2018).

2.9 Microalgae Biomass Separation Process

Once microalgae growth cycle is completed, biomass must be separated from water to recover the desired product. The high-water content of microalgae culture media, the small size of algal cells, in addition to low biomass concentration, makes the harvesting process costly and compromises its economic feasibility (Molina Grima et al., 2013; Razzak et al., 2017). Examples of dewatering process includes coagulation and flocculation as a step prior to flotation and sedimentation. Centrifugation and filtration are also used, among others (Molina Grima et al., 2013).

Figure 2.7 reports a biomass-water separation process representation. Once the dewatering is concluded, the following steps, depending on the final product, may include the dehydration of biomass which adds up to the cost of the biomass processing (Molina Grima et al., 2013).

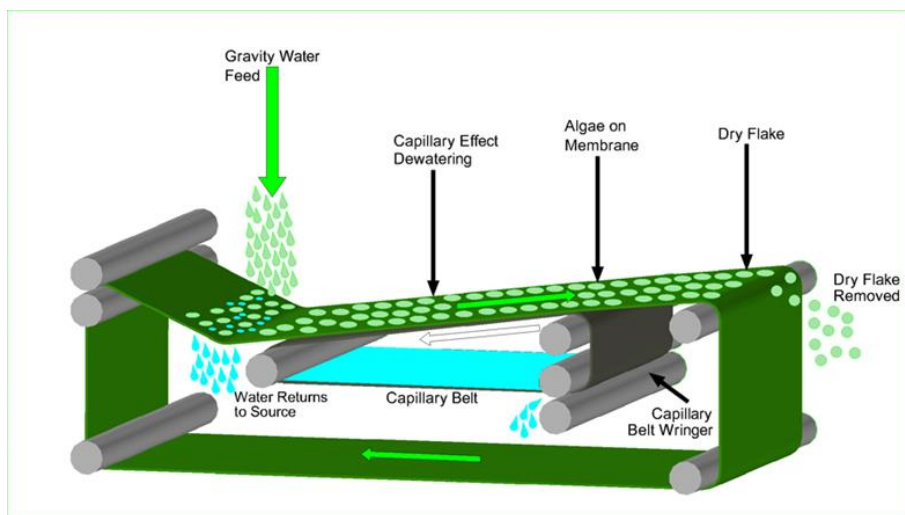


Figure 2.7 Schematic diagram of an algae culture dewatering process (Razzak et al., 2017).

2.10 CO₂ Capture by Microalgae

Different authors have reported the use of microalgae for CO₂ capture using either gaseous CO₂, flue gases and sodium bicarbonate. Table 2.1 presents a summary of some of the main contributions highlighting algae species, inorganic carbon source, conditions of pH and temperature, carbon conversion and the evaluation of Macroscopic Radiation Energy Balances (MREB) for establishing the Quantum Yield efficiency (QY).

Among the different species of microalgae, *Chlorella vulgaris* has been widely used to investigate carbon fixation. The use of soluble bicarbonates had been tested in *Chlorella vulgaris*, *Dunaliella salina*, *Dunaliella tertiolecta*, and *Chlorella sp.* Different temperatures and pH makes difficult a comparison in the carbon conversion. Despite the high CO₂ removal reported in some cases (Yeh et al., 2010, Lam & Lee, 2013), these values have been determined without considering the actual organic carbon formation. In addition, the application of radiation energy balances for establishing the quantum yield efficiencies are absent in all studies listed on Table 2.1.

Table 2.1 Microalgae Culture Species for CO₂ Capture Reported in the Technical Literature with the following reported: a) Inorganic carbon source, b) pH, c) Temperature, d) Carbon conversion, e) Macroscopic Radiation Energy Balances.

Author	Algae Species	Inorganic carbon source	Conditions of pH and Temperature (T)	Carbon conversion	MREB for QY
Keffer & Kleinheinz (2002)	<i>Chlorella vulgaris</i>	CO ₂	pH=9 room temperature (value not reported)	74% ¹	Not established
de Moraes & Costa (2007)	<i>Chlorella kessleri LEB 15</i> <i>Chlorella vulgaris LEB 12</i> <i>Scenedesmus obliquus LEB 22</i> <i>Spirulina sp.</i>	CO ₂	pH not controlled for <i>C. vulgaris</i> pH= 6.5-8.6 temperature reported not reported	Not reported	Not established
Yeh et al. (2010)	<i>ESP-31 Chlorella vulgaris</i> (Taiwan)	NaHCO ₃	pH: 5.8-11.9 not controlled T=25 °C	100%-88.3% ²	Not established
Lam & Lee (2013)	wild-type <i>Chlorella</i>	CO ₂	pH=4 T: 25-28 °C	CO ₂ removal efficiency ³ :1.5-	Not established

	<i>vulgaris.</i>			92%	
Lam & Lee (2013)	wild-type <i>Chlorella vulgaris</i>	NaHCO ₃	pH=4 and pH=8.5 T: 25-28 °C	CO ₂ removal efficiency ^{3:} 16.1-99%	Not established
(Kumar et al., 2014)	<i>Chlorella sorokiniana</i>	Flue gas	pH= 2.0- 8.0 not controlled T= 25 to 40 °C	CO ₂ removal efficiency ^{1:} 4.1%	Not established
Lohman et al. (2015)	<i>Chlorella vulgaris</i> (UTEX 395)	NaHCO ₃ , KHCO ₃ , NH ₄ HCO ₃ , Na ₂ CO ₃)	Maximum pH from 8.1-9.9 depending on carbon source T=24 C	Not reported	Not established
Abedini et al. (2015)	<i>Chlorella vulgaris</i> CCAP (211/19)	CO ₂ NaHCO ₃	pH not reported T= 25 °C	Not reported	Not established
Adamczyk et al. (2016)	<i>Chlorella vulgaris</i> <i>Nannochloropsis gaditana</i>	CO ₂	pH=7 T=25 °C	Not reported	Not established
Mokashi et al. (2016)	<i>Chlorella vulgaris</i>	NaHCO ₃	Temperature and pH not reported	Not reported	Not established
Kim et al (2017)	<i>Dunaliella salina</i>	CO ₂ (0.04%) +NaHCO ₃	pH= 8.0 (controlled) T=30 °C	91.4%	Not established
Kim et al. (2017)	<i>Dunaliella salina</i>	CO ₂	pH=8 (controlled) T=30 °C	3.59% ⁴	Not established
Zhang et al. (2019)	<i>Dunaliella tertiolecta</i> <i>Chlorella sp.</i>	NaHCO ₃	pH not controlled maximum pH=9.78 T= 25 °C	Not reported	Not established
Yadav et al. (2021)	<i>Chlorella vulgaris</i>	NaHCO ₃ /NaCl	pH=7.5 T=25 °C	0.5% ⁴	Not established

¹Based on concentration of CO₂ in the influent and effluent stream.

²Based on initial and final concentration of NaHCO₃.

³CO₂ removal efficiency: total biofixed CO₂/total input CO₂.

⁴Calculated from TOC, initial concentration of NaHCO₃, or CO₂, based on reported results.

Given the above-described lack of information, this PhD dissertation was planned to consider the design of a new *PhotoBioCREC* reactor allowing the simultaneous investigation of carbon conversion and quantum yield efficiencies of microalgae growth using soluble bicarbonates. As well, and in order to have results allowing PhotoBioCREC reactor scale up, with the anticipated photon utilization efficiencies, a kinetic model was considered to be established. It was the ultimate goal of this study to be able to describe organic carbon species (microalgae) and inorganic carbon species (sodium bicarbonate) changes at various irradiation time, with this data being extrapolatable to a scaled photobioreactor. This original approach has not been reported in the technical literature.

2.11 Conclusions

- Microalgae growth with soluble carbonates such as sodium bicarbonate, has the potential to overcome the limitations of low mass transfer and high energy input, associated with direct CO₂ feeds.
- Carbon content in microalgae culture media and visible light can be considered the primary factors affecting microalgae growth, and this considering other parameters such as nutrients, pH and temperature are carefully controlled.
- Quantum yield is a critical parameter to determine the efficiency of the microalgae culture process and has to be considered as key quantification parameter for biochemical fixation of CO₂.
- Photobioreactor design still offers challenges to make of this technology a suitable one for carbon dioxide uptake by microalgae, with a high efficiency and competitive cost.

Chapter 3

3 Research Objectives

The main goal of this research is to establish a new photobioreactor design unit (*PhotoBioCREC*) for microalgae culture, based on the exposure of microalgae cells, to a visible radiation field, during cultivation time.

3.1 Specific Objectives

- To design and implement a *PhotoBioCREC* cell unit for extended operation, with the following features: a) High mixing of the culture media, b) Undisturbed photon transmission to the culture, through the unit cell walls, c) Easy implementation of photon balances and quantum yields.
- To develop experiments in the designed unit, with microalgae CPCC 90 *Chlorella vulgaris*, growing with different sodium bicarbonate concentrations. This research follows the decay of inorganic carbon, the formation of total organic carbon and the irradiation transmittance.
- To determine the biochemical carbon conversion of soluble bicarbonates, by CPCC90 *Chlorella vulgaris*, using total organic carbon as an indicator.
- To establish Quantum Yield efficiency, on the basis of photon absorption determined by macroscopic energy balances in the *PhotoBioCREC* unit.
- To develop a kinetic model for the inorganic carbon consumption of sodium bicarbonate and the formation of total organic carbon using microalgae CPCC90 *Chlorella vulgaris*.
- To validate the developed model for microalgae growth kinetics, by comparing it with data obtained from experiments, carried out in the *PhotoBioCREC* unit, with CPCC90 *Chlorella vulgaris* and sodium bicarbonate nutrient.
- To establish a possible design for a scaled *PhotoBioCREC* prototype, based on a flow swirling principle, adequate for larger scale microalgae cultures, with its demonstration being effected via fluid dynamic and irradiation experiments.

Chapter 4

4 Materials and Methods

This chapter describes the materials used, and the analytical methods employed, in the present research, in order to achieve the proposed research goals described in Chapter 3.

4.1 Microalgae Strain

The microalgae strain selected for the research is the green microalgae CPCC90 *Chlorella vulgaris* obtained from the Canadian Phycological Culture Centre (CPCC) of the University of Waterloo, Canada. These microalgae species were chosen for experiments in the *PhotoBioCREC* unit since *Chlorella vulgaris* was found remarkably resistant to various culture conditions (pH, mixing, temperature), and contamination with other microalgae species (Sa et al, 2014).

4.2 Growth media

4.2.1 Modified Bold Basal Medium (MBBM)

The Modified Bold Basal Media used for all experiments, was obtained from Canadian Phycological Culture Center sterile and was ready to be used. The medium was prepared based on the composition reported by Stein (1973). Table 4.1 and Table 4.2 report the macro and micro-nutrients, used for the media preparation, respectively.

Table 4.1 Modified Bold Basal Media (Stein, 1973).

Substance	Stock solution	mL/Litre
KH ₂ PO ₄	8.75 g/500 mL	10 mL
CaCl ₂ •2H ₂ O	12.5 g/500 mL	1 mL
MgSO ₄ •7H ₂ O	37.5/500 mL	1 mL
NaNO ₃	125 g/500 mL	1 mL
K ₂ HPO ₄	37.5 g/500 mL	1 mL
NaCl	12.5 g/500 mL	1 ml
Na ₂ EDTA•2H ₂ O	10 g/L	1 mL
KOH	6.5 g/L	
FeSO ₄ •7H ₂ O	4.98 g/L	1 mL

H ₂ SO ₄ (concentrated)	1 mL/L	
Trace metal solution	See Table 2	1 mL
H ₃ BO ₃	5.75 g/500 mL	0.7 mL

Table 4.2 Trace Metal solution (Stein, 1973)

Substance	g/Litre
H ₃ BO ₃	2.86
MnCl ₂ •4H ₂ O	1.81
ZnSO ₄ •7H ₂ O	0.222
Na ₂ MoO ₄ •2H ₂ O	0.390
CuSO ₄ •5H ₂ O	0.079
Co(NO ₃) ₂ •6H ₂ O	0.0494

4.2.2 Inorganic Carbon Source

Sodium bicarbonate (NaHCO₃) was added as the inorganic carbon source, in all experiments, at four different nominal concentrations of 18 mM, 28 mM, 40 mM and 60 mM. The actual concentrations employed, and their standard deviations are reported in Table 4.3.

Table 4.3 Nominal and Experimental Concentrations of NaHCO₃ used in the Experiments.

Nominal Concentration (mM)	Actual Concentration (mM)
18	18.3 ± 1.4
28	28.8 ± 1.4
40	39.7 ± 0.5
60	56.45 ± 4.4

The levels of NaHCO₃ concentrations were selected based on Mokashi et al., (2016) results. This study reported the effects of 3 mM, 6 mM, and 12 mM concentrations of sodium bicarbonate on *Chlorella vulgaris*. Results obtained showed that the specific growth rate and the biomass concentration was higher for experimental runs with 12 mM sodium bicarbonate. In addition, Chun-Yen et al., (2010) tested concentrations of sodium bicarbonate ranging from 1.2 mM to 24 mM, on *Chlorella vulgaris C-C*. These authors reported a higher growth rate at 18 mM, with a 24 mM concentration showing a 3.9%

lower growth than the maximum rate reported for 18 mM. As a result, and consistent with the bicarbonate concentration levels selected by others, 18 mM, 28 mM, 40 mM and 60 mM were chosen for the present PhD research studies.

4.3 Experimental Setup

4.3.1 PhotoBioCREC Unit

A *PhotoBioCREC* unit was designed at the Chemical Reactor Engineering Center (CREC) at the University of Western Ontario. The 200 mL capacity unit was made of acrylic plastic using 3D printing. Four vertical baffles were included in the design. The *PhotoBioCREC* has a quartz window in one wall for irradiation measurements. The *PhotoBioCREC* was exposed to a cool white fluorescent lamp radiation on one side of the unit walls (the one opposite to the quartz window) and was placed over a stirrer plate.

Figure 4.1 describes *PhotoBioCREC* unit which has a unique photobioreactor design that optimizes the exposure of microalgae cells to photons, and consequently, their growth. Mixing is provided with a cross magnetic stirrer, located in the bottom unit section. This is complemented with vertical baffles which help to increase both mixing and turbulence.

Additionally, the *PhotoBioCREC* reactor has a semi-conical shape in the lower section, permitting the development of a vortex flow and counteracting at the same time, the formation of dead zones. The unit was made out of plexiglass, which transmits most of visible light, with an 0.5% material absorbance in the prototype walls (Altuglas International, 2016). This small plexiglass absorbance on the unit walls is considered critical for efficient microalgae culture.

Furthermore, a quartz window located in the center of the cell, allows irradiation measurements, taken with a fiber optic-spectrophotometer system, at various stages of microalgae growth. In addition, gamma alumina particles (0.3 g) of 1-2 mm diameter were added to the culture system to keep the reactor walls clean.

The system was complemented with a ventilation system to control the temperature during the experiments.

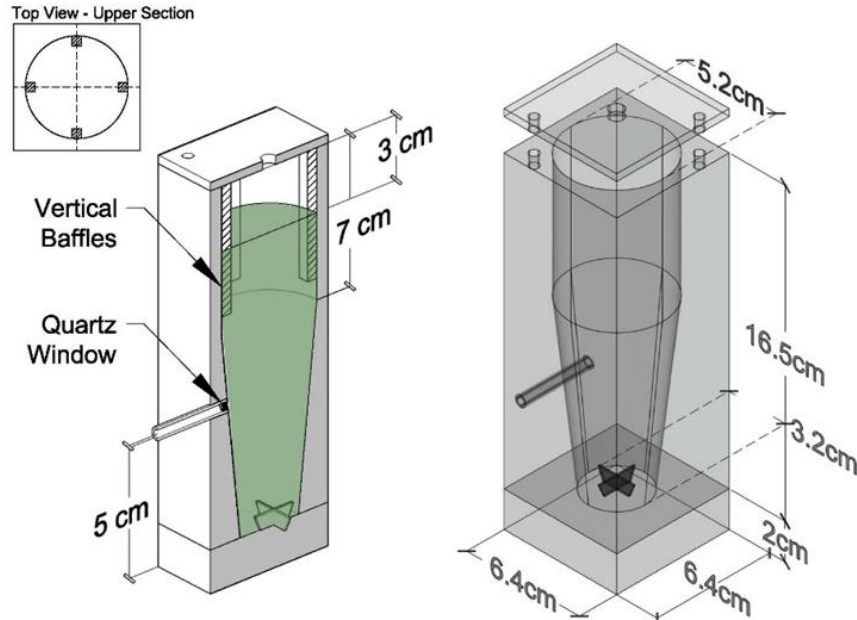


Figure 4.1 Schematic Description of the *PhotoBioCREC* Unit. Left: Longitudinal cross section showing the microalgae culture level, the baffle positions and the fiber optic conduit placed at 5cm from the bottom, for irradiation measurements with a spectrophotoradiometer. Right: Various photobioreactor dimensions (Cordoba-Perez & de Lasa, 2020).

4.3.2 Experiments in the *PhotoBioCREC* Unit

CPCC 90 *Chlorella vulgaris* was grown in a MBBM with four different nominal concentrations of NaHCO₃, ranging from 18 mM to 60 mM, in a 175 mL working volume. First, 157.5 mL of MBBM was added to the *PhotoBioCREC* unit. This was followed by the addition of the 17.5 mL of inoculum cells (10% of the liquid volume). Following this, the total initial average carbon concentration was quantified to be of 1.9 mM \pm 0.4 mM. After this step, the corresponding mass of sodium bicarbonate was added, and mixed for 15 minutes, to ensure that all NaHCO₃ was dissolved. A sample was taken

to quantify the initial inorganic carbon concentration. The pH was adjusted to 7.0 every 24 hours, with HCl 1.0 M and NaOH 1.0 M, as required.

Irradiation was supplied using cool white fluorescent lamp for 12 hours, followed by a 12-hour dark cycle. The average temperature recorded in the *PhotoBioCREC* unit during experiments was $24.3^{\circ}\text{C} \pm 0.5^{\circ}\text{C}$. The culture growth was monitored through the quantification of organic and inorganic carbon, the pH and transmission radiation measurements. Mixing was provided with a magnetic stirrer at 700 rpm. The experiments ran from 8 to 13 days, depending on the initial concentration of NaHCO_3 used. Samples were taken every 24 hours. Three experiments were conducted for each concentration of NaHCO_3 . Furthermore, average values and their standard deviations (SD) were reported.

Photos of the *PhotoBioCREC* prototype with microalgae CPCC90 *Chlorella vulgaris* are presented in Figure 4.2.

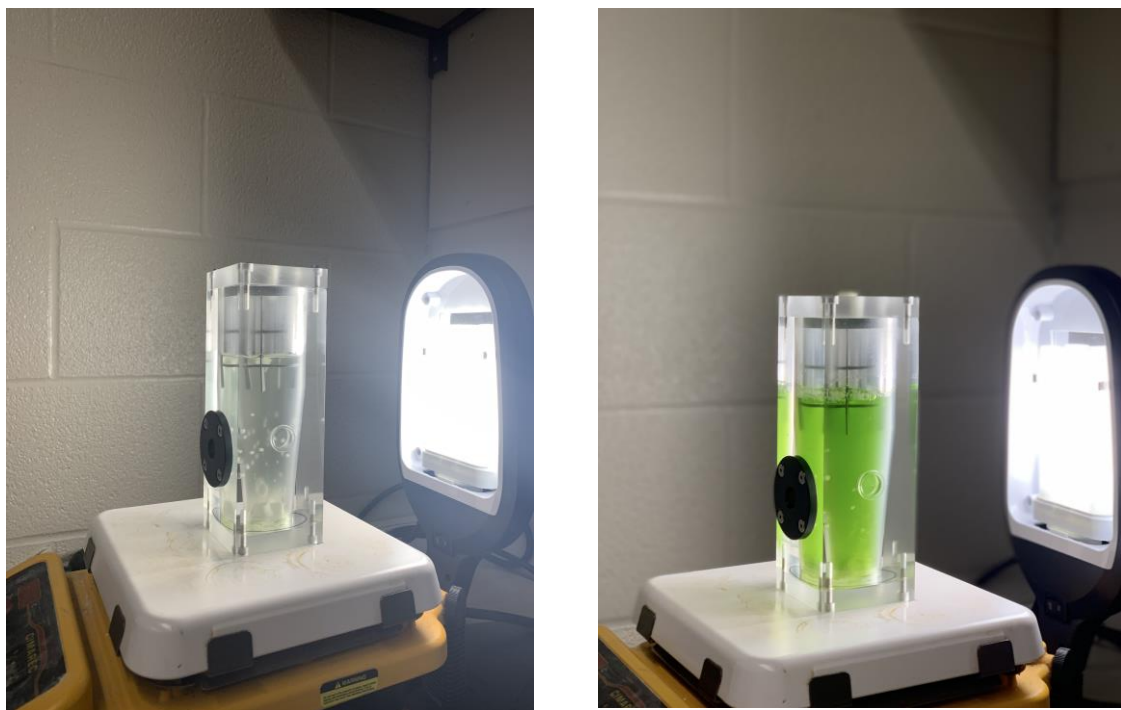


Figure 4.2 Different stages of CPCC90 *Chlorella vulgaris* growth in the *PhotoBioCREC* unit.

4.4 Analytical Methods

4.4.1 Total Organic Carbon (TOC)

The quantification of the total organic carbon was conducted using a TOC-Shimadzu Analyzer VCPH. Two collected 13 mL liquid samples, were pretreated with HCl 2.0 M in order to decrease the pH to 2.0. The two samples were sparged with nitrogen for 10 minutes, to eliminate inorganic carbon. After sparging, the sample was introduced in the autosampler Shimadzu ASI-V, to quantify the concentration of organic carbon in mg/L.

4.4.2 Inorganic Carbon Concentration

The determination of inorganic carbon concentration was performed using the derivative plot (Hage & Carr, 2011) titration, with a digital pH-meter Thermo Scientific Orion Star. Solution samples of 10 mL were titrated with 0.001M HCl while the volume (V) of the acid and the corresponding pH was recorded. The pH versus volume data was used to calculate the first derivative dp_H/dV . These derivative values were plotted as a function of HCl volume used, with the sharp peak in the plot corresponding to the end of the titration. The calibration of the HCl solution was conducted with sodium carbonate (Na_2CO_3). To avoid the interference of CO_2 in the determination of the titration end point, a methyl red indicator was added to the samples. When the colour changed to yellow, the samples were boiled for 1 minute, to eliminate the formed CO_2 . After the samples were cooled down, HCl was added to determine the true end point (Hage & Carr, 2011).

4.5 Irradiation Measurements

Irradiance measurements were taken using a StellarNet EPP2000C-25 LT16 Spectroradiometer (StellarNet, Inc) via an optical fibre cable, coupled to a photosensor. The optical fibre was housed in a stainless tube with the sensing end placed at the edge of the photobioreactor wall. This allowed one to take irradiance measurements with a wide optical angle.

Irradiance transmittance was recorded, for wavelengths ranging from 400 nm to 700 nm, at every 0.5 nm, every 24 hours. Figure 4.3 shows the fluorescent lamp spectrum. The highlighted green zones show the fraction of the spectrum where the chlorophyll displays absorption wavelengths (Lanfer Marquez & Borrmann, 2009). These absorption wavelengths are considered in the present study for quantum yields calculations.

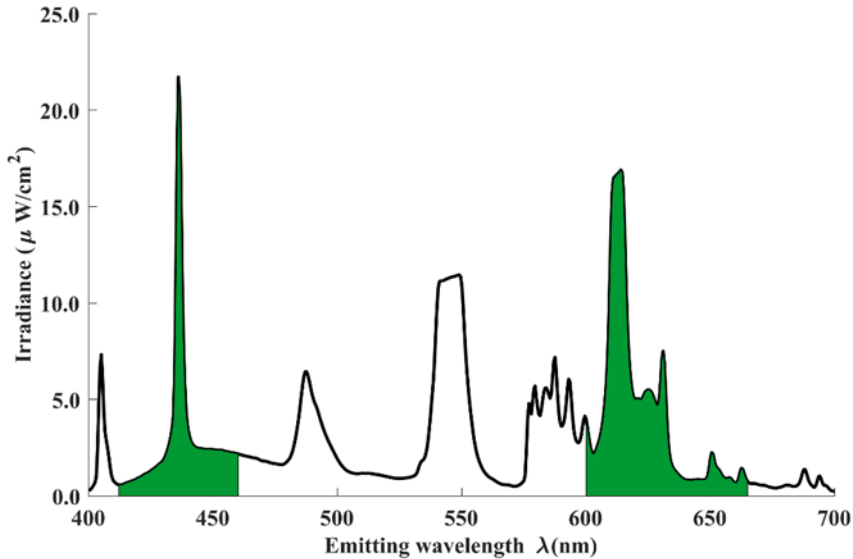


Figure 4.3 Irradiation Spectrum for Fluorescent Lamp. Zones highlighted in “green” describe the fraction of the spectrum where chlorophyll displays absorption wavelengths, which are included in quantum yield calculations (Cordoba-Perez & de Lasa, 2020)..

4.6 Algal Biomass Characterization

4.6.1 Elemental Analysis

The characterization of microalgae was achieved through the analysis of the cells of microalgae, by quantifying its elements, using combined elemental analysis, and Energy Dispersive X-ray Spectroscopy (EDX). To quantify carbon, hydrogen, nitrogen, and sulfur atomic element weight fractions in microalgae centrifugation was employed. To accomplish this, three centrifugation cycles were performed to remove any nutrients (Rosa et al., 2015). Following centrifugation and washing, the biomass was freeze dried

to keep an unaltered sample, before proceeding to analysis quantification. Figure 4.4 reports an SEM-EDX image. EDX analysis allowed to establish the elemental microalgal composition (C, N, O, H, S) which were used to determine later in Chapter 7 (Section 7.6), the biomass elemental formula.

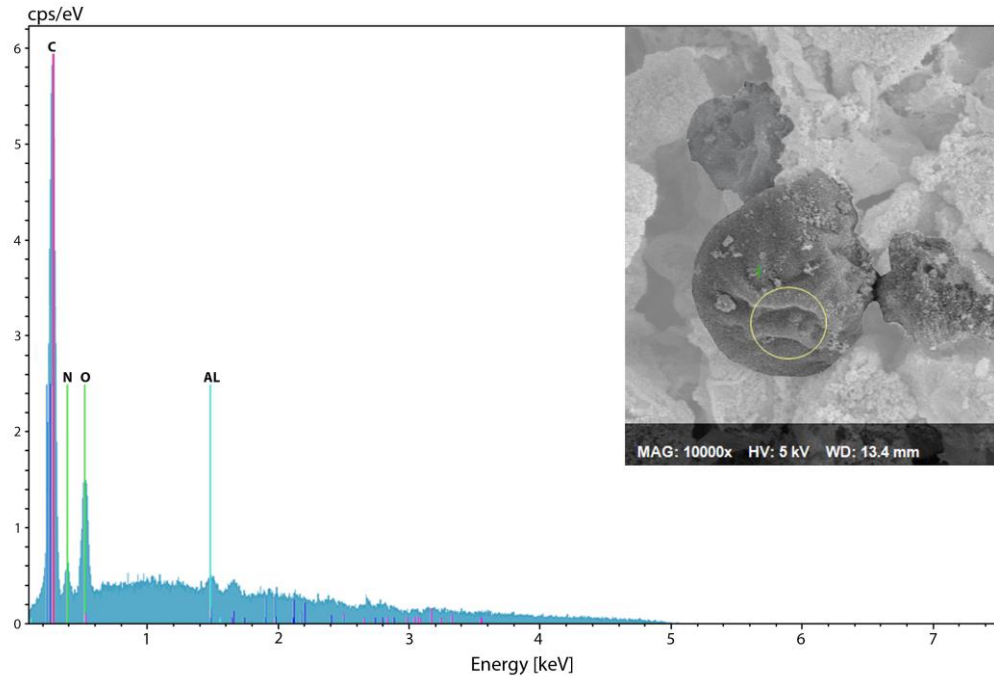


Figure 4.4 CPCC90 *Chlorella vulgaris* Cells Analysis with a) EDX and b) SEM. Samples correspond to a 12-day cultivation time and grown with nominal concentration of 60 mM of NaHCO₃.

4.6.2 Microalgae cell image analysis

The CPCC 90 *Chlorella vulgaris* was analyzed using a microscope Z1 Imager by Zeiss. Cell sizes were determined in the culture growth micrographs, utilizing a consistent 0 degrees direction, with this direction being used to define the microalgae cell size. This was complemented with a Scanning Electron Microscope (SEM) analysis. Sample preparation for SEM was based on the method reported by Percopo et al., (1997). This involved treating the samples with 1% glutaraldehyde (in MBBM) for 2.5 days at 4 °C. The resulting cells were washed with a MBBM buffer. Biomass was then treated with

osmium vapour for 1 hour. Following this, the filtered biomass was rinsed with water, to eliminate osmium. It was then dehydrated with ethanol, at different concentrations (30% to 100%). The ethanol dehydrated samples were dried using a Critical Point Dryer, followed by the needed tape coating for SEM analysis.

A typical SEM image is reported in Figure 4.4 (Section 4.6.1). Furthermore, in Figure 4.5 CPCC90 *Chlorella vulgaris* cell's shapes are also shown, with a quasi-spherical/ellipsoidal shape being observed. One can also notice that culture cells display a cell size distribution, consistently falling in the 4.0 to 6.0 μm size range, with a $\pm 0.8 \mu\text{m}$ SD, as shown in Figure 4.6. This cell sizes agree well with 2-10 μm cell sizes for *Chlorella vulgaris* reported by others (Sa et al., 2014).

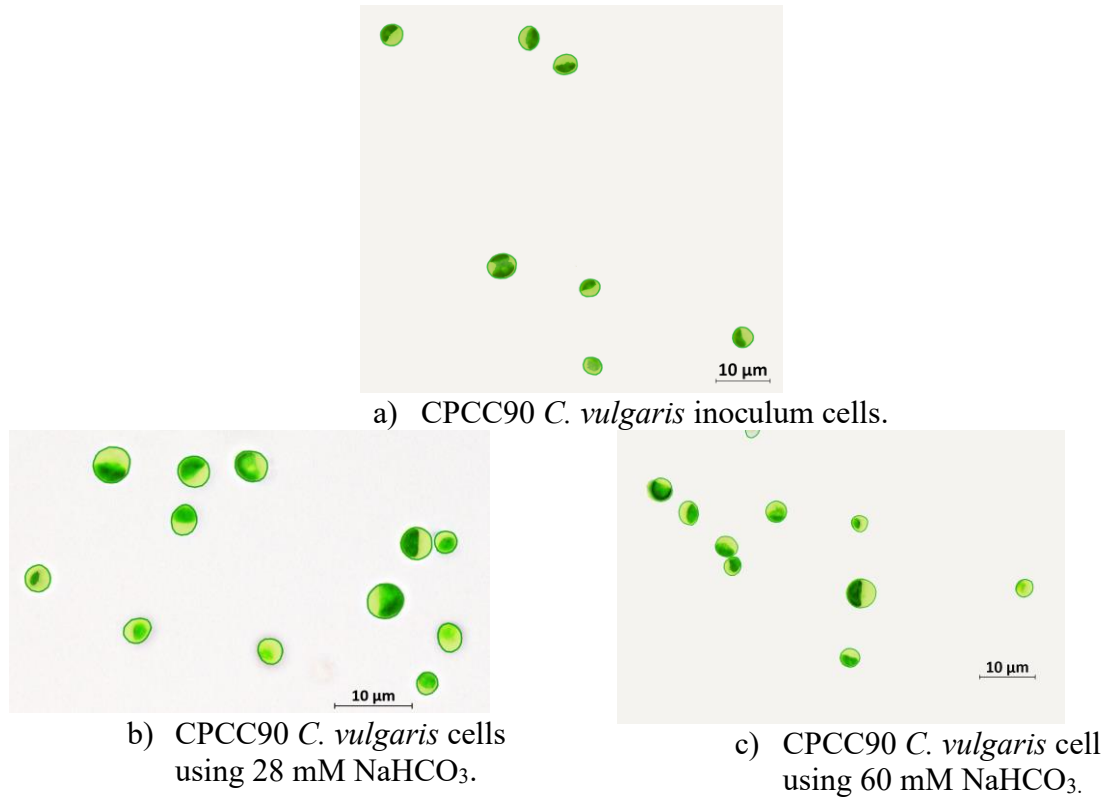


Figure 4.5 Microscope Images of CPCC90 *Chlorella vulgaris* cells: a) Show inoculum cells, b) show a case where a 28 mM NaHCO_3 solution was used and after 10 days of cultivation time, c) show a case where a 60 mM NaHCO_3 solution was used and after 12

days of culture. Contrast and cells boundary definition have been modified to improve the resolution of the images.

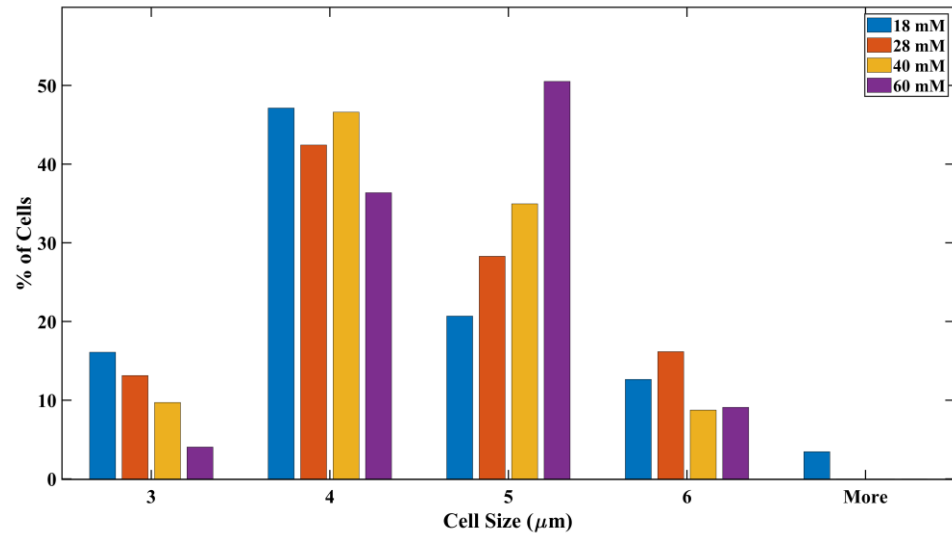


Figure 4.6 Cell size Distribution for Different Concentrations of Inorganic Carbon, as Sodium Bicarbonate: a) blue bars: 18 mM, b) orange bars: 28 mM, c) yellow bars: 40 mM, d) violet bars: 60 mM.

Chapter 5

5 Carbon Uptake by *Chlorella vulgaris* in a PhotoBioCREC Unit

This chapter reports the analysis of the biochemical conversion of sodium bicarbonate, into total organic carbon, as a measure of algal growth. Furthermore, pH results during the cultivation time are also described.

5.1 Carbon Concentration

Chlorella vulgaris was grown in a MBBM, with a NaHCO_3 inorganic supply of carbon culture media. Figure 5.1 reports the changes of the total inorganic and organic carbon concentrations during the cultivation time of *Chlorella vulgaris*, for all concentrations of NaHCO_3 .

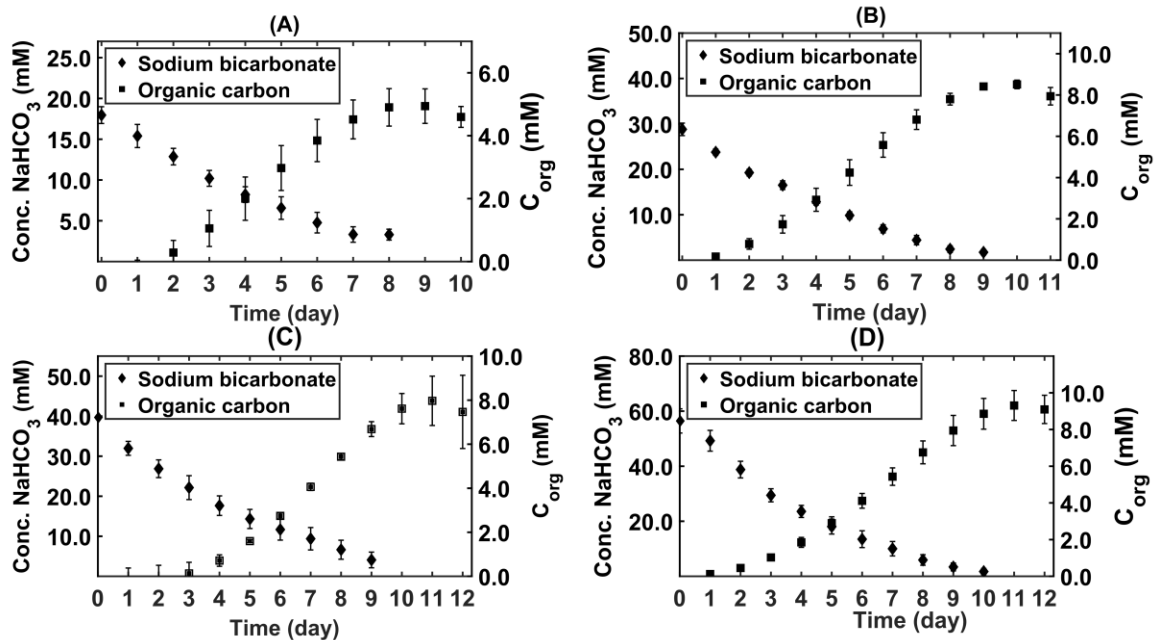


Figure 5.1 Total Inorganic Carbon and Total Organic Carbon Concentration Changes with Culture Time for the Different Nominal Concentrations of NaHCO_3 : (A) 18 mM, (B) 28 mM, (C) 40 mM and (D) 60 mM (standard deviation of 3 repeats).

One can observe in Figure 5.1, the anticipated progressive decay of inorganic carbon with a corresponding increase of total organic carbon. On the other hand, one can note that the cumulative organic carbon displays an S-shaped curve, achieving a maximum growth after 8 to 11 days of cultivation time, depending on the initial concentration of NaHCO_3 . Moreover, one can also notice that the rate of microalgae growth, assessed with the slope of the S-shaped organic carbon concentration curve, augments in average until day 6, and then decreases progressively.

For experiments with an initial concentration of 18 mM of NaHCO_3 , the value of the maximum concentration of total organic carbon achieved was 5.0 mM (see Figure 5.1.A). Furthermore, an increase in the value of total organic carbon concentration was observed for experiments with 28 mM NaHCO_3 concentration, reaching a maximum total organic carbon concentration of 8.5 mM (Figure 5.1.B). In the case of experiments with 40 mM and 60 mM of NaHCO_3 , the maximum organic carbon concentrations achieved were 8.0 mM (Figure 5.1.C) and 9.3 mM (Figure 5.1.D), respectively, at longer cultivation times of 11 days.

One can also remark that for the higher concentrations of inorganic carbon supply (40 mM and 60 mM), there were in both cases, longer initial lag phases, as well as a longer culture times to reach the maximum organic carbon concentration. Thus, it appears that *Chlorella vulgaris* requires more time to adapt to a higher level of dissolved inorganic carbon.

Therefore, the present study shows that the initial bicarbonate concentrations in the range studied, have a mild influence on the maximization of the carbon fixation by *Chlorella vulgaris*. One should mention that the observed initial bicarbonate effect on microalgae growth, is in line with the initial longer lag phases and suggested cell abundance, found while cultivating *N. salina* and using 24 mM of bicarbonate instead of 12 mM (White et al., 2013). In this respect, the higher bicarbonate concentration effect observed, can be justified as an inhibition of microalgae growth, even though this condition may lead to a high lipid concentration (Abedini et al., 2015; Tu et al., 2018).

5.1.1 pH Changes during Microalgae Growth

Regarding the use of sodium bicarbonate for microalgae cultivation, one can observe a steady pH increase trend, with this being due to the ion bicarbonate (HCO_3^-) decomposition, forming CO_2 and hydroxides (OH^-) catalyzed by carbonic anhydrase in the microalgae cells (Aizawa & Miyachi, 1986). Thus, every 24 hours, the pH was measured and adjusted to 7.0. Table 5.1 reports the pH value measured every day for all concentrations of sodium bicarbonate, and prior to the pH adjustment.

Table 5.1 pH Measurements during CPCC90 *Chlorella vulgaris* Growth.

Time (day)	NaHCO ₃ Concentration			
	18 mM pH ±SD	28 mM pH ±SD	40 mM pH ±SD	60 mM pH ±SD
1	8.3 ± 0.02	8.4 ± 0.1	8.4 ± 0.1	8.9 ± 0.2
2	8.5 ± 0.1	8.6 ± 0.02	8.3 ± 0.02	8.6 ± 0.05
3	8.8 ± 0.2	8.7 ± 0.1	8.4 ± 0.03	8.7 ± 0.1
4	9.1 ± 0.3	8.9 ± 0.2	8.5 ± 0.002	8.8 ± 0.1
5	9.4 ± 0.2	9.3 ± 0.2	8.7 ± 0.1	9.0 ± 0.1
6	9.3 ± 0.1	9.5 ± 0.1	8.9 ± 0.1	9.2 ± 0.1
7	8.8 ± 0.3	9.5 ± 0.1	9.1 ± 0.1	9.5 ± 0.2
8	7.6 ± 0.6	9.0 ± 0.5	9.3 ± 0.1	9.6 ± 0.02
9	7.1 ± 0.3	7.7 ± 0.5	9.2 ± 0.1	9.3 ± 0.4
10	7.2 ± 0.1	7.2 ± 0.1	8.8 ± 0.6	8.2 ± 0.7
11		7.3 ± 0.1	8.1 ± 0.5	7.3 ± 0.1
12			7.3 ± 0.2	7.3 ± 0.1

As reported in Table 5.1, as microalgae consumes inorganic carbon as bicarbonate ions, the pH increases progressively to a maximum value of 9.4. This is the case for

experiments with 18 mM of NaHCO₃. pH values of 9.5, 9.3 and 9.6 were found for runs with 28 mM, 40 mM and 60 mM of NaHCO₃, respectively.

One should notice that the maximum pH was reached, at different cultivation times, for runs with 28 mM, 40 mM or 60 mM of NaHCO₃. Once the maximum pH was attained, the increases in the pH became milder, displaying a 7.3 value at the end of the experiments, when presumably the ion bicarbonate fed was already depleted. Furthermore, it appears that the high pH values such as the ones observed in the present study, prevent bacterial contamination or avert the wild type of microalgal species from contaminating the culture (Wang et al., 2008). This is a positive effect for experiments developed which were carried out in non-sterile conditions.

5.2 Carbon Conversion by CPCC90 *Chlorella vulgaris*

Carbon utilization by microalgae is one of the most important culture parameters, coupled with the quantum yield, which is required to analyze the efficiency of the microalgae growth process. In this respect, one can envision the microalgae culture process as follows:

$$N_{in} \rightarrow N_{org} + unconverted\ N_{in} \quad \text{Equation 5.1}$$

With N_{in} representing the moles of inorganic carbon source, which in the case of the present study is sodium bicarbonate, and N_{org} representing the moles of organic carbon. Accordingly, one can estimate the carbon conversion by microalgae as:

$$\eta = \frac{\text{moles of organic carbon produced}}{\text{moles of initial inorganic carbon}} * 100 \quad \text{Equation 5.2}$$

Figure 5.2 reports the carbon conversion for the different concentrations of NaHCO₃ tested. It can be observed that the inorganic carbon conversion increases to a maximum value of 27%, in the runs with 18 mM NaHCO₃. A similar inorganic carbon conversion of 29.6% was reached for experiments with 28 mM NaHCO₃. On the other hand, when working with a higher concentration of inorganic carbon, the conversion into organic

carbon decreases. For instance, in the case of 40 mM of NaHCO_3 , the carbon conversion reached a maximum of 21% after 11 days of cultivation, while for experiments with 60 mM NaHCO_3 , this value was 17% after the same cultivation time.

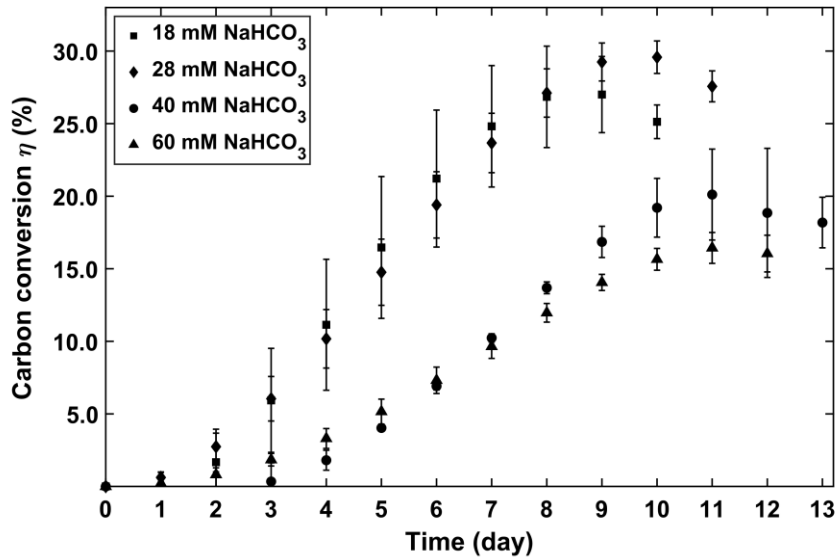


Figure 5.2 Conversion Efficiency of Inorganic Carbon provided as NaHCO_3 into Organic Carbon in the *PhotoBioCREC*.

On this basis, one can notice the following influence of bicarbonate concentration on the organic carbon formation as reported in Figure 5.2, as follows:

- Augmenting the bicarbonate concentration in the 18 mM to 28 mM of NaHCO_3 range, increases the inorganic carbon conversion,
- Raising the bicarbonate concentration from 28 mM to 40 mM of NaHCO_3 range, has no effect on the inorganic carbon conversion, and
- Augmenting the bicarbonate concentration in the 40 mM to 60 mM of NaHCO_3 range diminishes the inorganic carbon conversion.

As reported in the technical literature (Liu et al., 2017; Tu et al., 2018), microalgae growth processes are favored by higher substrate concentration until an optimum value. An increase in substrate concentration after the optimum level leads to inhibition of

microalgae growth, resulting in a lower carbon conversion and slower growth rates. Furthermore, in the case of using NaHCO_3 as a source of carbon, microalgae are exposed to salinity stress, that results in photosynthesis inhibition due to the changes in the osmotic pressure (Torzillo & Vonshak, 2013). Salt stress limits the fixation of CO_2 by inactivating the Rubisco enzyme (Torzillo & Vonshak, 2013).

Regarding the inorganic carbon obtained in *PhotoBioCREC*, it is important to remark that carbon dioxide fixation efficiencies have been reported in the technical literature, by other authors, for different microalgal strains including *C. vulgaris*, based on influent and effluent CO_2 or NaHCO_3 concentration differences. For instance, Keffer and Kleinheinz (2002) reported a 74% CO_2 fixation, by considering the doubtful assumption that the CO_2 concentration difference could be assigned to organic carbon only. A different approach was reported by Barahoei et al 2020, who determined a CO_2 utilization efficiency based on the theoretical yield of 1.88 kg of CO_2 recycled/100 kg biomass and the inlet CO_2 concentration. The maximum value of 35% carbon utilization efficiency was achieved when supplying 7% v CO_2 , in a bubble column photobioreactor (Barahoei et al., 2020).

Thus, the inorganic carbon conversion values reported in this chapter are valuable, given that they were obtained, using a rigorous inorganic carbon conversion analysis. They show typical inorganic carbon conversions in the 25-30%, at optimum bicarbonate concentrations.

5.3 Conclusions

- The culture of *Chlorella vulgaris* in a *PhotoBioCREC* unit leads to significant inorganic carbon conversions with a significant formation of organic carbon species.
- The culture pH must be monitored and adjusted periodically (every day) in order to prevent microalgae growth inhibition.

- The initial sodium bicarbonate concentrations do not lead to a higher carbon utilization efficiency. Inorganic carbon conversions are limited to levels that are 25-30% at their highest at the 18-28 mM bicarbonate concentrations.

Chapter 6

6 Macroscopic Radiation Energy Balances and Quantum Yields

An important parameter to establish photoreactor performance is the light utilization efficiency (Markager, 1993). This efficiency designated as quantum yield (QY), can be determined as the rate of organic carbon produced over the rate of absorbed photons. Considering that visible light supplies the energy required for the photosynthesis process performed by the *Chlorella vulgaris* in the *PhotoBioCREC* unit and that light absorption occurs only at specific wavelengths, this efficiency is critical to understand the carbon conversion efficiency in the *PhotoBioCREC*.

6.1 Methodology

As introduced in Chapter 4, a cool white fluorescent lamp was used to externally irradiate the *PhotoBioCREC* unit. The prototype was designed with a quartz window which allows the irradiation measurements to be performed with an optic spectro-photo-radiometer, every 24 hours, as reported in Figure 6.1. These measurements were performed within a range of 400 nm to 700 nm, at every 0.5 nm. However, since the energy consumed by the microalgae is only a fraction of the visible light spectrum, the chlorophyll absorption bands were considered, for the quantification of the rate of absorbed photons (see Figure 4.3). Three runs for each concentration were performed. As a result, in the present chapter, average values and their corresponding standard deviations (SD) are reported.

To be able to establish the quantum yield efficiency, one can calculate the rate of absorbed photons by considering the lamp emitted photons reaching the *PhotoBioCREC* reactor transparent wall. Macroscopic balances allow the calculation of absorbed photons (de Lasa et al., 2005), as the difference between the incident photons and transmitted photons:

$$P_a = P_i - P_t \quad \text{Equation 6.1}$$

where P_a is the rate of absorbed photons in the culture media, P_i the rate of photons reaching the *PhotoBioCREC* unit walls, and P_t the rate of photons transported throughout the *PhotoBioCREC* microalgae culture media. All units for rate of photons in Equation 6.1 are moles of photons s^{-1} .

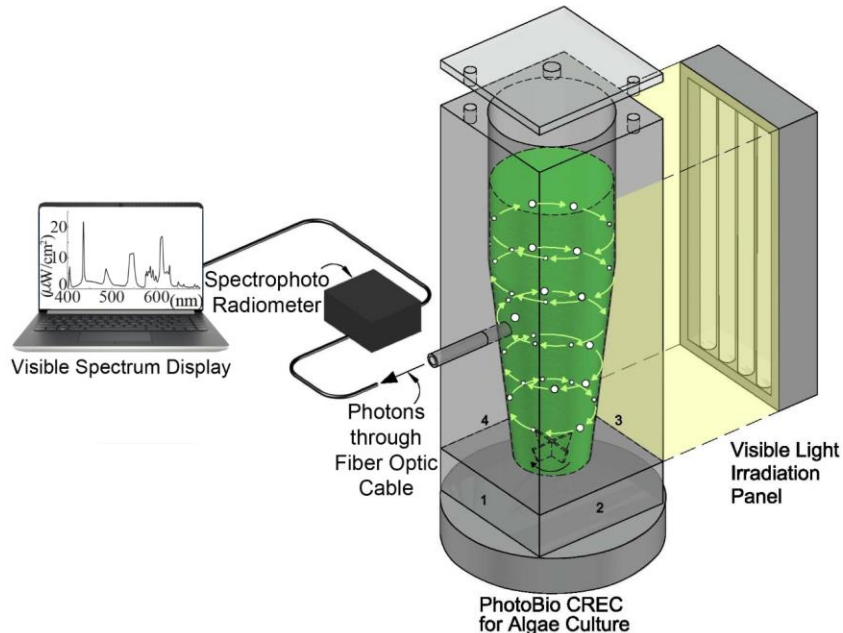


Figure 6.1 *PhotoBioCREC* Unit Setup for Irradiation Measurements (Cordoba-Perez & de Lasa, 2020).

Furthermore, based on photons absorbed rates by microalgae and the rates of organic carbon formed one can establish the quantum yield (QY), defined as the molar rate of organic carbon produced over the molar rate of photons absorbed as follows:

$$QY = \frac{N_{org}/_s}{\text{moles of photons absorbed by microalgae}/_s} \quad \text{Equation 6.2}$$

Considering that the moles of absorbed photons are estimated, for the main chlorophyll absorption spectrum bands, Equation 6.2 can be expressed as follows:

$$QY = \frac{\left[\frac{dN_{org}}{dt} \right]}{P_{a,\lambda}} * 100 \quad \text{Equation 6.3}$$

6.2 Observed Photon Absorption and Quantum Yields

The driving force for photosynthesis is sunlight. Once photons are absorbed in the chloroplast by chlorophyll pigments, a series of photochemical and redox reactions begin (Razzak et al., 2013). As a result and given the importance of visible light radiation for the consumption of inorganic carbon by the microalgae, irradiation measurements were effected. This was done to determine photon absorption efficiency, which is designated as the quantum yield.

Figure 6.2 reports the rate of photon absorption and its change with cultivation time, for the four concentrations of NaHCO₃. As described in Equation 6.1, the determination of photon absorption can be made by developing macroscopic irradiation energy balances in the *PhotoBioCREC* unit.

Regarding photon absorption in the *PhotoBioCREC* unit, one must consider the following:

- a) γ -alumina particles were added at a 0.05% volume concentration (volume of solid/liquid volume) to keep the photobioreactor walls free of microalgae deposition. Despite the fact that γ -alumina particles decreased transmitted radiation by less than 5% (e.g., Irradiance for a free of solids media was 2.21×10^{15} moles of photons cm⁻² s⁻¹ and irradiance with alumina particles loaded was 2.11×10^{15} moles of photons cm⁻² s⁻¹), it was found that their continuous motion and promoted shearing forces near the walls, was adequate to keep the reactor windows clean and without any significant microalgae deposit, all the times.

- b) At the beginning of the microalgae culture, the MBBM in the water yielded a liquid medium transparent to visible light. Under these initial conditions, there was very little photon absorption in the culture media (Kong & Vigil, 2014).
- c) However, later in the cultivation process, photons emitted by the light source became progressively absorbed via the different pigments in the microalgae cells (Kong & Vigil, 2014).
- d) Finally, and at the end of every run, starting around day 7, one was able to observe that the entire photon radiation flux was absorbed by the suspended algae.

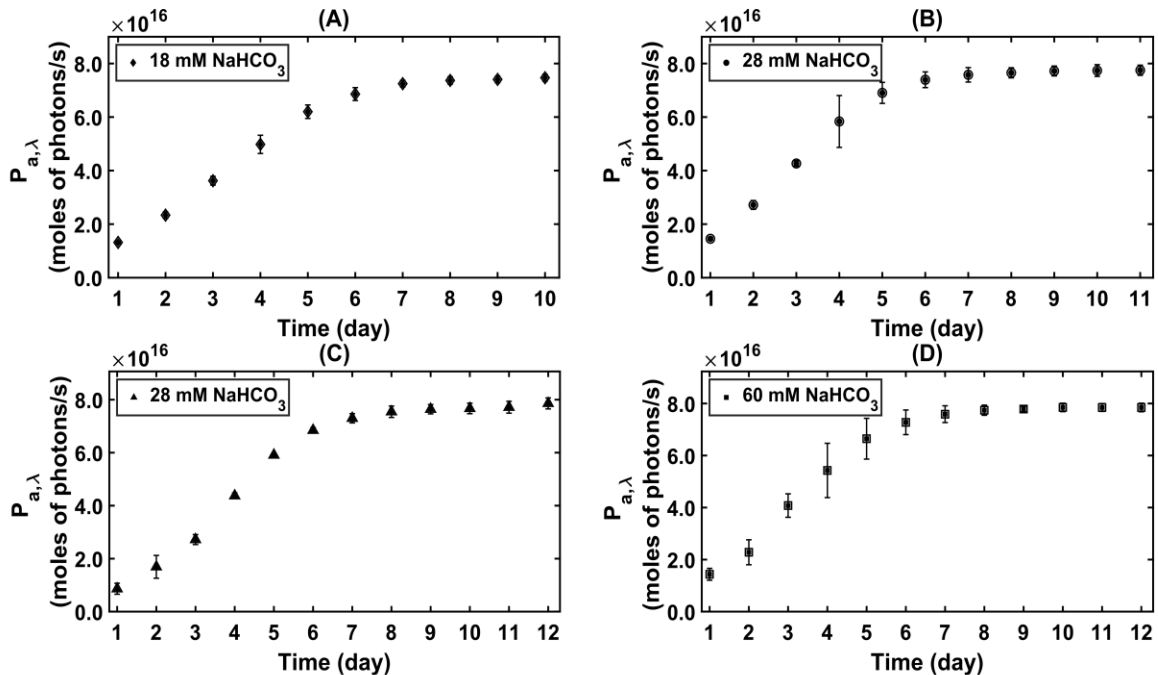


Figure 6.2 Rate of photon Absorption (Equation 6.1) for the Experiments with Concentrations of Sodium Bicarbonate of: (A) 18 mM, (B) 28 mM, (C) 40 mM and (D) 60 mM. Vertical bars represent the standard deviation of three runs.

On this basis, the QY as shown in Equation 6.3, allowed establishing the efficiency of microalgae growth per absorbed photon utilization rate. This represented the rate of absorbed photons required to produce the desired microalgae product formation rate.

To be able to calculate the QY, one must establish the time derivative of the organic carbon produced as microalgae, or the equivalent rate of organic carbon production. From the data reported in Figure 5.1, the dN_{org}/dt can be obtained for the four different concentrations of NaHCO_3 . This is reported in Figure 6.3A, B, C and D.

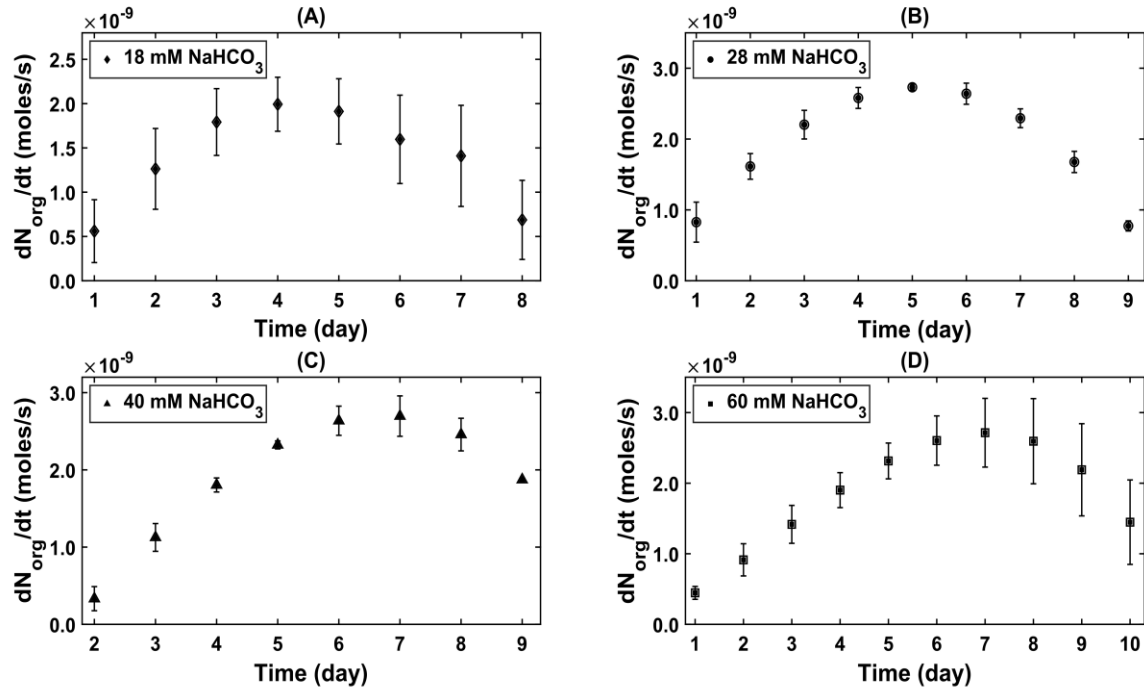


Figure 6.3 Rate of Organic Carbon Formation for the Different Concentrations of NaHCO_3 : (A) 18 mM, (B) 28 mM, (C) 40 mM, and (D) 60 mM. Vertical bars represent the standard deviation of three runs.

In addition, and based on the results obtained, concerning the rate of photon absorption and the total organic carbon production rate for CPCC90 *Chlorella vulgaris* growing with initial concentrations of NaHCO_3 of 40 mM (Figure 6.2C, Figure 6.3C) and 60 mM (Figure 6.2D and Figure 6.3D), it can be seen that a longer cultivation times are needed. This is the case to efficiently utilize the energy provided by the light source and the inorganic carbon when working with the higher concentration of NaHCO_3 .

Furthermore, Figure 6.4A, B, C and D describe the QY, using the data reported in Figure 6.2 and Figure 6.3.

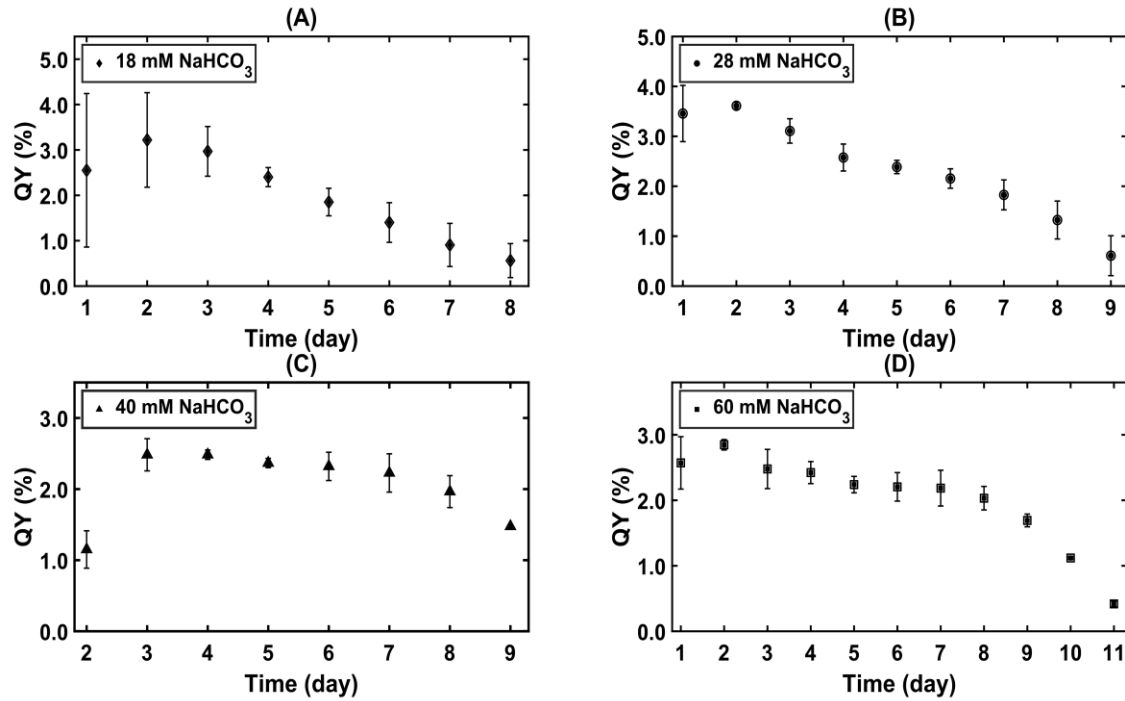


Figure 6.4 Percentual Quantum Yield (Equation 6.3) for *Chlorella vulgaris* with: (A) 18 mM NaHCO₃, (B) 28 mM NaHCO₃, (C) 40 mM of NaHCO₃ and (D) 60 mM of NaHCO₃. Vertical bars represent the standard deviations of three runs.

By reviewing the data reported in Figure 6.4A, one was able to see that the QY displayed a maximum value of 3.2%, for the experiments with 18 mM of NaHCO₃ at day 2 of cultivation. This decreased progressively from day 2 to day 7. A similar QY was achieved when microalgae were grown with 28 mM initial NaHCO₃ concentration, with the QY efficiency being 3.6% at day 2. Thus, one was able to see that the photochemical inorganic carbon conversion into biomass by microalgae, is a relatively slow process of variable QY efficiency. The QY values reported in Figure 6.4 can be explained as follow:

- a) At day 2, the rate of biomass formation is modest with relatively low P_a . This led to the highest QYs observed.

- b) After day 2, however, while microalgae continue to grow, the P_a stabilizes, reaching the total irradiated photon flux at day 6-7. This leads to QY values which are progressively reduced with cultivation time.

The analysis of these results can lead to establishing optimum operation conditions for cultivation time. For instance, when feeding *Chlorella vulgaris* with 18 mM of NaHCO₃, it can be envisioned that it is convenient to operate the *PhotoBioCREC* for 7 days only, in order to maximize carbon conversion, with an acceptable QY average of 2.0% for *Chlorella vulgaris*. Likewise, if the inorganic carbon concentration fed is 28 mM, one more day of operation to maximize inorganic carbon utilization leads to an average QY of 2.3%.

Moreover, for experiments with concentrations of NaHCO₃ of 40 mM (Figure 6.4C) and 60 mM (Figure 6.4D), one can see that a maximum photon utilization efficiency for organic carbon production is achieved at day 2 with values of 2.5% and 2.8%, respectively. Thus, one can envision that it is favorable to operate the photobioreactor for 8 days, when NaHCO₃ is supplied at 40 mM. In the case of 60 mM of NaHCO₃, limiting the operation of the *PhotoBioCREC* to 10 days allows maximizing carbon formation, and obtaining an adequate QY average of 1.9% for *Chlorella vulgaris*.

Regarding the QY values obtained for the different concentrations of NaHCO₃, one can conclude the following:

- a) P_a , which is the denominator in Equation 6.3, changes with cultivation time for all concentrations of NaHCO₃, studied in a similar manner.
- b) The dN_{org}/dt numerator in Equation 6.3, augments more rapidly for the lower concentrations of NaHCO₃ (18 mM and 28 mM).

As a result, lower concentrations of NaHCO₃ lead to a better photon utilization, as reflected by the higher QYs obtained.

6.3 Conclusions

- The transmitted radiation measurements allow one to establish macroscopic irradiation balances, with photon absorption steadily increasing with cultivation time.
- The average quantum yields evaluated, provide an encouraging photon utilization efficiency in the 1.9-2.3% range.
- The data obtained shows that the inorganic carbon concentrations influence the organic carbon formation rates, with lower values and extended lag phases observed at higher sodium bicarbonate concentrations.
- The rates of photon absorption and total organic carbon formation rates allow one to establish the best operation time in the *PhotoBioCREC* unit, in order to maximize utilization of light supply and total organic carbon production.

Chapter 7

7 Kinetics of Microalgae Culture

7.1 Introduction

Different kinetic models for microalgae growth have been published in the technical literature. The Monod model is widely used to predict the specific microorganism growth rate, under light saturation conditions (Monod, 1949). Later, in other studies, growth rate modifications have been reported including growth inhibition, due to both lack of nutrients and nutrient concentrations that are too high (Andrews, 1968; Martínez et al., 1999). Kumar & Das (2012) and Chang et al. (2016) used the logistic equation (Equation 7.1) to explain the different phases of the microalgae growth (lag, exponential and stationary), with the cell growth rate postulated, as being independent of the substrate concentration:

$$\frac{dX}{dt} = k_c X \left(1 - \frac{X}{X_{max}}\right) \quad \text{Equation 7.1}$$

where X represents the dry cell weight ($g L^{-1}$), X_{max} is the maximum dry cell weight ($g L^{-1}$) and K_c stands for the apparent specific growth rate of the microalgae (day^{-1})

Regarding the microalgae growth rate, few studies have determined algae growth kinetic parameters including the effect from inorganic carbon concentrations obtained from bicarbonate solutions. The focus has been on the use of gaseous CO₂ (Almomani, 2019; Jacob-Lopes et al., 2008).

Table 7.1 reports a summary of the kinetic models available in the technical literature, highlighting the main issues reading the reported kinetic models (a) the effect of mixing and radiation absorption, (b) the quantum yield evaluation, (c) the kinetic model development with the simultaneous measurement of total organic carbon (TOC) formed, and (d) the inorganic carbon substrate consumed.

Table 7.1 Microalgae Kinetic Models Reported in the Technical Literature.

Authors	Conditions of runs		Quantum Yield evaluation	Kinetics	
	Mixing evaluation	Radiation absorption evaluation		TOC/Biomass	Substrate (CO ₂ or NaHCO ₃)
Novak & Brune (1985)	?	No	No	First order and Monod	none
de Morais & Costa (2007)	No (intermittent aeration with air-CO ₂)	No	No	First order	None
Jacob-Lopes et al. (2008)	No (bubble column PBR)	No	No	First order	First order
Yeh et al. (2010)	Yes	No	No	First order and Monod model	None
Chun-Yen et al. (2010)	Yes	No	No	First order and Monod model	None
Kumar & Das (2012)	Yes	No	No	First order and logistic equation	None
Lam & Lee (2013)	Yes	No	No	First order	None
Chang et al. (2016)	?	No	No	First order, Logistic equation	None
Adamczyk et al. (2016)	?	No	No	Logistic equation	None
This study	Yes	Yes	Yes	Zero order	First order

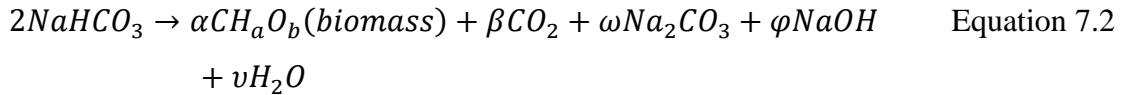
Notes: (a) The "yes" corresponds to a quantitative evaluation of either "the cell unit mixing" or "the cell unit radiation absorption" during runs, (b) The "No" corresponds to a lack of provided data regarding "mixing" or "radiation absorption", (c) The "?" symbol corresponds to cases where there is uncertainty regarding "the mixing conditions" or "the radiation absorption", and (d) The "zero order", "first order" or "the Monod model" corresponds to observed kinetics during experiments.

One can notice in Table 7.1, that even if this proposed kinetics can be considered valuable as first approximations, they still lack the following: (a) the development of macroscopic irradiation energy balances, (b) the assessment of carbon balances, (c) a critical review of kinetic model assumption applicability, and (d) the determination of kinetic parameters using statistical indicators.

Given the above, in the following sections of this chapter, a phenomenologically based growth kinetics for *CPCC90 Chlorella vulgaris* is rigorously established, using a wide range of bicarbonate concentrations.

7.2 Kinetic Model Development

Inorganic carbon species can be fed to the *PhotoBioCREC* unit, as bicarbonates. These species can be converted, in principle, into organic carbon as microalgal biomass, CO₂, sodium carbonate and sodium hydroxide. As a result, an overall bicarbonate conversion stoichiometry can be considered as follows:



with α , β , ω , φ and ν being the stoichiometric coefficients for organic carbon as biomass, for CO₂, for sodium carbonate, for sodium hydroxide and for water, respectively. On this basis, a kinetic model can be established by using the *PhotoBioCREC* unit data to arrive at the following conclusions:

- a) Algal growth takes places in a well-mixed *PhotoBioCREC* unit. This is considered adequate given the high mixing, which is the result of the important axial and circumferential promoted fluid motion in this unit.
- b) The incident irradiation passing through the flow media, containing the suspended alumina particles, remains steady during the entire algal growth period. This is achieved, because of the self-cleaning walls promoted by the circumferential motion of the alumina particles in the close to wall region.

As a result, under these conditions, one can postulate with confidence, that the changes in bicarbonate moles comply with the following species balance:

$$\frac{dN_{in}}{dt} = r_{in}V_f = -k_{in}C_{in}^nV_f \quad \text{Equation 7.3}$$

with N_{in} representing the moles of inorganic carbon, r_{in} being the molar rate of inorganic carbon consumption, C_{in} denotes the molar concentration of inorganic species, k_{in} representing the kinetic constant for the conversion of inorganic carbon species, and V_f standing for the liquid hold-up in the *PhotoBioCREC*.

Assuming that the V_f is constant, and given the unchanged fluid level, and the steady visible radiation provided to the *PhotoBioCREC*, Equation 7.2 becomes Equation 7.3, as follows:

$$\frac{dC_{in}}{dt} = -k_{in}C_{in}^n \quad \text{Equation 7.4}$$

With C_{in} representing the concentration of inorganic carbon species, fed as bicarbonates. Regarding Equation 7.3, one can also mention, as shown later in the present study, that sodium bicarbonate concentration displays a first order decay ($n=1$), which is an expected order of reaction for a unimolecular species consumption.

Furthermore, while sodium bicarbonate consumption is progressing, microalgae is steadily being formed, during a designated “growth phase”. Throughout this period, the CPCC90 *Chlorella vulgaris* growth can be described, using as a basis the total organic carbon (TOC) as follows:

$$\frac{dN_{org}}{dt} = r_{org}V_f = k_{org}C_{in}^m\theta_v V_f \quad \text{Equation 7.5}$$

$$\frac{dC_{org}}{dt} = k_{org}C_{in}^m\theta_v \quad \text{Equation 7.6}$$

with N_{org} representing the moles of total organic carbon, θ_v representing the microalgae matrix sites susceptible to reacting with bicarbonate inorganic molecules, in a condensation reaction with the m reaction order set to 1; r_{org} the molar rate of total organic carbon formation, k_{org} being the kinetic constant for the formation of total organic carbon, C_{org} is the concentration of total organic carbon.

Furthermore, and if the bicarbonate carbon containing species interact with microalgae sites at equilibrium, a Monod type of model can be described as follows:

$$\frac{dC_{org}}{dt} = r_{org} = \frac{k_{org}C_{in}}{1 + KC_{in}} \quad \text{Equation 7.7}$$

with K being the adsorption constant, and the vacant sites in the microalgae surface evaluated from a chemisorption model as $\theta_v = 1/(1 + KC_{in})$. Thus, Equation 7.3 and Equation 7.6 can be used to describe the sodium bicarbonate concentration changes, as well as the changes in carbon concentration contained in the microalgae (C_{org}) as defined using TOC.

In addition, one can also envisage that at $KC_{in} \gg 1$ conditions, Equation 7.6 becomes a zero-order reaction. The $KC_{in} \gg 1$ hypothesis included in the present model accounts for a sound bicarbonate-free site on microalgae surface interaction mechanism, which is likely the condition to be found for a bicarbonate decomposition reaction where one bicarbonate ion interacts with one free site on microalgae outer surface. If this is correct, the result is Equation 7.7, with this being consistent with the experimentally zero order observed during the microalgae growth period.

As a result, integrated forms of Equations 7.4 and 7.6 can be proposed for CPCC90 *Chlorella vulgaris* culture in a NaHCO₃ solution media:

- a) Inorganic carbon consumption:

$$C_{in} = C_{in_0} e^{-k_{int} t} \quad \text{Equation 7.8}$$

- b) Organic carbon formation:

$$C_{org} = u(t - t_{lag})\{k_{org,j}(t - t_{lag})[1 - u(t - t_f)] + u(t - t_f)C_{org}^{max}\} \quad \text{Equation 7.9}$$

with t_{lag} and t_f corresponding to the beginning of the lag phase, and the end of the growth phase, respectively; C_{org}^{max} being the maximum organic carbon concentration at

the end of the growth phase. Equation 7.8 represents the decay of inorganic species, involving an exponential decay function which was found to be first order; and Equation 7.9 representing a zero-order reaction, with a Heaviside function selected to represent the growth induction period, and the growth arrest time.

Furthermore, a ratio between the integrated form of Equation 7.7 evaluated at the maximum organic carbon concentration, and the initial inorganic carbon concentration, can be established. One can obtain the maximum concentration of total organic carbon based on the initial inorganic carbon concentration (C_{in_0}) as:

$$\frac{C_{org}^{max}}{C_{in_0}} = \frac{1}{C_{in_0}} k_{org} (t_f - t_{lag}) = \frac{k_{org}}{C_{in_0}} \tau \quad \text{Equation 7.10}$$

with τ representing the growth phase time.

Furthermore, the selectivity conversion of inorganic carbon into *Chlorella vulgaris* can be calculated as:

$$\text{Selectivity} = \frac{C_{org}}{(C_{in_0} - C_{in})} * 100 \quad \text{Equation 7.11}$$

7.3 Kinetic Parameters

Table 7.2 reports the reaction order and the reaction rate constant, for the inorganic carbon (bicarbonate) consumption. One should note that few studies in the literature have reported the inorganic carbon conversion kinetic parameters. One should mention that the kinetic model obtained in our research is consistent with Jacob-Lopes, Gimenes Scoparo & Teixeira Franco (2008), who reported a first order removal of gaseous CO₂, in the aqueous phase by a cyanobacteria species.

Table 7.2 Kinetic Parameters for Inorganic Carbon Consumption.

Parameter	Value
n	0.95 ± 0.09
$k_{in} \{(mmole L^{-1})^{0.05} day^{-1}\}$	0.26 ± 0.09

Moreover, Figure 7.1(a), Figure 7.1(b), Figure 7.1(c) and Figure 7.1(d) report the NaHCO_3 concentration changes with culture time, at four different initial concentrations, showing the good agreement between the experimental and the predicted concentrations.

Microalgae biomass growth can be tracked using the progressive total organic carbon concentration increase with culture time. The kinetic parameters for total organic carbon are presented in Table 7.3, for the different bicarbonate concentrations. The results are consistent with the already described TOC observed: (a) there is a kinetic constant increase in the 18 mM to 28 mM range, (b) there is a stable value of the kinetic constant for 28 mM, 40 mM and 60 mM concentrations of NaHCO_3 . Furthermore, the reported results confirm the effective applicability of the proposed zero order model, for the biotransformation of inorganic carbon into organic matter, by the CPCC90 *Chlorella vulgaris*, during the growth phase, for all bicarbonate concentrations.

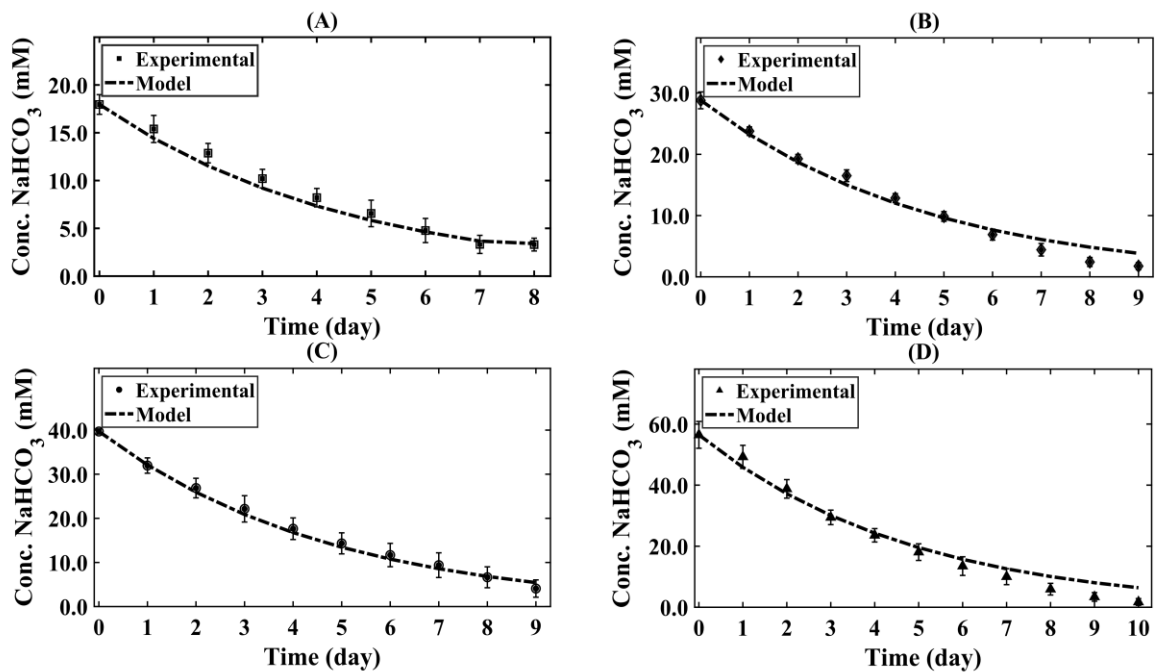


Figure 7.1 NaHCO_3 Concentration Changes with culture time. Experimental and model predicted values (Equation 7.8) for nominal initial concentrations of (A) 18 mM, (B) 28 mM, (C) 40 mM, (D) 60 mM. Note: reported results include at least 3 repeats.

Table 7.3 Reaction Rate Constants for Total Organic Carbon Formation and Growth Phase time.

Nominal conc. of NaHCO ₃ (mM)	k_{org} (mmole L ⁻¹ day ⁻¹)	τ (day)
18	0.86 ± 0.13	6
28	1.18 ± 0.05	7.2
40	1.06 ± 0.08	8
60	1.02 ± 0.11	9

Figure 7.2(A), Figure 7.2(B), Figure 7.2(C) and Figure 7.2(D), show that TOC increases with culture time, during the growth phase, with the predicted organic carbon concentration for the growth phase, following the proposed zero-order model closely, during the 2-10 days period. This consistent zero order model agrees with the Monod model, with bicarbonate carbon concentrations being supplied at relatively high levels (Chun-Yen et al., 2010; Yeh et al., 2010).

Figure 7.2 also shows that a maximum organic carbon concentration is reached in all cases, after 8 or 11 days of algae culture. This maximum organic carbon concentration can be influenced by the initial bicarbonate, which follows a non-linear trend, as reported in Figure 7.3. Therefore, the maximum organic carbon concentration (C_{org}^{max}) predicted by the proposed kinetic model, can be related to the initial inorganic carbon concentration, provided as NaHCO₃, using γ and δ parameters, and estimated with a nonlinear regression as follows:

$$C_{org}^{max} = \gamma C_{in_0} = \gamma_0 C_{in_0} e^{(-\delta C_{in_0})} \quad \text{Equation 7.12}$$

Figure 7.3 shows the ability of the proposed model to predict maximum organic carbon concentrations using both Equation 10 and Equation 12. Furthermore, Figure 7.3 demonstrates the adequacy of the γ and δ parameters calculated via nonlinear regression.

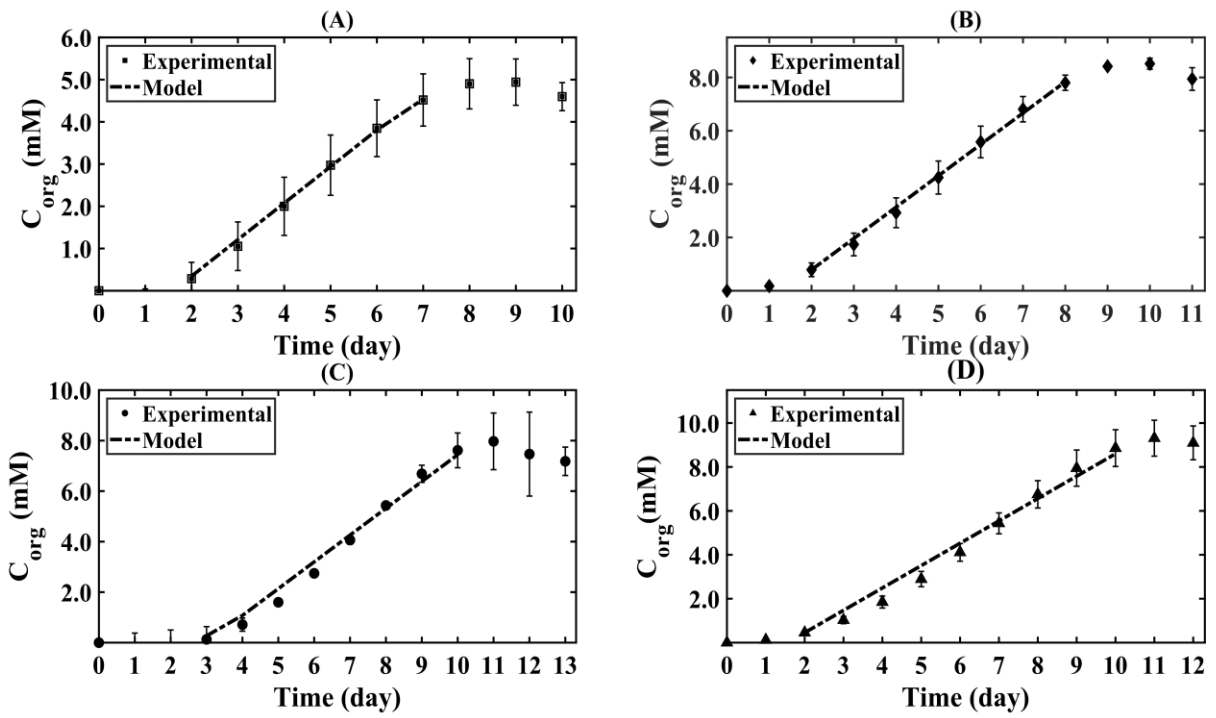


Figure 7.2 Concentrations of Total Organic Carbon with Culture Time. Experimental and model predicted values (Equation 7.9 for growth phase) for Nominal concentrations of NaHCO_3 : (A) 18 mM, (B) 28 mM, (C) 40 mM and (D) 60 mM.

Furthermore, and regarding the selective conversion of inorganic carbon into *Chlorella vulgaris*, the maximum selectivity was found to be for the initial concentration of 18 mM of bicarbonate species as shown in Table 7.4. Selectivity decreased with the increase of the initial sodium bicarbonate concentration. These results yielded stoichiometric coefficients close to $\alpha = 0.33$, $\varphi = 1$, $\beta + \omega = 1.67$, in Equation 7.2, and showed the promise of the bicarbonate conversion by *Chlorella vulgaris* via photosynthesis, in the *PhotoBioCREC*.

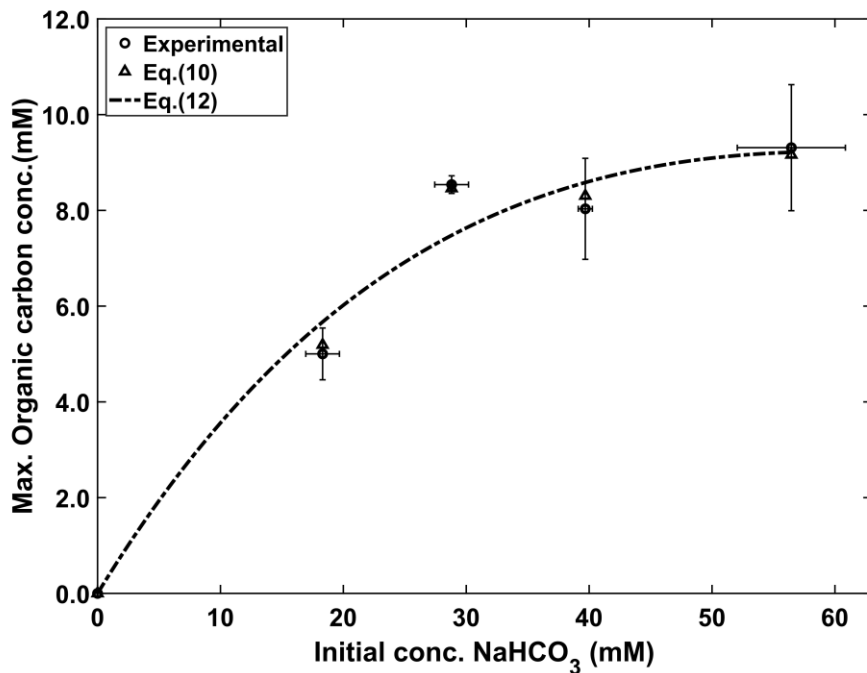


Figure 7.3 Maximum Concentrations of Total Organic Carbon as a Function of Initial NaHCO₃ Concentration. Note $\gamma = 0.42 \pm 0.04$ and $\delta = 0.02 \pm 0.004$ of Equation 7.12.

Table 7.4 Maximum Selectivity for the Different Inorganic Carbon Concentrations Based on Equation 7.12. Average values of 3 runs and standard deviations are reported.

Initial Conc. NaHCO ₃ (mM)	Selectivity (%)
18	33.0 ± 2.0
28	31.6 ± 1.8
40	22.8 ± 3.1
60	17.0 ± 1.4

7.4 Kinetic Model

The kinetic modelling allows the prediction of the *PhotoBioCREC* performance, and the efficiency of carbon uptake by microalgae. During the lag phase, microorganisms adapt to the growth conditions, such as nutrients, temperature and mixing, that can result in a partial inhibition of cell division (Monod, 1949). As a result, the Heaviside function

included in the model, and presented in Equation 7.9, allows one to properly account for these phenomena, predicting a close to null increase of biomass or total organic carbon concentration during the lag phase. On the other hand, for the growth phase, the proposed model allows the prediction of total organic carbon concentration until it reaches the maximum value. As shown in Figure 7.2(A), Figure 7.2(B), Figure 7.2(C) and Figure 7.2(D), after reaching the maximum concentration, there is a decline in the growth rate, as a result of the depletion of inorganic carbon supply.

Consequently, the kinetic model proposed in this research allowed us, in principle, to predict the CPCC 90 *Chlorella vulgaris* growth rate, both for carbon conversion and maximum carbon fixation. In addition, and given the experimental runs developed in the *PhotoBioCREC*, with concurrent macroscopic energy balances being established, this model allowed the evaluation of photon utilization efficiency, observed to be as high as 3.6%, as previously reported in Chapter 6.

Figure 7.4(A), Figure 7.4(B), Figure 7.4(C) and Figure 7.4(D) report the good agreement between the total organic carbon concentration, as predicted by the model developed in the present study, and the experimental results obtained in the present study, in the *PhotoBioCREC* unit.

Additionally, the validity of the proposed kinetic model for determining the conversion of inorganic carbon into organic carbon, can be analyzed by comparing the model predicted values with the experimental results. Figure 7.5 confirms the adequacy of the model proposed for CPCC90 Chlorella vulgaris. As a result, the proposed model of the present study can be considered as suitable for the prediction inorganic carbon converted, organic carbon formed and the prediction of carbon capture.

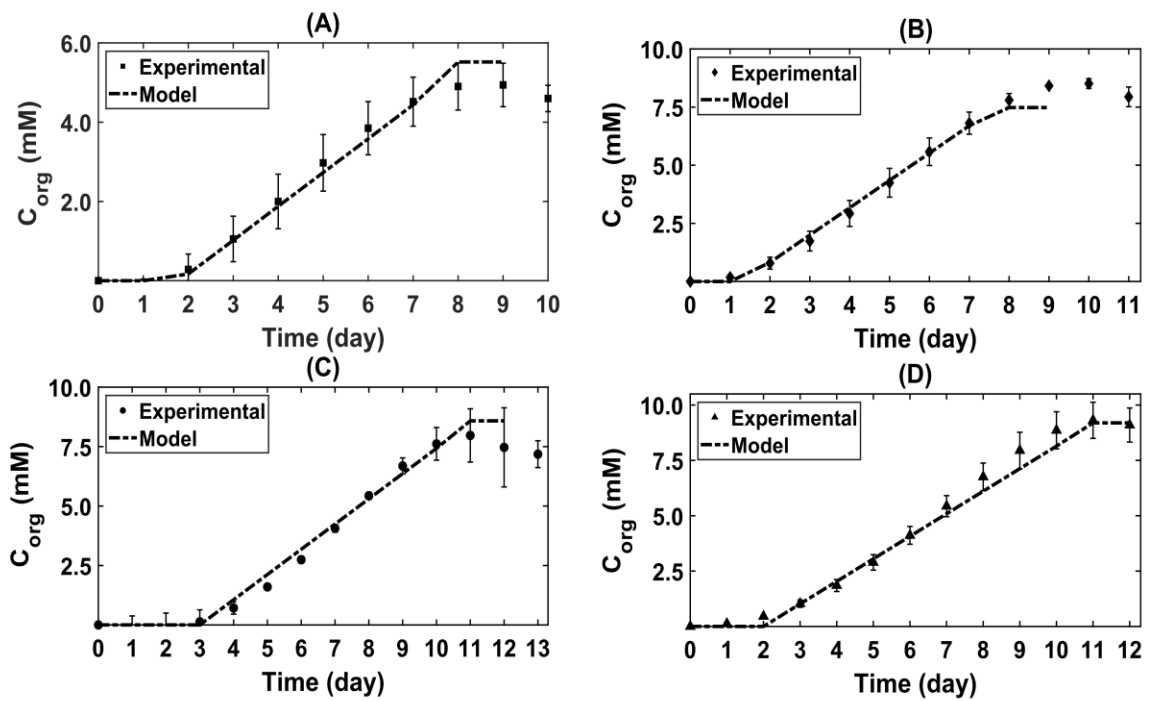


Figure 7.4 Comparison between Experimental Results and Predicted Values from the Proposed Kinetic Model (Equation 7.9), for the determination of Total Organic Carbon Concentration for Different Initial Nominal Concentrations of NaHCO₃: (A) 18 mM, (B) 28 mM, (C) 40 mM, and (D) 60 mM.

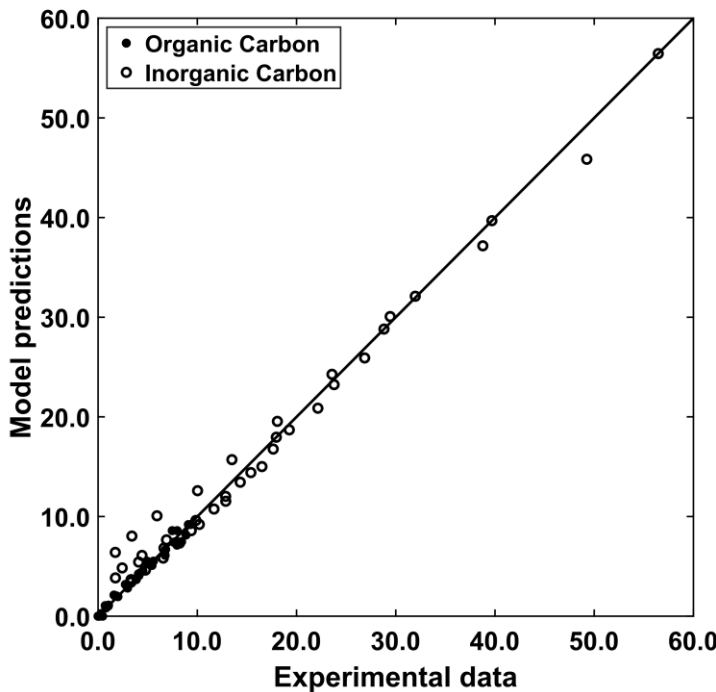


Figure 7.5 Comparison of Predicted and Observed Total Organic Carbon for the sodium Bicarbonate Concentrations of the present study.

7.5 Biomass Composition

The elemental composition of microalgal biomass was determined via combined CHNS (Elemental Carbon, Hydrogen, Nitrogen and Sulfur) and EDX (Energy Dispersive X-Ray) analysis. Table 7.5 shows that the carbon, hydrogen, oxygen and nitrogen elemental components of the CPCC90 *Chlorella vulgaris* of the present study, agree with the data reported in the literature. In particular, the observed nitrogen content in the CPCC90 *C. vulgaris* confirmed the expected protein content (Arif et al., 2021). In addition, the CPCC90 *C. vulgaris* grown with NaHCO₃, had a reported low sulfur content, which makes it a good biofuel feedstock, with low sulfur oxide emissions (Arif et al., 2021).

Finally, one can also notice the negligible sodium content, in the CPCC90 *C. vulgaris* elemental composition. This allows one to anticipate the full recycle of sodium in the CO₂ capture process, which is consistent with Equation 7.1. Thus, and on this basis, a

proximate formula for CPCC90 *Chlorella vulgaris* biomass was established as $CH_{1.8}O_{0.39}$.

Table 7.5 Elemental Analysis of the Cells of the CPCC90 *Chlorella vulgaris* Using Combined CHNS and EDX Elemental Analyses. Reported results are an average value for repeats with a ± 0.003 being the largest standard deviation.

Composition (%)	This study <i>CPCC Chlorella vulgaris</i>	Literature <i>Chlorella vulgaris</i> (Raheem et al., 2015)
Carbon	55.1	46.1-50.39
Hydrogen	8.2	6.01-6.41
Oxygen ¹	29.0	19.1-25.00
Nitrogen	7.1	9.01-14.77
Sulfur	0.6	0.4-6.05
Molar ratios		
H/C	1.8	1.43
C/N	9.1	
O/C	0.39	0.339

¹ Data calculated from combined CHNS and EDX analyses.

7.6 Conclusions

- A *PhotoBioCREC* prototype with controlled mixing and radiation conditions, provides a suitable experimental prototype, for the establishment of *Chlorella vulgaris* culture kinetics.
- Measurements of sodium bicarbonate and TOC changes with culture time, show an up to 33% selective conversion of bicarbonates into microalgae, establishing *Chlorella vulgaris* photosynthesis in the *PhotoBioCREC*, as a promising process for carbon capture.
- The proposed kinetics allows one to predict both bicarbonate concentration and organic carbon concentration changes, during various *Chlorella vulgaris* growth phases, when using an ample 18 mM to 60 mM range of sodium bicarbonate initial concentrations.

- The proposed model also reliably permits one to establish maximum *Chlorella vulgaris* microalgae concentrations, for various initial bicarbonate concentrations.

Chapter 8

8 *PhotoBioCREC Scaled Swirl Reactor Prototype*

The scaled *PhotoBioCREC* unit described in Chapter 4, was designed to establish microalgal kinetics. This kinetic model reported in Chapter 7 could make possible, in the near future, the prediction of the performance of a *PhotoBioCREC Swirl Reactor*, designed at the Chemical Reactor Engineering Centre (CREC), as part of this PhD Dissertation. This chapter describes the *PhotoBioCREC Swirl Reactor*, and presents relevant results obtained, concerning both fluid dynamics and irradiation.

8.1 Description of the *PhotoBioCREC Swirl Reactor*

The *PhotoBioCREC Swirl Reactor* was configured with a central annular section of 10.3 L, made of two vertical placed, concentric cylindrical quartz glass tubes. This central section is surrounded by four equally spaced reflector units, made of polished metal. A total of 8 externally placed fluorescent lamps irradiate the annular section of the *PhotoBioCREC Swirl Reactor*.

The *PhotoBioCREC Swirl Reactor* and auxiliary components is described in Figure 8.1: (a) an irradiated section, (b) a pump to recirculate the water, (c) a gas flow to recirculate the particles and (d) a storage tank to fill up the reactor.

During the preliminary experiments, the *PhotoBioCREC Swirl Reactor* was run with water only. The photobioreactor operates as follows: (a) once water and alumina particles reach the bottom section of the reactor, they are recirculated back, using two separated recirculation systems: one for the liquid and one for the particles, (b) water is recirculated to the top of the unit using a water pump. A filter placed at the water pump admission prevents alumina particles from reaching the water pump moving parts. These alumina particles move upwards due to a gas flow. This gas could be nitrogen or a mixture of CO₂-air, which can enhance microalgae growth.

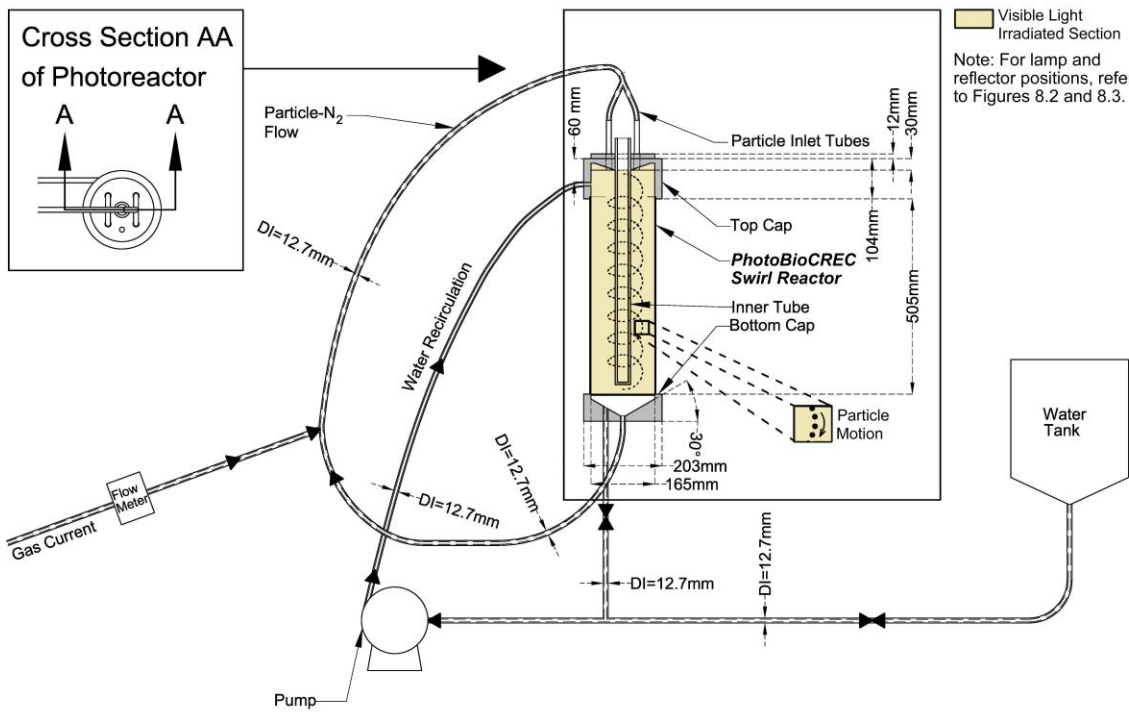


Figure 8.1 General Schematic Diagram of the *PhotoBioCREC Swirl Reactor* and the Experimental System.

The water suspended solids are fed from the top of the unit to the irradiated section, via four equally circumferentially distributed ports measuring 12.7 mm each. As well, the water flow reaching the top of the unit is fed tangentially to the *PhotoBioCREC Swirl Reactor* via a 9.5 mm inlet, inducing a combined swirl of particle flow, throughout the irradiated reactor section. The generated swirl flow is predicted to: a) enhance microalgae cell exposure to the visible light irradiation, reducing the effects of limited irradiation, when the culture concentration increases (Pruvost et al., 2002), b) prevent microalgal deposition on the unit walls, given that the swirling motion is dominant (Loubière et al., 2008).

Figure 8.2 provides additional details of the *PhotoBioCREC Swirl Reactor* radiation section. It consists, as already described, of an annular section with the microalgae cells and suspended particles flowing downwards, with a considerable circumferential

velocity. The design considerations allow one to extend the residence time of microalgae cells in the unit, improving the irradiation efficiency.

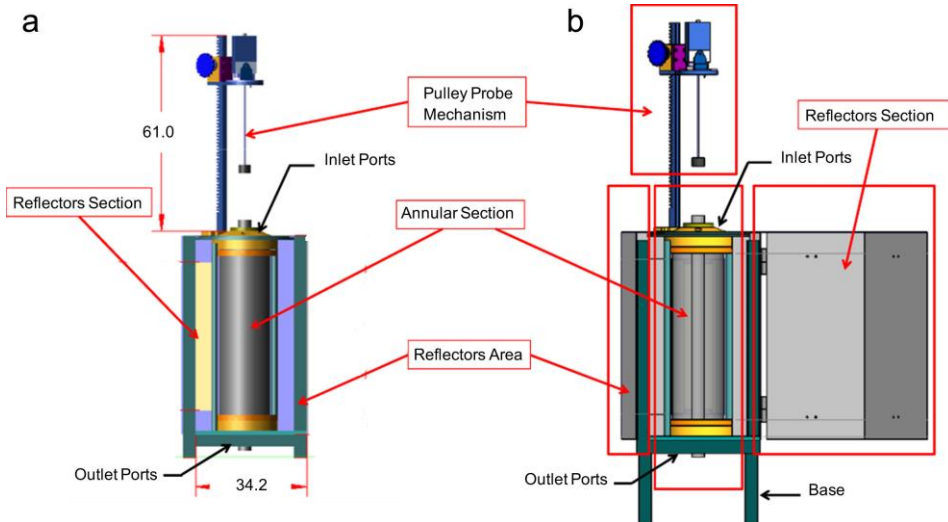


Figure 8.2 Diagram of the PhotoBioCREC Swirl Reactor a) inner reflectors and front annular section view, (b) unit side view (Valadés-Pelayo et al., 2015).

The radiation section is complemented with the following: (a) a reflector section with four reflectors and eight lamps in total, (b) a pulley mechanism to introduce a probe, along the central axis of the annular section, at different heights and azimuthal angles. The four reflectors are arranged at 90 degrees from each other. Each reflector has a 46.2 cm length and 15.7 cm width. There are two lamps in each reflector. Details of the position of the reflectors are shown in Figure 8.3. Eight lamps of visible light irradiation can be used in this photobioreactor.

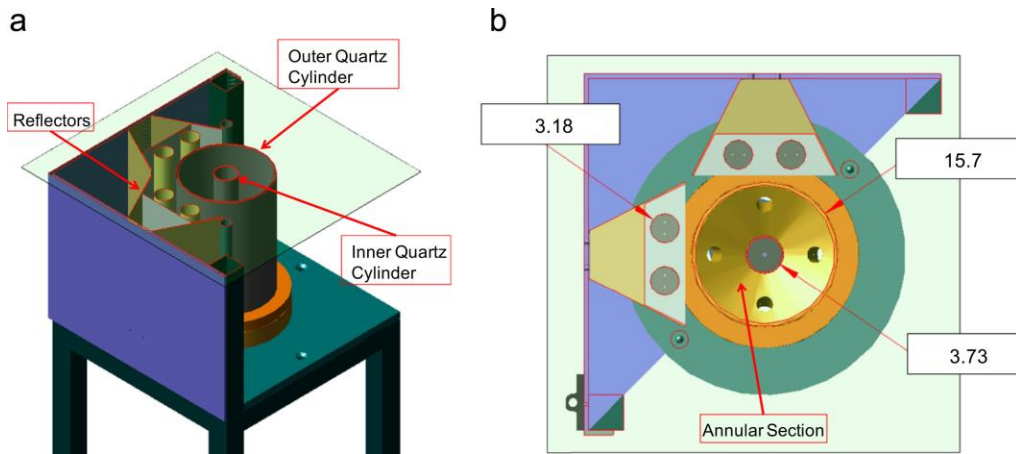


Figure 8.3 Schematic Diagram Showing Lamps and their Relative Location in the Reflectors. The (a) axonometric view and (b) top view. Dimensions reported in centimeters (Valadés-Pelayo et al., 2015).

8.2 Image Analysis for Tangential and Axial Velocity Determination in the *PhotoBioCREC Swirl Reactor*.

The tangential and axial particle velocity in the *PhotoBioCREC Swirl Reactor* were determined through video image analysis using a graphic editor software. The process of frame analysis involved (a) the use of individual video frames, (b) a grid of a set size on *PhotoBioCREC Swirl Reactor* established, (c) the use of pixels dimensions of the extracted frames. These dimensions from the extracted frames were related to the actual dimensions in centimeters.

In each frame, particles were located based on their (x, y) position in pixels (Position 1, Figure 8.4). The particles were followed in the next frames to register the new position (Position 2, Figure 8.4), and with this information the Δx and Δy were calculated. Using the corresponding conversion factor established for the reactor size as mentioned above, and since there were 60 frames per second, the velocity (axial and tangential) in cm/s was calculated for each particle. Moreover, particles trajectories were followed at different positions along the axial axis, as a result, a velocity profile of the *PhotoBioCREC Swirl Reactor* was established.



Figure 8.4 Image Analysis. Particle trajectories are tracked in different frames, establishing the x and y position. Particles highlighted in black represent the particles tracked. The red lines provide a reference for x and y position changes of the selected particles.

8.3 Fluid Dynamics of the *PhotoBioCREC Swirl Reactor*

In the *PhotoBioCREC Swirl Reactor*, a swirling particle flow is promoted, generating a particle-fluid descending vortex. To assess the extent of this, axial and tangential particle velocities were determined using image analysis. With the images extracted from videos and the process of calculation described in section 8.2, we were able to track numerous particles, to calculate their velocity components, as well as to determine their trajectories. Using these data, both axial and tangential velocities were obtained.

Figure 8.5 reports the tangential particle velocity, for both normal co-axial flow and for the swirling flow. One can see that, in this case, there is a significant increase of the tangential velocity from an average 4.0 cm/s to 11.5 cm/s. Furthermore, Figure 8.5 also

shows that the tangential particle velocity remains in a close range along the axial reactor length, with this showing little dissipation of the swirl, along the reactor unit.

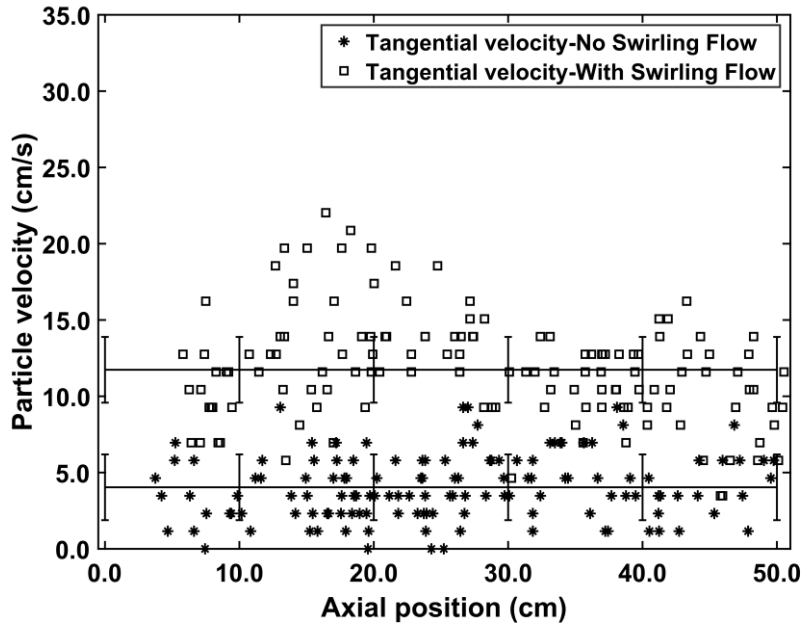


Figure 8.5 Effect of Swirl Flow on Particle Tangential Velocity.

Furthermore, and regarding axial velocity, Figure 8.6 shows that the average velocity of the particles remains unaffected by the swirl. One can see that particles display a mean axial velocity of 18.1 cm/s without the swirl, and a 19.5 cm/s with swirl flow.

As a result, the proposed *PhotoBioCREC Swirl Reactor* is effective in creating a rotating flow field with little dissipation of the swirl along the vertical axis. This increases microalgae cell radiation exposure time, which enhances photosynthesis efficiency.

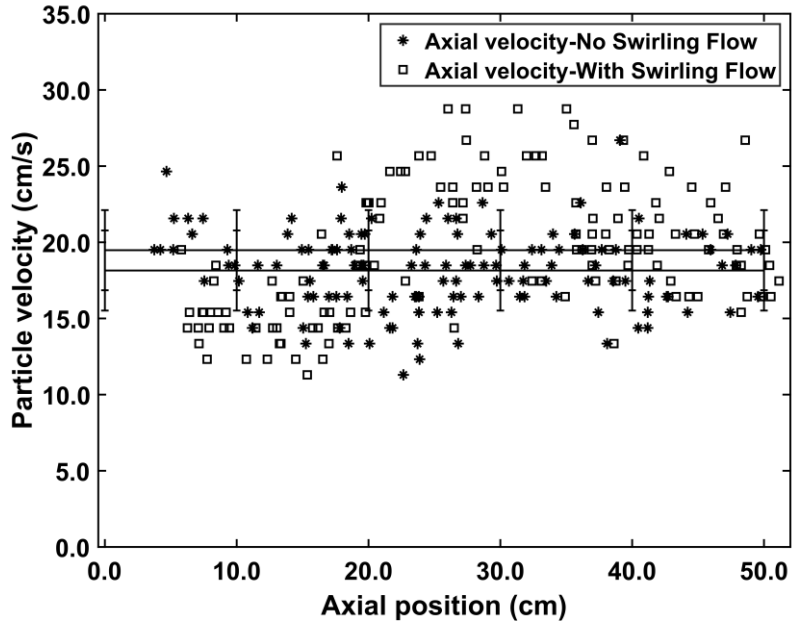


Figure 8.6 Effect of Swirling Flow on Particle Axial Velocity.

8.4 Irradiation Measurements in the *PhotoBioCREC Swirl Reactor*.

Irradiation measurements in the *PhotoBioCREC Swirl Reactor* taken with suspended alumina particles suspended in water, allow one to establish photon absorption by these alumina particles.

Figure 8.7 reports the irradiance transmittance when the *PhotoBioCREC Swirl Reactor* is loaded with alumina particles at a 0.2% concentration (volume of solid/liquid volume). Measurements were taken at the 0-cm axial and four azimuthal angular positions. Quantified differences between irradiation transmittance were 15%. This confirms the limited ability of the alumina particles, at the selected conditions of the *PhotoBioCREC Swirl Reactor*, to absorb radiation in the 400 nm-700 nm range.

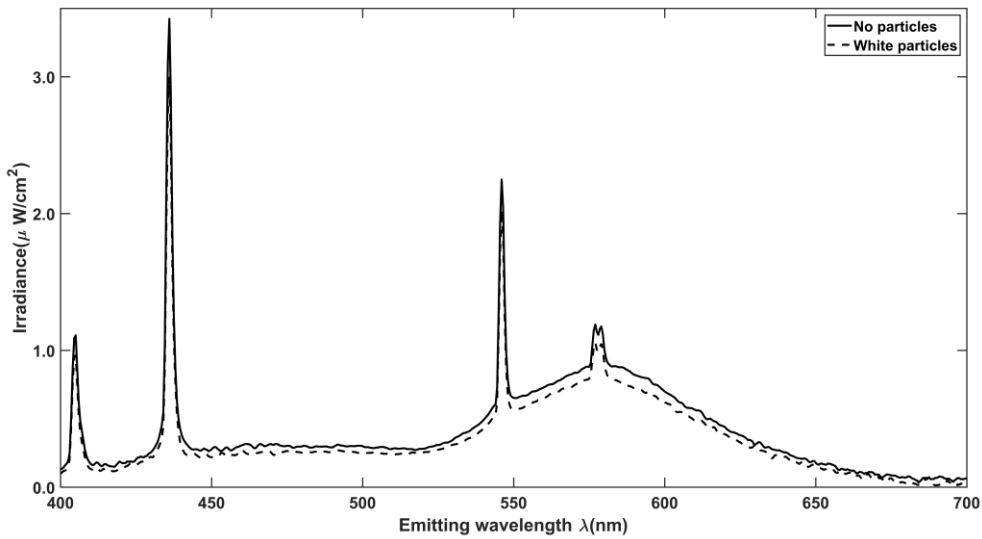


Figure 8.7 Comparison of the Visible Radiation spectra for water (continuous line) and water with alumina particles (dash lines). Measurements were performed at $Z=0$ cm and four azimuthal positions in the 400 nm-70 nm range. Standard deviations $\pm 2\%$.

Moreover, an irradiance axial profile for the *PhotoBioCREC Swirl Reactor* was established, as reported in Figure 8.8, which shows the axial radiation distribution. One can thus confirm that there is an observable light transmittance reduction, when alumina particles are loaded at a 0.2% concentration.

However, after developing a Macroscopic Radiation Balance in the *PhotoBioCREC Swirl Reactor*, it was found that alumina particles absorbed only 6.4% of the photons reaching the inner reactor surface. This photon absorption by the alumina particles is in line with the photon absorption reported previously, when using the *PhotoBioCREC* unit.

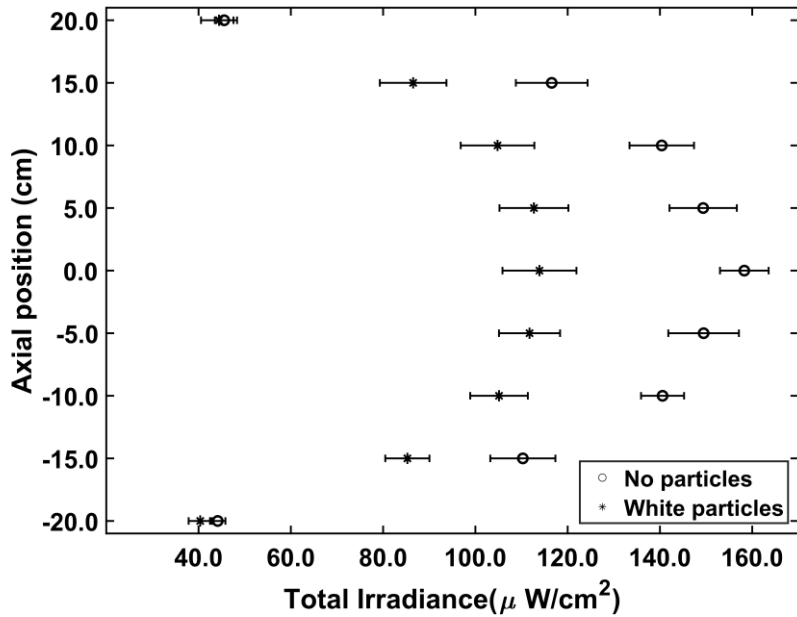


Figure 8.8 Axial Radiation distribution Profile at Various axial Positions. Measurements effected at four azimuthal positions.

Furthermore, Figure 8.9 reports the total transmittance at the Z=0 axial position and different azimuthal angles. One can notice the consistency of the I/I_0 , at various azimuthal positions, thus allowing the *PhotoBioCREC Swirl Reactor* to be analyzed, using a restricted “pie shape” control volume. This type of approach has the advantage of reducing considerably, the various numerical calculations required, for future studies, using this photoreactor.

While these findings are valuable, further experimentation is in our view required, to re-establish the optimal alumina particle concentration, in the *PhotoBioCREC Swirl Reactor*. These alumina particles, in combination with the promoted swirl flow, are relevant because they keep the photobioreactor walls clean, without algae deposition.

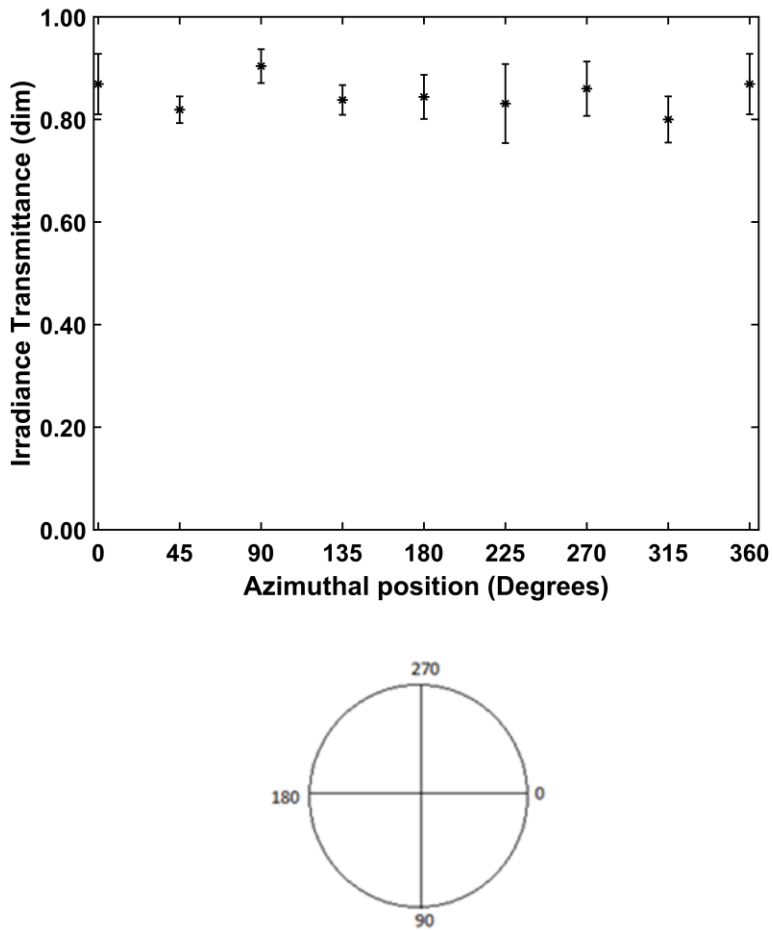


Figure 8.9 Dimensionless Transmitted Radiative Flux at Z=0 cm and at Different Azimuthal Positions shown in the Diagram.

Furthermore, since there is a recirculation of the fluid, there are short periods of time when the microalgae cells are not exposed to the visible irradiation light. In this regard, experiments in the *PhotoBioCREC* unit, can also allow one to determine the effect of short dark-light cycles during irradiation time.

Even though experiments with *Chlorella vulgaris* were not performed in the *PhotoBioCREC Swirl Reactor* in the context of this research, the provided fluid dynamics and irradiation measurements obtained in the *PhotoBioCREC Swirl Reactor*, and presented in this PhD Dissertation, provide important data for the evaluation of the

microalgae growth performance, in this scaled bioreactor. This proposed future evaluation should include both experiments and numerical CFD calculations, including the culture algae growth kinetics, reported in Chapter 7.

8.5 Conclusions

- The *PhotoBioCREC Swirl Reactor* provides a design concept that involves a significant vortex flow, with an important tangential particle velocity, in the near-wall region. This particle tangential velocity helps to increase microalgae cell residence time, and photon absorption through transparent reactor walls, free of algae deposition.
- The future development of the *PhotoBioCREC Swirl Reactor* prototype will significantly benefit from the established *Chlorella vulgaris* growth kinetics and from photon absorption and fluid dynamics studies reported in this PhD Dissertation.

Chapter 9

9 Conclusions, Future Work and Research Outcomes

9.1 Conclusions

The main contributions of this thesis can be summarized as follow:

- a) Runs were performed in the 0.175 L *PhotoBioCREC* unit with *Chlorella vulgaris* growing in sodium bicarbonate solutions. Culture growth was successfully monitored using total organic carbon and inorganic carbon concentrations, and irradiation transmittance. The formed microalgae were characterized using high resolution microscopy, SEM-EDX and CHNS elemental analysis.
- b) Inorganic carbon conversion as high as 29.6% at 18-28 mM of sodium bicarbonate solutions, were established for *Chlorella vulgaris* growth. It was proven that increasing the inorganic carbon supply as sodium bicarbonate in the 40-60 mM does not lead to higher inorganic carbon utilization efficiencies. Instead, under these higher bicarbonate concentration conditions, the lag phase is extended, and the total organic carbon formation rates slow down.
- c) Macroscopic energy balances allowed the successful determination of the photon absorption rates of *Chlorella vulgaris* culture, in the 0.175 L *PhotoBioCREC* unit. It was observed that photon absorption rates increased with culture time, reaching a constant maximum value after 7 days of microalgae cultivation, on average.
- d) Quantum yield efficiencies for *Chlorella vulgaris* growing in sodium bicarbonate solutions, in the 0.175 L *PhotoBioCREC* unit, were calculated and provided encouraging 1.9-2.3% light utilization efficiencies, towards carbon fixation by microalgae.
- e) Both quantum yields and carbon utilization efficiencies allowed the definition of optimum conditions for *Chlorella vulgaris* growth in 0.175 L *PhotoBioCREC*

unit. In this case, the goal was to maximize energy and inorganic carbon utilization.

- f) A new kinetic model was successfully established to predict total organic carbon and inorganic carbon concentrations, during *Chlorella vulgaris* growth phase, when using sodium bicarbonate concentrations, in the 18 mM to 60 mM range.
- g) Fluid dynamics studies were developed using a scaled 10.3 L *PhotoBioCREC Swirl Reactor* prototype with an induced swirl. This reactor can preserve all the beneficial microalgae growth features, demonstrated in the 0.175 L *PhotoBioCREC* Unit.

9.2 Future work

The recommendations of future research, based on the findings of this PhD thesis Dissertation are:

- a) To investigate the effect of a higher culture pH on *Chlorella vulgaris* growth rate, in the *PhotoBioCREC* unit using sodium bicarbonate solutions as the microalgae growth media.
- b) To optimize the alumina particle concentration in the *PhotoBioCREC Swirl Reactor* that in combination with the promoted swirl flow, can maintain the reactor walls clean, during microalgae growth, ensuring a constant irradiation transmittance.
- c) To investigate microalgae growth in the *PhotoBioCREC Swirl Reactor*, combining CFD simulation and the kinetic model reported in this PhD Dissertation.
- d) To characterize microalgae biomass obtained with the different sodium bicarbonate concentrations including carbohydrates, lipids, proteins, and calorific values

9.3 Research Outcomes

The research objectives presented in Chapter 3 of this PhD Dissertation were met, and the results obtained from this research were published as a research paper, with a second one pending publication. M. Cordoba-Perez is the first author for both articles. In addition, there was a conference presentation that was made by the same author, based on the outcomes of this research.

- **Cordoba-Perez, M.**; de Lasa, H. CO₂ Derived Carbon Capture Using Microalgae and Sodium Bicarbonate in a *PhotoBioCREC* Unit: Kinetic Modeling. *Processes*. 2021; 9(8):1296. <https://doi.org/10.3390/pr9081296>
- **Cordoba-Perez, M.**; de Lasa, Hugo. CO₂-Derived Carbon Capture and Photon Absorption Efficiency by Microalgae in Novel *PhotoBioCREC*. *Industrial and Engineering Chemistry Research*, 2020, 59 (33), 14710-14716. <https://doi.org/10.1021/acs.iecr.0c02319>
- **Cordoba-Perez, M.**; de Lasa, H. CO₂ Capture and Photon Absorption Efficiency by Microalgae in Novel *PhotoBioCREC*. Canadian Chemical Engineering Conference 2020. Ottawa, Canada, October 2020 (held Virtually due to COVID-19)

Bibliography

- Abdel-Raouf, N., Al-Homaidan, A. A., & Ibraheem, I. B. M. (2012). Microalgae and wastewater treatment. *Saudi Journal of Biological Sciences*, 19(3), 257–275. <https://doi.org/10.1016/j.sjbs.2012.04.005>
- Abedini, H., Malekzadeh, M., Jalilian, F., & Vossoughi, M. (2015). Effect of various carbon sources on biomass and lipid production of *Chlorella vulgaris* during nutrient sufficient and nitrogen starvation conditions. *Bioresource Technology*, 180, 311–317. <https://doi.org/10.1016/j.biortech.2014.12.076>
- Acién Fernández, F. G., Fernández Sevilla, J. M., & Molina Grima, E. (2013). Photobioreactors for the production of microalgae. *Reviews in Environmental Science and Biotechnology*, 12, 131–151. <https://doi.org/10.1007/s11157-012-9307-6>
- Adamczyk, M., Lasek, J., & Skawińska, A. (2016). CO₂ Biofixation and Growth Kinetics of *Chlorella vulgaris* and *Nannochloropsis gaditana*. *Applied Biochemistry and Biotechnology*, 179(7), 1248–1261. <https://doi.org/10.1007/s12010-016-2062-3>
- Aizawa, K., & Miyachi, S. (1986). Carbonic anhydrase and CO₂ concentrating mechanisms in microalgae and cyanobacteria. *FEMS Microbiology Letters*, 39(3), 215–233. <https://doi.org/10.1111/j.1574-6968.1986.tb01860.x>
- Almomani, F. A. (2019). Assessment and modeling of microalgae growth considering the effects OF CO₂, nutrients, dissolved organic carbon and solar irradiation. *Journal of Environmental Management*, 247 (June), 738–748. <https://doi.org/10.1016/j.jenvman.2019.06.085>
- Altuglas International. (2016). *Plexiglas optical and transmission characteristics*. <https://www.plexiglas.com/en/literature/literature-plexiglas-sheet/>
- Andersen, R. A. (2005). Algal Culturing Techniques. In R. A. Andersen (Ed.), *Elsevier Inc. Elsevier Inc.*
- Andrews, J. F. (1968). A mathematical model for the continuous culture of microorganisms utilizing inhibitory substrates. *Biotechnology and Bioengineering*, 10(6), 707–723. <https://doi.org/10.1002/bit.260100602>
- Arif, M., Li, Y., El-Dalatony, M. M., Zhang, C., Li, X., & Salama, E. S. (2021). A complete characterization of microalgal biomass through FTIR/TGA/CHNS analysis: An approach for biofuel generation and nutrients removal. *Renewable Energy*, 163, 1973–1982. <https://doi.org/10.1016/j.renene.2020.10.066>
- Barahoei, M., Hatamipour, M. S., & Afsharzadeh, S. (2020). CO₂ capturing by *chlorella vulgaris* in a bubble column photo-bioreactor; Effect of bubble size on CO₂ removal and growth rate. *Journal of CO₂ Utilization*, 37, 9–19. <https://doi.org/10.1016/j.jcou.2019.11.023>
- Blanch, H. W. W., Clark, D. S. S., & Clarck, D. S. (1996). *Biochemical Engineering*. Marcel Dekker, Inc.

- Bolton, J. R., & Hall, D. O. (1991). The Maximum Efficiency of Photosynthesis. *Photochemistry and Photobiology*, 53(4), 545–548. <https://doi.org/10.1111/j.1751-1097.1991.tb03668.x>
- Buis, A. (2019). NASA's Jet Propulsion Laboratory. The Atmosphere: Getting a Handle on Carbon Dioxide. <https://climate.nasa.gov/news/2915/the-atmosphere-getting-a-handle-on-carbon-dioxide/>
- Carvalho, J., Matsudo, M., Bezerra, R., Ferreira-Camargo, L., & Sato, S. (2014). Microalgae Bioreactors. In R. Bajpai, A. Prokop, & M. Zappi (Eds.), *Algal Biorefineries: Volume 1: Cultivation of Cells and Products* (pp. 83–126). Springer Dordrecht Heidelberg.
- Chang, H.-X., Huang, Y., Fu, Q., Liao, Q., & Zhu, X. (2016). Kinetic characteristics and modeling of microalgae *Chlorella vulgaris* growth and CO₂ biofixation considering the coupled effects of light intensity and dissolved inorganic carbon. *BIORESOURCE TECHNOLOGY*, 206, 231–238. <https://doi.org/10.1016/j.biortech.2016.01.087>
- Chi, Z., Fallon, J. V. O., & Chen, S. (2011). Bicarbonate produced from carbon capture for algae culture. *Trends in Biotechnology*, 29(11), 537–541. <https://doi.org/10.1016/j.tibtech.2011.06.006>
- Chi, Z., Xie, Y., Elloy, F., Zheng, Y., Hu, Y., & Chen, S. (2013). Bicarbonate-based Integrated Carbon Capture and Algae Production System with alkalihalophilic cyanobacterium. *Bioresource Technology*, 133, 513–521. <https://doi.org/10.1016/j.biortech.2013.01.150>
- Chisti, Y. (2007). Biodiesel from microalgae. *Biotechnology Advances*, 25, 294–306. <https://doi.org/10.1016/j.tibtech.2007.12.002>
- Chisti, Y. (2016). Large-Scale Production of Algal Biomass: Photobioreactors. In F. Bux & Y. Chisti (Eds.), *Algae Biotechnology. Products and Processes* (pp. 21–40). Springer International Publishing Switzerland. https://doi.org/10.1007/978-3-319-12334-9_3
- Chiu, S. Y., Kao, C. Y., Huang, T. T., Lin, C. J., Ong, S. C., Chen, C. Da, Chang, J. S., & Lin, C. S. (2011). Microalgal biomass production and on-site bioremediation of carbon dioxide, nitrogen oxide and sulfur dioxide from flue gas using *Chlorella sp.* cultures. *Bioresource Technology*, 102(19), 9135–9142. <https://doi.org/10.1016/j.biortech.2011.06.091>
- Christenson, L., & Sims, R. (2011). Production and harvesting of microalgae for wastewater treatment, biofuels, and bioproducts. *Biotechnology Advances*, 29(6), 686–702. <https://doi.org/10.1016/j.biotechadv.2011.05.015>
- Chun-Yen, C., Yeh, K.-L., Huei-Meei, S., Yung-Chung, L., Wen-Ming, C., & Jo-Shu, C. (2010). Strategies to Enhance Cell Growth and Achieve High-Level Oil Production of a *Chlorella vulgaris* Isolate. *Biotechnology Progress*, 26(3), 679–686. <https://doi.org/10.1002/btpr.381>

- Colman, B., & Rotatore, C. (1995). *Photosynthetic inorganic carbon uptake and accumulation in two marine diatoms.* 18, 919–924.
- Converti, A., Casazza, A. A., Ortiz, E. Y., Perego, P., & Del Borghi, M. (2009). Effect of temperature and nitrogen concentration on the growth and lipid content of *Nannochloropsis oculata* and *Chlorella vulgaris* for biodiesel production. *Chemical Engineering and Processing: Process Intensification*, 48(6), 1146–1151. <https://doi.org/10.1016/j.cep.2009.03.006>
- Cordoba-Perez, M., & De Lasa, H. (2020). CO₂-derived carbon capture and photon absorption efficiency by microalgae in novel *PhotoBioCREC*. *Industrial and Engineering Chemistry Research*, 59(33), 14710–14716. <https://doi.org/10.1021/acs.iecr.0c02319>
- De Godos, I., González, C., Becares, E., García-Encina, P. A., & Muñoz, R. (2009). Simultaneous nutrients and carbon removal during pretreated swine slurry degradation in a tubular biofilm photobioreactor. *Applied Microbiology and Biotechnology*, 82(1), 187–194. <https://doi.org/10.1007/s00253-008-1825-3>
- de Lasa, H., Serrano, B., & Salaices, M. (2005). *Photocatalytic Reaction Engineering*. Springer Science+Business Media New York.
- de Morais, M. G., & Costa, J. A. V. (2007). Carbon dioxide fixation by *Chlorella kessleri*, *C. vulgaris*, *Scenedesmus obliquus* and *Spirulina sp.* cultivated in flasks and vertical tubular photobioreactors. *Biotechnology Letters*, 29(9), 1349–1352. <https://doi.org/10.1007/s10529-007-9394-6>
- Devgoswami, C., Kalita, M. C., Talukdar, J., Bora, R., & Sharma, P. (2011). Studies on the growth behavior of *Chlorella*, *Haematococcus* and *Scenedesmus sp.* in culture media with different concentrations of sodium bicarbonate and carbon dioxide gas. *African Journal of Biotechnology*, 10(61), 13128–13138. <https://doi.org/10.5897/AJB11.888>
- Dillschneider, R., & Posten, C. (2013). Closed Bioreactors as Tools for Microalgae. In J. W. Lee (Ed.), *Advanced Biofuels and Bioproducts* (Vol. 9781461433, pp. 1–1122). Springer Science+Business Media New York. <https://doi.org/10.1007/978-1-4614-3348-4>
- Duan, Y., & Shi, F. (2014). Bioreactor design for algal growth as a sustainable energy source. In F. Shi (Ed.), *Reactor and process design in sustainable energy technology*. Elsevier B.V.
- Emerson, R. (1958). The quantum yield of photosynthesis. *Annual Review of Plant Physiology*, 9(1), 1–24. [https://doi.org/10.1016/0014-5793\(90\)81390-A](https://doi.org/10.1016/0014-5793(90)81390-A)
- Emerson, R., & Lewis, C. M. (1941). Carbon Dioxide Exchange and the Measurement of the Quantum Yield of Photosynthesis. *American Journal of Botany*, 28(9), 789–804.

- Falkowski, P. G., & Raven, J. A. (2007). Aquatic Photosynthesis. In *Aquatic Photosynthesis* (Second edi). Princeton University Press. <https://doi.org/10.1515/9781400849727>
- Fayyaz, M., Chew, K. W., Show, P. L., Ling, T. C., Ng, I. S., & Chang, J. S. (2020). Genetic engineering of microalgae for enhanced biorefinery capabilities. *Biotechnology Advances*, 43(May), 107554. <https://doi.org/10.1016/j.biotechadv.2020.107554>
- Gharabaghi, M., Delavai Amrei, H., Moosavi Zenooz, A., Shahrivar Guzullo, J., & Zokaei Ashtiani, F. (2015). Biofuels: Bioethanol, Biodiesel, Biogas, Biohydrogen from Plants and Microalgae. In R. D. Lichtfouse E., Schwarzbauer J. (Ed.), *CO₂ Sequestration, Biofuels and Depollution* (pp. 234–252). Springer, Cham. https://doi.org/https://doi.org/10.1007/978-3-319-11906-9_6
- Giordano, M., Beardall, J., & Raven, J. A. (2005). CO₂ CONCENTRATING MECHANISMS IN ALGAE: Mechanisms, Environmental Modulation, and Evolution. *Annual Review of Plant Biology*, 56(1), 99–131. <https://doi.org/10.1146/annurev.arplant.56.032604.144052>
- Godbole, V., Pal, M. K., & Gautam, P. (2021). A critical perspective on the scope of interdisciplinary approaches used in fourth-generation biofuel production. *Algal Research*, 58(May), 102436. <https://doi.org/10.1016/j.algal.2021.102436>
- Gonçalves, A. L., Pires, J. C. M., & Simões, M. (2017). A review on the use of microalgal consortia for wastewater treatment. *Algal Research*, 24, 403–415. <https://doi.org/10.1016/j.algal.2016.11.008>
- González-López, C. V., Acién Fernández, F. G., Fernández-Sevilla, J. M., Sánchez Fernández, J. F., & Molina Grima, E. (2012). Development of a process for efficient use of CO₂ from flue gases in the production of photosynthetic microorganisms. *Biotechnology and Bioengineering*, 109(7), 1637–1650. <https://doi.org/10.1002/bit.24446>
- Gouveia, L. (2011). Microalgae as a Feedstock for biofuels. In *Microalgae as Feedstock for Biofuels*. <https://doi.org/10.1007/978-3-642-17997-6>
- Govindjee, R., Rabinowitch, E., & Govindjee. (1968). Maximum quantum yield and action spectrum of photosynthesis and fluorescence in *chlorella*. *Biochimica et Biophysica Acta*, 162(4), 539–544. [https://doi.org/10.1016/0005-2728\(68\)90061-3](https://doi.org/10.1016/0005-2728(68)90061-3)
- Graham, L. E., Graham, J. M., & Wilcox, L. W. (2009). *Algae* (L. W. Wilcox (ed.); 2nd ed). Pearson Benjaming Cummings.
- Gris, B., Sforza, E., Vecchiato, L., & Bertucco, A. (2014). Development of a process for an efficient exploitation of CO₂ captured from flue gases as liquid carbonates for chlorella protothecoides cultivation. *Industrial and Engineering Chemistry Research*, 53, 16678–16688. <https://doi.org/10.1021/ie502336d>

- Gupta, P. L., Lee, S. M., & Choi, H. J. (2015). A mini review: photobioreactors for large scale algal cultivation. *World Journal of Microbiology and Biotechnology*, 31(9), 1409–1417. <https://doi.org/10.1007/s11274-015-1892-4>
- Hage, D. S., & Carr, J. D. (2011). *Analytical Chemistry and Quantitative Analysis*. Prentice Hall.
- Harel, M., & Place, A. R. (2004). Heterotrophic Production of Marine Algae for Aquaculture. In *Handbook of Microalgal Culture* (pp. 513–524). <https://doi.org/10.1002/9780470995280.ch31>
- Ho, S. H., Chen, C. Y., Lee, D. J., & Chang, J. S. (2011). Perspectives on microalgal CO₂-emission mitigation systems-A review. *Biotechnology Advances*, 29(2), 189–198. <https://doi.org/10.1016/j.biotechadv.2010.11.001>
- Hu, Q. (2004). Environmental Effects on Cell Composition. In A. Richmond (Ed.), *Handbook of Microalgal Culture: Biotechnology and Applied Phycology* (pp. 83–93). Blackwell Publishing Ltd. <https://doi.org/10.1002/9780470995280.ch5>
- Huertas, I. E., Colman, B., Espie, G. S., & Lubian, L. M. (2000). Active Transport of CO₂ by three species of marine microalgae. *Journal of Phycology*, 36, 314–320.
- IEA. (2020). *Key World Energy Statistics 2020*, IEA, Paris. <https://www.iea.org/reports/key-world-energy-statistics-2020>
- IPCC. (2014). Summary for Polymakers. In: Climate Change 2014: Mitigation of Climate change. Contribution of Working Group III to the Fifth Assessment Report of the intergovernmental Panel on Climate Change. In Panel on Climate Change. <https://doi.org/10.4324/9781315071961-11>
- Jacob-Lopes, E., Gimenes Scoparo, C. H., & Teixeira Franco, T. (2008). Rates of CO₂ removal by Aphanothecace microscopica Nägeli in tubular photobioreactors. *Chemical Engineering and Processing: Process Intensification*, 47(8), 1365–1373. <https://doi.org/10.1016/j.cep.2007.06.004>
- Jutidamrongphan, W., Park, K. Y., Lee, K., Kim, D., Lim, B. R., & Lee, J. W. (2015). Effect of carbon dioxide injection on photosynthetic wastewater treatment using microalgae *Chlorella vulgaris* and *Euglena gracilis*. *Desalination and Water Treatment*, 54(13), 3654–3660. <https://doi.org/10.1080/19443994.2014.923197>
- Kaplan, A., & Reinhold, L. (1999). CO₂ Concentrating Mechanisms in Microorganisms. *Annual Review Plant Physiology Plant Molecular Biology*, 50, 539–570. <https://doi.org/10.1139/b05-907>
- Keffer, J. E., & Kleinheinz, G. T. (2002). Use of Chlorella vulgaris for CO₂ mitigation in a photobioreactor. *Journal of Industrial Microbiology and Biotechnology*, 29(5), 275–280. <https://doi.org/10.1038/sj.jim.7000313>
- Kim, G., Heo, J., Kim, H., & Han, J. (2017). Bicarbonate-based cultivation of *Dunaliella salina* for enhancing carbon utilization efficiency. *Bioresource Technology*, 237, 72–77. <https://doi.org/10.1016/j.biortech.2017.04.009>

- Kong, B., & Vigil, R. D. (2014). Simulation of photosynthetically active radiation distribution in algal photobioreactors using a multidimensional spectral radiation model. *Bioresource Technology*, 158, 141–148. <https://doi.org/10.1016/j.biortech.2014.01.052>
- Kumar, K., Banerjee, D., & Das, D. (2014). Carbon dioxide sequestration from industrial flue gas by Chlorella sorokiniana. *Bioresource Technology*, 152, 225–233. <https://doi.org/10.1016/j.biortech.2013.10.098>
- Kumar, K., & Das, D. (2012). Growth characteristics of *Chlorella sorokiniana* in airlift and bubble column photobioreactors. *Bioresource Technology*, 116, 307–313. <https://doi.org/10.1016/j.biortech.2012.03.074>
- Kumar, K., Dasgupta, C. N., Nayak, B., Lindblad, P., & Das, D. (2011). Development of suitable photobioreactors for CO₂ sequestration addressing global warming using green algae and cyanobacteria. *Bioresource Technology*, 102(8), 4945–4953. <https://doi.org/10.1016/j.biortech.2011.01.054>
- Kumar, K., Mishra, S. K., Shrivastav, A., Park, M. S., & Yang, J. W. (2015). Recent trends in the mass cultivation of algae in raceway ponds. *Renewable and Sustainable Energy Reviews*, 51, 875–885. <https://doi.org/10.1016/j.rser.2015.06.033>
- Kumar, M., Jeon, J., Choi, J., & Kim, S. R. (2018). Rapid and efficient genetic transformation of the green microalga Chlorella vulgaris. *Journal of Applied Phycology*, 30(3), 1735–1745. <https://doi.org/10.1007/s10811-018-1396-3>
- Kumar, P. K., Vijaya Krishna, S., Verma, K., Pooja, K., Bhagawan, D., & Himabindu, V. (2018). Phycoremediation of sewage wastewater and industrial flue gases for biomass generation from microalgae. *South African Journal of Chemical Engineering*, 25, 133–146. <https://doi.org/10.1016/j.sajce.2018.04.006>
- Lam, M. K., & Lee, K. T. (2013). Effect of carbon source towards the growth of Chlorella vulgaris for CO₂ bio-mitigation and biodiesel production. *International Journal of Greenhouse Gas Control*, 14, 169–176. <https://doi.org/10.1016/j.ijggc.2013.01.016>
- Lam, M. K., Lee, K. T., & Mohamed, A. R. (2012). Current status and challenges on microalgae-based carbon capture. *International Journal of Greenhouse Gas Control*, 10, 456–469. <https://doi.org/10.1016/j.ijggc.2012.07.010>
- Lanfer Marquez, U. M., & Borrmann, D. (2009). Chlorophylls. In T. Bechtold & R. Mussak (Eds.), *Handbook of Natural Colorants of Natural Colorants* (pp. 243–252).
- Lara-Gil, J. A., Álvarez, M. M., & Pacheco, A. (2014). Toxicity of flue gas components from cement plants in microalgae CO₂ mitigation systems. *Journal of Applied Phycology*, 26(1), 357–368. <https://doi.org/10.1007/s10811-013-0136-y>

- Lee, E., Jalalizadeh, M., & Zhang, Q. (2015). Growth kinetic models for microalgae cultivation: A review. *Algal Research*, 12, 497–512. <https://doi.org/10.1016/j.algal.2015.10.004>
- Li, J., Li, C., Lan, C. Q., & Liao, D. (2018). Effects of sodium bicarbonate on cell growth, lipid accumulation, and morphology of *Chlorella vulgaris*. *Microbial Cell Factories*, 17, 1–10.
- Liu, B. H., & Lee, Y. K. (2000). Secondary carotenoids formation by the green alga *Chlorococcum* sp. *Journal of Applied Phycology*, 12(3–5), 301–307. <https://doi.org/10.1023/a:1008185212724>
- Liu, X., Ying, K., Chen, G., Zhou, C., Zhang, W., Zhang, X., Cai, Z., Holmes, T., & Tao, Y. (2017). Growth of *Chlorella vulgaris* and nutrient removal in the wastewater in response to intermittent carbon dioxide. *Chemosphere*, 186, 977–985. <https://doi.org/10.1016/j.chemosphere.2017.07.160>
- Lewis, N. S., & Nocera, D. G. (2006). Powering the planet: Chemical challenges in solar energy utilization. *Proceedings of the National Academy of Science of the United States of America*, 103(43), 15729–15735.
- Li, Y., Horsman, M., Wu, N., Lan, C. Q., & Dubois-Calero, N. (2008). Biofuels from microalgae. *Biotechnology Progress*, 24(4), 815–819. <https://doi.org/10.1021/bp.070371k>
- Liu, B. H., & Lee, Y. K. (2000). Secondary carotenoids formation by the green alga *Chlorococcum* sp. *Journal of Applied Phycology*, 12(3–5), 301–307. <https://doi.org/10.1023/a:1008185212724>
- Lizzul, A. M., Hellier, P., Purton, S., Baganz, F., Ladommato, N., & Campos, L. (2014). Combined remediation and lipid production using *Chlorella sorokiniana* grown on wastewater and exhaust gases. *Bioresource Technology*, 151, 12–18. <https://doi.org/10.1016/j.biortech.2013.10.040>
- Lohman, E. J., Gardner, R. D., Pedersen, T., Peyton, B. M., Cooksey, K. E., & Gerlach, R. (2015). Optimized inorganic carbon regime for enhanced growth and lipid accumulation in *Chlorella vulgaris*
- Luisa Gouveia. Biotechnology for Biofuels, 8(1), 1–13. <https://doi.org/10.1186/s13068-015-0265-4>
- Long, S. P., Zhu, X. G., Naidu, S. L., & Ort, D. R. (2006). Can improvement in photosynthesis increase crop yields? *Plant, Cell and Environment*, 29(3), 315–330. <https://doi.org/10.1111/j.1365-3040.2005.01493.x>
- Loubière, K., Olivo, E., Bougaran, G., Pruvost, J., Robert, R., & Legrand, J. (2008). A new photobioreactor for continuous microalgal production in hatcheries based on external-loop airlift and swirling flow. *Biotechnology and Bioengineering*, 102(1), 132–147. <https://doi.org/10.1002/bit.22035>

- Markager, S. (1993). Light Absorption and Quantum Yield for Growth in Five Species of Marine Macroalga. *Journal of Phycology*, 29(1), 54–63. <https://doi.org/10.1111/j.1529-8817.1993.tb00279.x>
- Martínez, M. E., Jiménez, J. M., & El Yousfi, F. (1999). Influence of phosphorus concentration and temperature on growth and phosphorus uptake by the microalga *Scenedesmus obliquus*. *Bioresource Technology*, 67(3), 233–240. [https://doi.org/10.1016/S0960-8524\(98\)00120-5](https://doi.org/10.1016/S0960-8524(98)00120-5)
- Masahiko, M., Watanabe, Y., & Saiki, H. (2000). High Photosynthetic productivity of Green Microalga *Chlorella sorokiniana*. *Applied Biochemistry and Biotechnology*, 87, 203–218.
- Masojídek, J., Torzillo, G., Koblížek, M., & Torzillo, G. (2013). Photosynthesis in Microalgae. Handbook of Microalgal Culture: *Applied Phycology and Biotechnology*, April 21–36. <https://doi.org/10.1002/9781118567166.ch2>
- Matsumoto, H., Hamasaki, A., Sioji, N., & Ikuta, Y. (1997). Influence of CO₂, SO₂ and no in flue gas on microalgae productivity. In *Journal of Chemical Engineering of Japan* (Vol. 30, Issue 4, pp. 620–624). <https://doi.org/10.1252/jcej.30.620>
- Mauzerall, D. (2013). Thermodynamics of primary photosynthesis. *Photosynthesis Research*, 116(2–3), 363–366. <https://doi.org/10.1007/s11120-013-9919-x>
- Melis, A. (2009). Solar energy conversion efficiencies in photosynthesis: Minimizing the chlorophyll antennae to maximize efficiency. *Plant Science*, 177(177), 272–280. <https://doi.org/10.1016/j.plantsci.2009.06.005>
- Metting, F. B. (1996). Biodiversity and application of microalgae. *Journal of Industrial Microbiology and Biotechnology*, 17(5–6), 477–489. <https://doi.org/10.1007/bf01574779>
- Mokashi, K., Shetty, V., George, S. A., & Sibi, G. (2016). Sodium Bicarbonate as Inorganic Carbon Source for Higher Biomass and Lipid Production Integrated Carbon Capture in *Chlorella vulgaris*. *Achievements in the Life Sciences*. <https://doi.org/10.1016/j.als.2016.05.011>
- Molina Grima, E., Acién Fernández, F. G., & Robles Medina, A. (2013). Downstream Processing of Cell Mass and Products. In A. Richmond & Q. Hu (Eds.), *Handbook of Microalgal Culture: applied phycology and biotechnology* (Second Edi, pp. 267–309). Wiley.
- Monod, J. (1949). The Growth of Bacterial Cultures. *Annual Reviews in Microbiology*, 3(1), 371–394.
- Morita, M., Watanabe, Y., & Saiki, H. (2001). Evaluation of photobioreactor heat balance for predicting changes in culture medium temperature due to light irradiation. *Biotechnology and Bioengineering*, 74(6), 466–475. <https://doi.org/10.1002/bit.1137>

- Moroney, J. V., & Somanchi, A. (2002). How Do Algae Concentrate CO₂ to Increase the Efficiency of Photosynthetic Carbon Fixation? *Plant Physiology*, 119(1), 9–16. <https://doi.org/10.1104/pp.119.1.9>
- Negoro, M., Shioji, N., Miyamoto, K., & Micira, Y. (1991). Growth of Microalgae in High CO₂ Gas and Effects of SOX and NOX. *Applied Biochemistry and Biotechnology*, 28–29(1), 877–886. <https://doi.org/10.1007/BF02922657>
- Norashikin, M. N., Loh, S. H., Aziz, A., & Cha, T. S. (2018). Metabolic engineering of fatty acid biosynthesis in *Chlorella vulgaris* using an endogenous omega-3 fatty acid desaturase gene with its promoter. *Algal Research*, 31(February), 262–275. <https://doi.org/10.1016/j.algal.2018.02.020>
- Novak, J. T., & Brune, D. E. (1985). Inorganic carbon limited growth kinetics of some freshwater algae. *Water Research*, 19(2), 215–225. [https://doi.org/10.1016/0043-1354\(85\)90203-9](https://doi.org/10.1016/0043-1354(85)90203-9)
- Nwoba, E. G., Parlevliet, D. A., Laird, D. W., Alameh, K., & Moheimani, N. R. (2019). Light management technologies for increasing algal photobioreactor efficiency. *Algal Research*, 39(January), 101433. <https://doi.org/10.1016/j.algal.2019.101433>
- Olivieri, G., Salatino, P., & Marzocchella, A. (2014). Advances in photobioreactors for intensive microalgal production: Configurations, operating strategies and applications. *Journal of Chemical Technology and Biotechnology*, 89(2), 178–195. <https://doi.org/10.1002/jctb.4218>
- Pandey, A., Lee, D.-J., Chisti, Y., & Soccoll, C. R. (Eds.). (2014a). *Biofuels from microalgae* (First Edit). Elsevier B.V.
- Pandey, A., Lee, D. J., Chisti, Y., & Soccoll, C. R. (Eds.). (2014b). *Biofuels from Algae* (First edit). Elsevier B.V.
- Percopo, I., Montresor, M., Taxonomy, D. S., Zoologica, S., & Dohrn, A. (1997). *Microalgae preparation for scanning electron microscopy: Dehydration*. <https://www.assemblemarine.org/assets/Uploads/Documents/tool-box/Preparation-for-Scanning-Electron-Microscopy1.pdf>
- Perry, S., Perry, R. H., Green, D. W., & Maloney, J. O. (1997). Perry's chemical engineers' handbook. In *Choice Reviews Online* (7th ed., Vol. 38, Issue 02). McGraw-Hill. <https://doi.org/10.5860/choice.38-0966>
- Pires, J. C. M., Alvim-Ferraz, M. C. M., Martins, F. G., & Simões, M. (2012). Carbon dioxide capture from flue gases using microalgae: Engineering aspects and biorefinery concept. *Renewable and Sustainable Energy Reviews*, 16(5), 3043–3053. <https://doi.org/10.1016/j.rser.2012.02.055>
- Pruvost, J., Legrand, J., Legentilhomme, P., & Muller-Feuga, A. (2002). Lagrangian trajectory model for turbulent swirling flow in an annular cell: Comparison with residence time distribution measurements. *Chemical Engineering Science*, 57(7), 1205–1215. [https://doi.org/10.1016/S0009-2509\(02\)00009-X](https://doi.org/10.1016/S0009-2509(02)00009-X)

- Raheem, A., Sivasangar, S., Wan Azlina, W. A. K. G., Taufiq Yap, Y. H., Danquah, M. K., & Harun, R. (2015). Thermogravimetric study of *Chlorella vulgaris* for syngas production. *Algal Research*, 12, 52–59. <https://doi.org/10.1016/j.algal.2015.08.003>
- Rasmussen, M., & Minteer, S. D. (2014). Photobioelectrochemistry: Solar Energy Conversion and Biofuel Production with Photosynthetic Catalysts. *Journal of The Electrochemical Society*, 161(10), H647–H655. <https://doi.org/10.1149/2.0651410jes>
- Razzak, S. A., Ali, S. A. M., Hossain, M. M., & de Lasa, H. (2017). Biological CO₂ fixation with production of microalgae in wastewater – A review. *Renewable and Sustainable Energy Reviews*, 76(March), 379–390. <https://doi.org/10.1016/j.rser.2017.02.038>
- Razzak, S. A., Hossain, M. M., Lucky, R. A., Bassi, A. S., & de Lasa, H. I. (2013). Integrated CO₂ capture, wastewater treatment and biofuel production by microalgae culturing - A review. *Renewable and Sustainable Energy Reviews*, 27, 622–653. <https://doi.org/10.1016/j.rser.2013.05.063>
- Rosa, G. M. da, Moraes, L., Cardias, B. B., Souza, M. da R. A. Z. de, & Costa, J. A. V. (2015). Chemical absorption and CO₂ biofixation via the cultivation of *Spirulina* in semicontinuous mode with nutrient recycle. *Bioresource Technology*, 192, 321–327. <https://doi.org/10.1016/j.biortech.2015.05.020>
- Sa, C., Zebib, B., Merah, O., & Pontalier, P. (2014). Morphology, composition, production, processing and applications of *Chlorella vulgaris*: A review. *Renewable and Sustainable Energy Reviews*, 35, 265–278. <https://doi.org/10.1016/j.rser.2014.04.007>
- Sayre, R. (2010). Microalgae: The Potential for Carbon Capture. *BioScience*, 60(9), 722–727. <https://doi.org/10.1525/bio.2010.60.9.9>
- Shi, F. (Ed.). (2014). Bioreactor design for algal growth as a sustainable energy source. In *Reactor and process design in sustainable energy technology*. Elsevier B.V.
- Singh, J., & Dhar, D. W. (2019). Overview of carbon capture technology: Microalgal biorefinery concept and state-of-the-art. *Frontiers in Marine Science*, 6(FEB), 1–9. <https://doi.org/10.3389/fmars.2019.00029>
- Singh, S. P., & Singh, P. (2015). Effect of temperature and light on the growth of algae species: A review. *Renewable and Sustainable Energy Reviews*, 50, 431–444. <https://doi.org/10.1016/j.rser.2015.05.024>
- Solovchenko, A., & Khozin-Goldberg, I. (2013). High-CO₂ tolerance in microalgae: Possible mechanisms and implications for biotechnology and bioremediation. *Biotechnology Letters*, 35(11), 1745–1752. <https://doi.org/10.1007/s10529-013-1274-7>

- Spalding, M. H. (2008). Microalgal carbon-dioxide-concentrating mechanisms: Chlamydomonas inorganic carbon transporters. *Journal of Experimental Botany*, 59(7), 1463–1473. <https://doi.org/10.1093/jxb/erm128>
- Spolaore, P., Joannis-Cassan, C., Duran, E., & Isambert, A. (2006). Commercial applications of microalgae. *Journal of Bioscience and Bioengineering*, 101(2), 87–96. <https://doi.org/10.1263/jbb.101.87>
- Sproles, A. E., Fields, F. J., Smalley, T. N., Le, C. H., Badary, A., & Mayfield, S. P. (2021). Recent advancements in the genetic engineering of microalgae. *Algal Research*, 53(December 2020), 102158. <https://doi.org/10.1016/j.algal.2020.102158>
- Stein, J. (Ed.). (1973). *Handbook of Phycological methods. Culture methods and growth measurements*. Cambridge University Press.
- Stocker, T. ., Qin, D., Plattner, G.-K., Alexander, L. ., Allen, S. K., Bindoff, N. ., Breón, F.-M., Church, J. A., Cubasch, U., Emori, S., Foster, P., Friedlingstein, P., & Gillet, N. (2013). Technical Summary In: Climate Change 2013: The physical Science Basis. Contribution of working Group I to the Fifth Assessment Report of the Intergovernmental Panel on climate change. In Climate Change 2013 - The Physical Science Basis. <https://doi.org/10.1017/cbo9781107415324.005>
- Talebi, A. F., Tohidfar, M., Tabatabaei, M., Bagheri, A., Mohsenpor, M., & Mohtashami, S. K. (2013). Genetic manipulation, a feasible tool to enhance unique characteristic of *Chlorella vulgaris* as a feedstock for biodiesel production. *Molecular Biology Reports*, 40(7), 4421–4428. <https://doi.org/10.1007/s11033-013-2532-4>
- Taylor, T. G., & Tainter, J. A. (2016). The Nexus of Population, Energy, Innovation, and Complexity. *American Journal of Economics and Sociology*, 75(4), 1005–1043. <https://doi.org/10.1111/ajes.12162>
- Thomas, D. M., Mechery, J., & Paulose, S. V. (2016). Carbon dioxide capture strategies from flue gas using microalgae: a review. *Environmental Science and Pollution Research*, 23, 16926–16940. <https://doi.org/10.1007/s11356-016-7158-3>
- Torzillo, G., & Vonshak, A. (2013). Environmental Stress Physiology with Reference to mass culture. In A. Richmond & Q. Hu (Eds.), *Handbook of Microalgal Culture. Applied phycology and biotechnology* (Second edi, pp. 90–113). Wiley.
- Tu, Z., Liu, L., Lin, W., Xie, Z., & Luo, J. (2018). Potential of using sodium bicarbonate as external carbon source to cultivate microalga in non-sterile condition. *Bioresource Technology*, 266(June), 109–115. <https://doi.org/10.1016/j.biortech.2018.06.076>
- U.S. DOE 2010. National Algal Biofuels Technology Roadmap. U.S. Department of Energy, Office of Energy Efficiency and Renewable Energy, Biomass Program. Visit <http://biomass.energy.gov> for more information

- Vadlamani, A., Pendyala, B., Viamajala, S., & Varanasi, S. (2019). High Productivity Cultivation of Microalgae without Concentrated CO₂ Input. *ACS Sustainable Chemistry and Engineering*, 7(2), 1933–1943. <https://doi.org/10.1021/acssuschemeng.8b04094>
- Vadlamani, A., Viamajala, S., Pendyala, B., & Varanasi, S. (2017). Cultivation of Microalgae at Extreme Alkaline pH Conditions: A Novel Approach for Biofuel Production. *ACS Sustainable Chemistry and Engineering*, 5, 7284–7294. <https://doi.org/10.1021/acssuschemeng.7b01534>
- Valades-Pelayo, P. J. (2014). Scale-Up Methodology for Bench-Scale Slurry Photocatalytic Reactors Using Combined Irradiation and Kinetic Modelling [Western University]. In *Electronic Thesis and Dissertation Repository*. <https://doi.org/10.1016/j.ces.2013.12.013>
- Valadés-Pelayo, P. J., Guayaquil Sosa, F., Serrano, B., & de Lasa, H. (2015). Photocatalytic reactor under different external irradiance conditions: Validation of a fully predictive radiation absorption model. *Chemical Engineering Science*, 126, 42–54. <https://doi.org/10.1016/j.ces.2014.12.003>
- Vuppaldadiyam, A. K., Yao, J. G., Florin, N., George, A., Wang, X., Labeeuw, L., Jiang, Y., Davis, R. W., Abbas, A., Ralph, P., Fennell, P. S., & Zhao, M. (2018). Impact of Flue Gas Compounds on Microalgae and Mechanisms for Carbon Assimilation and Utilization. *ChemSusChem*, 11(2), 334–355. <https://doi.org/10.1002/cssc.201701611>
- Wang, B., Lan, C. Q., & Horsman, M. (2012). Closed photobioreactors for production of microalgal biomasses. *Biotechnology Advances*, 30(4), 904–912. <https://doi.org/10.1016/j.biotechadv.2012.01.019>
- Wang, B., Li, Y., Wu, N., & Lan, C. Q. (2008). CO₂ bio-mitigation using microalgae. *Applied Microbiology and Biotechnology*, 79(5), 707–718. <https://doi.org/10.1007/s00253-008-1518-y>
- White, D., Pagarette, A., Rooks, P., & Ali, S. T. (2013). The effect of sodium bicarbonate supplementation on growth and biochemical composition of marine microalgae cultures. *Journal of Applied Phycology*, 25, 153–165. <https://doi.org/10.1007/s10811-012-9849-6>
- Yadav, G., Karemire, A., Dash, S. K., & Sen, R. (2015). Performance evaluation of a green process for microalgal CO₂ sequestration in closed photobioreactor using flue gas generated in-situ. *Bioresource Technology*, 191, 399–406. <https://doi.org/10.1016/j.biortech.2015.04.040>
- Yadav, N., Gupta, N., & Singh, D. P. (2021). Ameliorating Effect of Bicarbonate on Salinity Induced Changes in the Growth, Nutrient Status, Cell Constituents and Photosynthetic Attributes of Microalga *Chlorella vulgaris*. *Bulletin of Environmental Contamination and Toxicology*. <https://doi.org/10.1007/s00128-021-03135-5>

- Yeh, K.-L., Chang, J., & Chen, W. (2010). Effect of light supply and carbon source on cell growth and cellular composition of a newly isolated microalga Chlorella vulgaris. *Engineering in Life Sciences*, 10(3), 201–208. <https://doi.org/10.1002/elsc.200900116>
- Yen, H. W., Ho, S. H., Chen, C. Y., & Chang, J. S. (2015). CO₂, NOx and SOx removal from flue gas via microalgae cultivation: A critical review. *Biotechnology Journal*, 10(6), 829–839. <https://doi.org/10.1002/biot.201400707>
- Zhang, R. L., Wang, J. H., Cheng, L. Y., Tang, Y. J., & Chi, Z. Y. (2019). Selection of microalgae strains for bicarbonate-based integrated carbon capture and algal production system to produce lipid. *International Journal of Green Energy*, 16(11), 825–833. <https://doi.org/10.1080/15435075.2019.1641103>
- Zhao, B., & Su, Y. (2014). Process effect of microalgal-carbon dioxide fixation and biomass production: A review. *Renewable and Sustainable Energy Reviews*, 31, 121–132. <https://doi.org/10.1016/j.rser.2013.11.054>
- Zhu, X. G., Long, S. P., & Ort, D. R. (2008). What is the maximum efficiency with which photosynthesis can convert solar energy into biomass? *Current Opinion in Biotechnology*, 19(2), 153–159. <https://doi.org/10.1016/j.copbio.2008.02.004>

Curriculum Vitae

Name:	Maureen D. Córdoba Pérez
Post-secondary Education and Degrees:	Ph.D. in Chemical and Biochemical Engineering University of Western Ontario London, Ontario, Canada 2016-2021.
	B.Sc. in Chemical Engineering Universidad de Costa Rica San José, Costa Rica 2005-2011
Honours and Awards:	Postgraduate Scholarship. University of Costa Rica 2016-2021
Related Work Experience	Graduate Teaching Assistant University of Western Ontario 2016-2021
	Graduate Research Assistant University of Western Ontario 2016-2021
	Assistant Professor University of Costa Rica 2011-2016
Publications:	
	Cordoba-Perez, M; de Lasa, Hugo. CO ₂ -Derived Carbon Capture and Photon Absorption Efficiency by Microalgae in Novel <i>PhotoBioCREC</i> . Industrial and Engineering Chemistry Research, 2020, 59 (33), 14710-14716. https://doi.org/10.1021/acs.iecr.0c02319
	Cordoba-Perez, M.; de Lasa, H. CO ₂ Derived Carbon Capture Using Microalgae and Sodium Bicarbonate in a PhotoBioCREC Unit: Kinetic Modeling. Processes. 2021; 9(8):1296. https://doi.org/10.3390/pr9081296
	Córdoba Pérez, M., Molina Córdoba, M. Determinación del efecto de la concentración de celulosa, celobiosa y NaOH en la hidrólisis para la producción de etanol a partir del rastrojo de la piña. Ingeniería, 2014, 24 (2), 35-51. DOI 10.15517/RING.V24I2.11767.